Universidad Autónoma de Madrid

Departamento de Biología Molecular
Facultad de Ciencias

Functional characterization of Frataxin isoforms and mechanisms of regulation of frataxin expression

Mauro Agrò

Madrid, 2019

INDEX

Abbreviation List

Aco1: Aconitase 1

Aco2: Aconitase 2

AEBSF: 4-(2-aminoethyl)benzenesulfonyl fluoride hydrochloride

ATP: Adenosine Tri-Phosphate

BDNF: Brain-Derived Neurotrophic Factor

BML-210: N-phenyl-N'-(2-Aminophenyl) hexamethylenediamide

BSA: Bovine Serum Albumine

cAMP: Cyclic Adenosine Mono Phosphate

CEPO: Carbamylated Erythropoietin

CNS: Central Nervous System

Cpm: Cyclopamine

CREB: cAMP Response Element-Binding protein

CV: Complex V / ATP Synthase

DAPI: 4′,6-diamidino-2-phenylindole

dbcAMP: Dibutyryl Cyclic Adenosine Monophosphate / Bucladesine

DMEM: Dulbecco's Modified Eagle Medium

DMSO: Dimethyl Sulfoxide

DNA: Deoxyribonucleic Acid

DTT: Dithiothreitol

ECL: Enhanced ChemiLuminescence

EDTA: Ethylene Diamine Tetraacetic Acid

EGF: Epidermal Growth Factor

EGTA: Ethylene Glycol-bis(β-aminoethyl ether)-N,N,N,N-Tetraacetic Acid

EPO: Erythropoietin

ETR: Electron Transport Chain

FBS: Fetal Bovine Serum

FCCP: Carbonyl cyanide 4-(trifluoromethoxy) phenylhydrazone

FNDC5: Fibronectin Type III Domain Containing 5

FRDA: Friedreich's Ataxia

FXN: Frataxin

GABA: γ-AminoButyric Acid

GAPDH: Glyceraldehyde 3-phosphate dehydrogenase

GDNF: Glial-cell Derived Neurotrophic Factor

GFP: Green Fluorescent Protein

HBSP: Helix B Small Peptide

HBSS: Hank's Balanced Salt Solution

HEK 293T: Human Embryonic Kidney 293 cells with SV40 large antigen

HEPES: 4-(2-hydroxyethyl)-1-piperazineethanesulfonic acid

HDAC: Hystone Deacetylase

hrFGF: Human Recombinant Fibroblast Growth Factor

IDH: Isocitrate Dehydrogenase

IDLVs: Integration-Deficient Lentiviral Vectors

IL-6: Interleukin-6

INFγ : Interferon-γ

iPS: Induced Pluripotent Stem cells

IREs: Iron Responsive Elements

ISCs: Iron-Sulfur Clusters

ISCU: Iron-Sulfur Cluster assembly enzyme

MOI: Multiplicity of Infection

MIP-1α : Macrophage Inflammatory Protein-1α

mRNA: Messenger Ribonucleic Acid

MPP: Mitochondrial Processing Peptidase

MTS: Mitochondrial Targeting Sequence

MTT: 3-(4,5-Dimethylthiazol-2-Yl)-2,5-Diphenyltetrazolium Bromide

NAD^+/NADH: Nicotinamide Adenine Dinucleotide Oxidized/Reduced

NADP: Nicotinamide Adenine Dinucleotide Phosphate

NDUFS3: NADH Dehydrogenase Ubiquinone Iron-Sulfur protein 3

NEAA: Non-Essential Amino Acids

NGF: Nerve Growth Factor

NK: Natural Killer cells

NMDAR: N-Methyl-D-Aspartate Receptor

NRF: Nuclear Respiratory Factor

NT-3: Neurotrophin-3

OCR: Oxygen Consumption Rate

OMScs: Olfactory Mesenchymal Stem cells

PARP: Poly ADP-Ribose Polymerase

PBS: Phosphate Saline Buffer

PCR: Polymerase Chain Reaction

PFA: Paraformaldehyde

PGC-1alpha: Peroxisome Proliferator-Activated Receptor Gamma Coactivator - 1alpha

PMS: Phenazine Methosulfate

PPAR-γ: Peroxisome Proliferator-Activated Receptor gamma

qPCR: Quantitative Polymerase Chain Reaction

qRT-PCR: Quantitative Retro Transcribed Polymerase Chain Reaction

ROS: Reactive Oxygen Species

SCF: Stem Cell Factor

SDS: Sodium Dodecyl Sulfate

SHH: Sonic Hedgehog

STAT: Signal Transducer and Activator of Transcription

TFAM: Mitochondrial Transcriptional Factor A

TGF-β: Transforming Growth Factor β

TMB: 3,3', 5,5' – tetramethylbenzidine

TRF1: Transferrin Receptor 1

TrK: Tyrosine Receptor Kinase

VDAC: Voltage-Dependent Anion Channel

VEGF: Vascular Endothelial Growth Factor

YAC: Yeast Artificial Chromosome

YFH1: Yeast Frataxin Homologue 1

Summary:

Friedreich's Ataxia (FRDA) is a mainly neurodegenerative recessive disease caused by the deficiency of frataxin protein. This deficiency is mostly due to the expansion of the GAA triplet located in the first intron of frataxin gene. This mutation leads to the reduction in the levels of the protein, which fall around 20-30% of normal levels. Frataxin, in its canonical mature form, is a protein localized to the mitochondria, where it exerts its roles, mostly involved in iron storage, in the formation and regulation of Iron-Sulfur clusters and in maintaining mitochondrial homeostasis.

Recently the existence of different isoforms of frataxin with an extra-mitochondrial localization has been indicated. We found that the overexpression of both mitochondrial isoform I and cytosolic isoform II is able to improve mitochondrial respiration in FRDA patient cells, increasing basal respiration rates and oxygen consumption rates and incrementing the levels of mitochondrial biomarkers like VDAC and Aconitase. Besides, the overexpression of canonical Isoform I is directly affecting the development of mitochondrial network, exerting a positive effect on both the number of isolated mitochondria as well as the number of mitochondria structured in networks. Finally, both isoforms seem to interact with Fe-S cluster containing proteins, like cytosolic and mitochondrial Aconitase, being also able to protect the enzymes in an oxidative-stressing environment.

The regulation of frataxin gene expression is another issue of major interest for its possible therapeutic relevance. Several factors including Erythropoietin and some Epo-mimetic molecules have been reported to increase frataxin levels. There are some drawbacks, since canonical Epo can cause hematocrit problems, while some of the derivative peptides described are known to be highly unstable, with a very low half-life in the organism. For this reason, we decided to focus on a retro-enantiomeric version of a HBSP-based peptide, called EPO2. We described in this work the positive regulatory effects on frataxin of this synthetic epomimetic peptide, both *in vitro* in several cell models and *in vivo* in the cerebellum of wild type mice.

Finally, we reported the effects of spontaneous physical activity in wild type mouse cerebellum on frataxin expression. Frataxin levels appeared positively modulated after exercise, suggesting a post-transcriptional regulation mechanism. We investigated for possible mediators of this beneficial effect by qPCRs and through a cytokine array which highlighted the upregulation of several factors, including the neurotrophin NT-3, SHH protein, MIP-1α and IFN-γ, pointing the way to a multi-layered regulatory complex behind frataxin modulation set up by physical exercise.

Together, these results give more insight on part of the mechanisms underlying frataxin regulation, which could prove useful in the development of potential new strategies in the treatment of FRDA.

Resumen:

La Ataxía de Friedreich (FRDA) es una enfermedad predominantemente neurodegenerativa causada por la deficiencia de la proteína Frataxina. Esta deficiencia es mayormente debida a la expansión del triplete GAA localizado en el primer intrón del gen de la frataxina, la cual es responsable de la reducción de los niveles de la proteína, que se sitúan alrededor de un 20-30% de los niveles normales. La frataxina, en su forma canónica madura, es una proteína mitocondrial involucrada en el almacenamiento de hierro, la formación y regulación de centros hierro-azufre y el mantenimiento de una correcta homeostasis mitocondrial.

Estudios recientes han observado la existencia de diferentes isoformas de frataxina de localización extra-mitocondrial. En este trabajo hemos demostrado que la sobreexpresión de ambas isoformas de frataxina, la isoforma I mitocondrial y la isoforma II citosólica, es capaz de mejorar la respiración mitocondrial en células de paciente de FRDA, incrementando los niveles de respiración basal y la tasa de consumo de oxígeno, aumentando, también, el nivel de biomarcadores mitocondriales como por ejemplo VDAC y Aconitasa. Además, la sobreexpresión de la isoforma I es directamente responsable de inducir una mejora en el desarrollo de la red mitocondrial, ejerciendo un efecto positivo en el aumento de mitocondrias aisladas y en el número de mitocondrias estructuradas en red. Finalmente, ambas isoformas parecen interactuar con los centros Fe-S contenidos en las proteínas, como por ejemplo de la aconitasa mitocondrial y la citosólica, y además protegen a estas enzimas en condiciones de estrés oxidativo.

La regulación de la expresión del gen de la frataxina es otro tema de gran interés por su posible relevancia terapéutica. Se ha visto que varios factores son capaces de incrementar los niveles de frataxina, entre los cuales figuran la Eritropoyetina y algunas moléculas Epo-mimeticas. Existen algunos inconvenientes debido al hecho de que el péptido Epo canónico puede provocar problemas en el hematocrito, mientras que algunos de los análogos descritos parecen ser altamente inestables, con una vida media en el organismo muy corta. Por estas razones, hemos decidido enfocarnos en una versión retro-enantiomérica de un péptido basado en HBSP, llamado EPO2. Hemos descrito en este trabajo los efectos positivos de este péptido epomimetico sobre la expresión de frataxina, *in vitro* en distintos modelos celulares e *in vivo* en el cerebelo de ratones *wild-type*.

Finalmente, hemos observado los efectos de la actividad física espontánea sobre los niveles de frataxina en el cerebelo de ratones *wild-type*. Estos niveles parecen estar modulados positivamente después del ejercicio, y nuestros resultados sugieren un mecanismo de regulación post-transcriptional. Hemos estudiado los posibles mediadores de este efecto beneficioso mediante qPCR y a través de un *array* de citoquinas, permitiéndonos identificar el aumento de

distintos factores, incluyendo la neurotrofina NT-3, la proteína SHH, MIP-1α y IFN-γ, lo cual indica un complejo mecanismo regulatorio detrás del aumento de los niveles de frataxina inducido por el ejercicio físico.

En conjunto, estos resultados nos han permitido profundizar en una parte de los mecanismos que subyacen a la regulación de frataxina, lo cual podría ser de gran utilidad para el desarrollo de nuevas estrategias potenciales en el tratamiento de la FRDA.

Introduction

1. Friedreich's Ataxia:

Friedreich's Ataxia (FRDA) is an inherited autosomal recessive disease described for the first time by Dr. Nikolaus Friedreich in 1863. It belongs to a group of rare neurological disorders called Autosomal Recessive Cerebellar Ataxias (ARCAs) which are characterized by a degeneration and/or a defective development of the spinocerebellar system. FRDA is the less "rare" of the ataxias, affecting roughly 1-2 every 50000 Caucasians.

Being an ataxia, it is characterized by the lack of motor coordination; the development of the disease is slow, but steady during the lifespan of an individual, with the first symptoms starting to show themselves during childhood. Not all the symptoms show at the same time, but often the earliest ones include poor articulation of phonemes (dysarthria), blurred vision (diplopia), difficulties in swallowing (dysphagia), uncontrolled movements of the eyes (nystagmus), abnormal reflexes of lower extremities (Babinsky response), and loss of proprioception. In addition to neurological symptoms, a high number of patients also show extra-neurological signs, as mitochondrial energy production deficit in muscle (Lodi, Cooper et al. 1999), skeletal abnormalities such as scoliosis and *pes cavus* (Parkinson, Boesch et al. 2013), type II diabetes (Cnop, Mulder et al. 2013), glucose intolerance (Finocchiaro, Baio et al. 1988) and hypertrophic cardiomyopathy (Regner, Lagedrost et al. 2012).

Even though the disease has always been described as an early onset neurodegenerative disease, recent findings indicate that it is possibly composed by two "steps": a developmental hypoplasia mainly affecting the spinal cord and medulla, and a neurodegenerative process mainly affecting the cerebellum. Thus, the patients are born with a neuronal deficiency in the spinal cord and medulla and with normal cerebellar nuclei, which are bound to slowly neurodegenerate over time (Mascalchi, Toschi et al. 2016). Neuropathologic and imaging studies show that the development of the disease begins with an atrophy of spinal ganglia, spinal cord and of the medulla oblongata, followed by a neurodegenerative process of the cerebellum with a focus on the deep nuclei (especially the dentate nucleus) where a degeneration of the glutamatergic neurons and of the corticonuclear synaptic terminals containing γ-aminobutyric acid (GABA) takes place. In later stages of the disease, other areas affected are represented by cerebellar vermis and cortex (Koeppen and Mazurkiewicz 2013). Furthermore, recent findings indicate there is a direct glial cells contribution during FRDA development, shown both in Drosophila (Navarro, Ohmann et al. 2010) and by our group in human astrocytes (Loria and Diaz-Nido 2015). These results have been further confirmed by analyzing plasma levels, in FRDA patients, of glial markers such as the Glial

Fibrillary Acidic Protein (GFAP), along other factors indicating neuronal damage such as the Ubiquitin Carboxy-terminal Hydrolase L1 (UCH-L1) and the Neurofilament-Light Chain (NfL), which could be used as potential biomarkers to achieve a better understanding of disease progression (Zeitlberger, Thomas-Black et al. 2018).

1.1. Molecular bases of FRDA:

Friedreich's ataxia originates from mutations in FRDA gene, located at the chromosome 9p13 (Chamberlain, Shaw et al. 1988; Campuzano, Montermini et al. 1996). This gene, also known as X25, encodes for frataxin (FXN) protein, a ubiquitous protein, mostly localized in mitochondria. X25 gene is composed by 7 exons (Baralle, Pastor et al. 2008) spanning around 80kb, but only the first five exons are responsible of codifying for FXN protein. The most common mutation in FRDA patients is the expansion of the GAA (guanine-adenine-adenine) triplet contained in the first intron of the gene (Campuzano, Montermini et al. 1996; Cossee, Schmitt et al. 1997): a certain number of GAA repeats is present even in non-patients, with up to 60-70 GAA repeats being non-dangerous, while patients possess a number of repeats spanning from 70 up to 1700 (Fig.1).

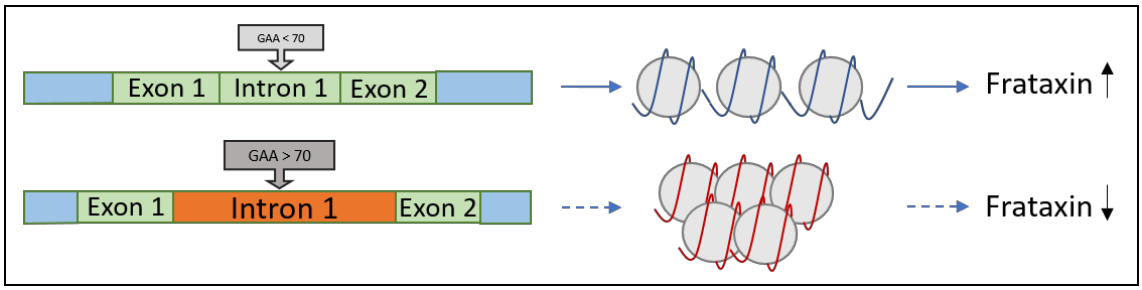

Figure 1 - Effects of GAA repeats on Frataxin levels. GAA expansion induces heterochromatin domains which ultimately lead to reduced levels of the protein

The GAA expansion is the major cause of the disease, being present in homozygosis in 95% of patients, while the rest are commonly compound heterozygous for the expansion and a point mutation (De Castro, Garcia-Planells et al. 2000). Up to 30 point mutations have been identified, including both missense and nonsense mutations, giving rise to either anomalous or truncated versions of FXN protein. No homozygous patients with point-mutations have been identified (Galea, Huq et al. 2016).

The GAA triplet expansion causes a significant reduction in transcription levels, with mechanisms not yet fully established and still controversial. One possible cause could be the induction of "sticky DNA" aberrant structures that could physically block the RNA polymerase II, thus hindering its movement along the DNA template (Sakamoto, Ohshima et al. 2001). Another mechanism hypothesized involves the formation at the GAA expansion of aberrant DNA/RNA hybrid structures, called R-loops, that could ultimately lead to an aberrant termination of transcription (Butler and Napierala 2015). This reduction in transcription levels would be also followed by a gradual heterochromatization of FXN gene (Kumari and Usdin 2012). Previous studies showed that FRDA patients actually do possess a very condensed chromatin, due to the deacetylation and hypermethylation of histones, so GAA repeats could provoke both phenomena at the same time: a reduction in transcription rates and the induction of heterochromatin domains (Yandim, Natisvili et al. 2013).

There are evidences of a direct correlation between the number of GAA repeats and the amount of protein: the higher the number of repeats, the lower the amount of frataxin. Therefore, even another conclusion can be drawn: the higher the number of repeats, the sooner the symptoms are bound to appear, and this applies also to the intensity of such symptoms (Evans-Galea, Carrodus et al. 2012)

2. Frataxin: structure and functions

Frataxin is a ubiquitous protein with major abundance in tissues in which there is a high energetic demand, such as brain, heart, liver, pancreas and spinal cord. In its canonical mature form, frataxin localizes inside the mitochondria (Campuzano, Montermini et al. 1997), associated with the inner membrane. It is synthesized as a precursor protein (210aa, 23kDa) that is then processed, cleaved and sent to the mitochondria, process mediated by the mitochondrial targeting sequence (MTS) that the precursor possesses on the N-terminal domain. The protein complex responsible of the precursor processing is the mitochondrial processing peptidase (MPP) that cleaves the precursor producing an intermediate form (42-210, 19 kDa) that is then further processed to free the mature form of frataxin (81-210, 14,2 kDa). The molar ratio between these two forms is thought to be modulable, with FRDA patients shifting towards a faster conversion of the 42-210 form into the 81-210 one. Furthermore, the 42-210 form exists in mono- and oligomeric configurations, similarly to several components of the Fe-S cluster assembly machinery (Gakh, Bedekovics et al. 2010)

Over the course of time, there have been described many alternative forms of frataxin protein (or *isoforms*): the first ones have been described by Campuzano (Campuzano, Montermini et al.

1997) originated though an alternative splicing event in intron 4; another one has been described by Pianese (Pianese, Tammaro et al. 2002) containing exon 5b and not 5a.

Recently, another group (Xia, Cao et al. 2012) described even more isoforms with different cellular localization and tissue distribution. These new isoforms are called FXN II and FXN III (*Fig.2*): in both of them the MTS is absent, so they are not localized in the mitochondria. FXN II is transcribed from a different starting point and possess a different first exon (Exon 1b /Δ18), while FXN III is obtained through an alternative splicing of exon 1a (exon 1a, Δ141).

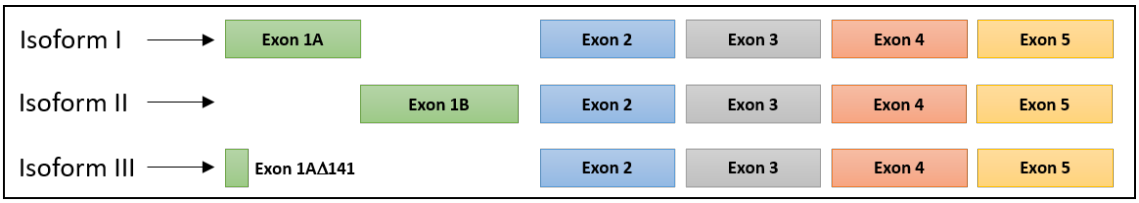

Figure 2 - Diagram showing differences between Frataxin isoforms (I, II and III in order) following Xia et al. results

According to the work of Xia et al., these isoforms seem to be tissue-specific, with the Isoform II localized mainly in the cerebellum and Isoform III mostly abundant in heart. Furthermore, their cellular distributions seem to be different too, with the II being cytosolic and the III being nuclear. Isoform II might be involved in protecting iron-sulfur clusters (ISCs) from oxidative damage, while Isoform III might activate the biogenesis of mitochondrial ISCs, according to the description provided by Xia. Previous work from our laboratory has demonstrated that by delivering the whole 135kb FXN genomic locus to FRDA patient cells, all the isoforms are detectable in cells from healthy subjects and patients (Perez-Luz, Gimenez-Cassina et al. 2015).

As for frataxin functions, several hypotheses are postulated on the important cellular functions in which frataxin play a role (Fig.3):

It is thought that frataxin is capable to bind iron and regulate its storage inside the mitochondria (Isaya, O'Neill et al. 2004), by forming a complex which can accumulate many iron atoms (Fig 3 – a). Frataxin is also involved in protecting iron from oxidation that could occur inside the mitochondria and to supply it to other proteins (Adamec, Rusnak et al. 2000; Gakh, Adamec et al. 2002), such as the ferrochelatase (heme synthesis, Fig. 3 - b) (Bencze, Yoon et al. 2007). Other potential targets of the iron transferring include the Iron-Sulfur Cluster assembly enzyme (ISCU) and Cysteine desulfurase NFS1 (encoded by NSF1 gene), involved in the formation of Iron-Sulfur Clusters (ISCs).

In addition, frataxin itself participates in ISCs formation directly, by stabilizing the ternary complex of ISCU/NFS1/ISD11 (Fig 3 – c), otherwise the ternary complex would not be correctly

formed, and it would be unable to transfer Fe-S clusters to other proteins (Colin, Martelli et al. 2013). Furthermore, also the 42-210 oligomeric form of frataxin has been shown to possess the ability of forming stable complexes with NFS1/ISD11, which could act as a backup Fe-S cluster formation mechanism under the appropriate metabolic activation switch (Gakh, Bedekovics et al. 2010).

Apart from participating in the ISCs formation, Frataxin is also probably involved in the repair of ISCs (such as the one of mitochondrial aconitase) by protecting them from the prooxidant action and maintaining them in the $[4Fe\text{-}4S]^{2+}$ active form (Fig 3 – d), (Bulteau, O'Neill et al. 2004).

Another postulated function is the possible interaction of Frataxin with components of the electron transport chain, in particular with the succinate dehydrogenase (Complex II, Fig 3 - e) (Gonzalez-Cabo, Vazquez-Manrique et al. 2005), thus increasing electron transport and oxidative phosphorylation itself.

Last, Frataxin may participate in the antioxidant response of cells in conjunction with the Peroxisome proliferator-activated receptor gamma coactivator 1-alpha (PGC1-alpha) (Marmolino 2011) and the nuclear factor-E2-related factor-2 (Nrf2) (Shan, Schoenfeld et al. 2013), both downregulated in FRDA cells (Fig 3 – f).

Even though there still is some debate on the exact roles performed by Frataxin, it is clear that all of these functions are part of the same net and that frataxin deficiency leads to an deregulated iron metabolism and to defective ISCs which, in turn, mean that iron could react with reactive oxygen species (ROS) in order to produce further damage in the mitochondria and, thus, in the whole cell.

ISCs are key elements of several cellular metabolic pathways and are needed to maintain correct homeostasis, in practically all living organism, from archaea to eukaryotes. Many enzymes involved in nucleic acid, amino acid and lipid metabolism or DNA repair machinery contain iron-sulfur clusters, thus marking the importance of these cofactors (Fontecave 2006). For this reason, their assembly is strictly regulated by cells with a complex controlled system involving many partners, including 18 mitochondrial cluster assembly proteins (ISC) and 11 cytosolic assembly proteins (CIA), underlying the existence of different isoforms of the ISCs assembly machinery distributed in different cellular compartments (Rouault and Maio 2017). The postulated assembly process involves the synthesis of a *de novo* [2Fe-2S] cluster by an early-acting ISC machinery. This cluster is then processed by a late-acting machinery to produce the functional [4Fe-4S] clusters which are either transported to the corresponding mitochondrial target apoproteins or exported to the cytosol to be assembled to cytosolic targets by the CIA machinery (Braymer and Lill 2017). Finally, frataxin is thought to have a role on ISCs formation process, by acting as a

metabolic switch by determining the allocation, in mitochondria, of iron used for ISCs synthesis (Chiang, Kovacevic et al. 2016)

As for the different isoforms, they are thought to be involved in protecting ISCs from oxidative damage (Iso II) and activating ISCs biogenesis (Iso III) (Xia, Cao et al. 2012); however, their precise function has not yet been fully described yet. Precisely, further developments in these fields will be one of the aims of this thesis.

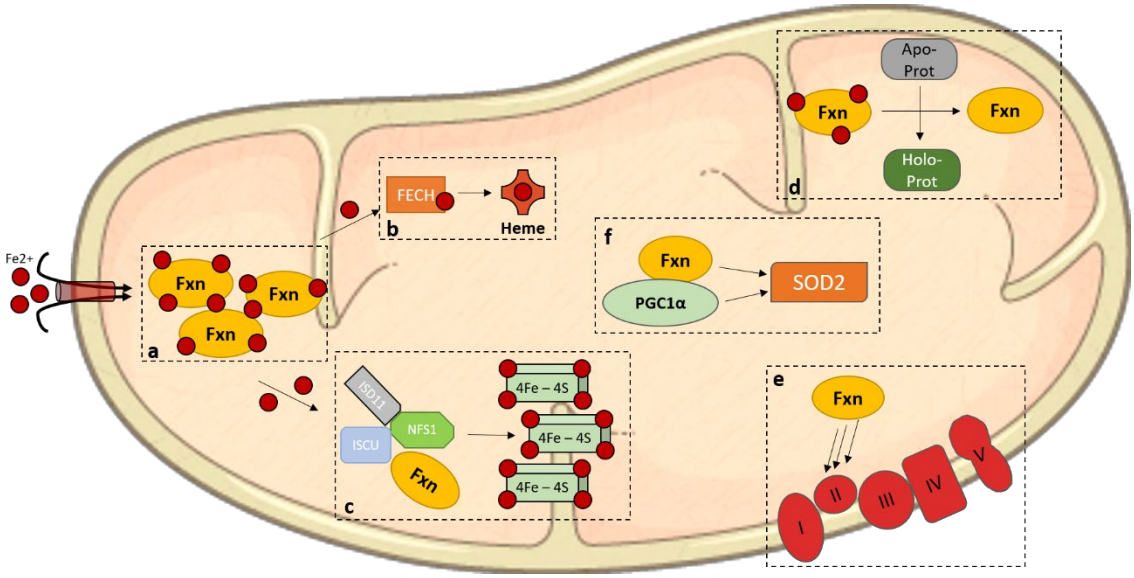

Figure 3 - Diagram showing Frataxin postulated functions. **a**) Iron binding and storage, **b**) Iron donor to Ferrochelatase during Heme biosynthesis, **c**) Iron donor and physical stabilizer of the ISCU/NSF1/ISD11 complex during ISCs biosynthesis, **d**) Transfer and reparation of ISCs to recipient proteins, **e**) Interaction with Succinate Dehydrogenase (Complex II) to improve OXPHOS, **f**) Participation with PGC1α in antioxidant response by activating Superoxide Dismutase 2

3. Frataxin in mitochondrial metabolism and biogenesis

Being frataxin a mitochondrial protein involved in all the functions we have previously unraveled and with such a strong impact on this organelle, it is clear that mitochondrial biogenesis and metabolism study is a key factor for FRDA research. Starting from organisms like *C. elegans* and yeast, frataxin deficiency leads to impairments in components of the OXPHOS (Complex II, in particular, following the work of Gonzalez-Cabo (Gonzalez-Cabo, Vazquez-Manrique et al. 2005). Moving up the evolutionary ladder, it is known that, in myocardial tissue and blood from patients, the OXPHOS is impaired and that they show abnormalities in complex I, II and III (Rotig, de Lonlay et al. 1997) (Salehi, Kamalidehghan et al. 2014), but little is known about the most affected tissues like brain and cerebellum. Recent studies in frataxin-deficient mouse (see section 4) cerebellum have shown that PGC-1α which is involved in mitochondrial biogenesis, is strongly downregulated compared to its levels in WT mice both at asymptomatic (P30, 60, 90) and at symptomatic (P270) ages, suggesting an early impairment of PGC-1α and its mitochondrial biogenetic roles. These findings were also confirmed for the factors downstream of PGC-1α, such as the Nuclear Respiratory Factor 1 (NRF1) and the Mitochondrial Transcriptional Factor A (TFAM or mtTFA) suggesting that the PGC1α/TFAM/NRF1 mitochondrial biogenesis pathway in the cerebellum of these mice is strongly impaired which could lead to the dysfunction typical of FRDA. Moreover, even the function of the subunits of the respiratory complex is compromised, with the activity of Complex I, II and IV significantly diminished in the cerebellum of KIKO mice (Lin, Magrane et al. 2017). Similar findings were also confirmed in KIKO brain tissue, but, more importantly, in patient fibroblasts and whole blood (Jasoliya, McMackin et al. 2017), thus correlating the decreased mitochondrial biogenesis with low frataxin expression and suggesting mitochondrial biogenesis as a FRDA biomarker.

Interestingly, Jasoliya also showed that overexpression of canonical frataxin is directly related to the increment of Voltage-Dependent Anion Channel (VDAC) protein, confirming the direct effect of frataxin upon mitochondrial biogenesis. In this picture, unknown are the functions of the cytosolic frataxin isoform II which could be involved in preserving iron homeostasis, and thus mitochondrial correct functioning, “from the outside” of the mitochondria itself: in cytosol. We have already said that the canonical isoform of frataxin is involved in stabilizing the iron-sulfur cluster of mitochondrial aconitase (Aco2), but it is also known that there is another, cytosolic, form of Aconitase (Aco1 or IREB1) which has shown moonlight activity: when intracellular iron levels are low, Aco1 binds to Iron Responsive Elements (IREs) located on the mRNAs of ferritin (thus inhibiting its translation, being ferritin involved in iron storage) and of transferrin (involved in iron import from the outside of the cell), stabilizing its mRNA. When intracellular iron levels are not low anymore, the protein becomes a fully-fledged aconitase,

incorporating an iron sulfur cluster and restoring the balance between ferritin and transferrin (Seznec, Simon et al. 2005).

4. FRDA: Experimental models

Cellular and animal models that allow for a better understanding of the processes happening during FRDA development, are mandatory for unraveling the biological functions of frataxin and its isoforms as well as to permit the discovery of potential new therapeutic approaches. Being frataxin a phylogenetically highly conserved protein, over the years a high number of different models, cellular or animal, have been characterized, which allows for a better view of the mechanisms underlying the disease. Unicellular models like *E. coli* or *S. cerevisiae* have the credit to have allowed for the characterization of frataxin and its functions and have been fundamental in opening the way for more "complex" systems reproducing the more characteristic aspects of the disease: between these models, the most useful has been the yeast *Saccharomyces cerevisiae*, due the discovery of the analogue gene Yeast Frataxin Homolog 1 (YFH1). It was, then, possible to create a strain expressing no YFH1 thus seeing features similar to the ones observed in patients: impaired oxidative phosphorylation, iron accumulation and a higher sensitivity to oxidative stress (Foury and Cazzalini 1997).

In the following table, some of the models used in literature can be found:

Model	Features	Reference
Unicellular Models		
E. coli	Deletion of the homologous Fxn gene does not provoke iron accumulation or oxidative stress.	(Li, Ohshima et al. 1999)
Saccharomyces cerevisiae	Deletion of the homologous Fxn gene causes iron accumulation, impaired OXPHOS and increased sensitivity to oxidative stress.	(Foury and Cazzalini 1997)
Invertebrate Models		
C. elegans	Silencing Fxn induces increased sensitivity to oxidative stress and reduced life span.	(Vazquez-Manrique, Gonzalez-Cabo et al. 2006)

Drosophila melanogaster	Fxn silencing induces ISCs and Heme formation deficiency, aconitase activity reduction, increased sensitivity to oxidative stress and an overall reduced life span.	(Anderson, Kirby et al. 2005; Navarro, Ohmann et al. 2010; Calap-Quintana, Navarro et al. 2018)
Neural cell Models		
SH-SY5Y	*FXN* silencing through shRNA provokes mitochondrial dysfunctions, higher oxidative stress, cell cycle arrest in G1 and p53-triggered apoptosis.	(Bolinches-Amoros, Molla et al. 2014) (Palomo, Cerrato et al. 2011)
Astrocytes	*FXN* silencing causes altered mitochondrial morphology and higher sensitivity to oxidative stress, inhibition of cell proliferation and decreased viability.	(Loria and Diaz-Nido 2015)
Schwann cells	*FXN* silencing induces activation of inflammatory pathways and apoptotic genes, decreased cell viability and proliferation.	(Lu, Schoenfeld et al. 2009)
Primary cultures of rat DRG neurons	Frataxin depletion caused mitochondrial membrane potential decrease, neurite degeneration, altered calcium homeostasis and apoptosis.	(Mincheva-Tasheva, Obis et al. 2014)
Primary cultures of mouse brain neurons	Frataxin depletion induced activation of Caspase-3 and caused apoptotic cell death.	(Katsu-Jimenez, Loria et al. 2016)
Models derived from FRDA patients		
Lymphocytes	Increased sensitivity to oxidative damage, ISCs proteins deficiency.	(Rotig, de Lonlay et al. 1997)

Fibroblasts	Increased sensitivity to oxidative damage, ISCs proteins deficiency.	(Sturm, Bistrich et al. 2005)
iPS derived Neurons	Impairment in mitochondrial homeostasis, maturation delay.	(Hick, Wattenhofer-Donze et al. 2013)
Mammalian Animal Models		
KIKI	Knock-in in homozygosis with ~126 GAA repeats. Approximately 70% of fxn levels compared to healthy mice.	(Miranda, Santos et al. 2002)
KIKO	Knock-in with ~230 repeats and knock-out on the other allele. Around 30% of fxn levels compared to healthy mice.	(Miranda, Santos et al. 2002)
YG8R	Murine frataxin delete with a YAC expressing human fxn containing GAA expansion. Mild phenotype.	(Al-Mahdawi, Pinto et al. 2006)
YG8sR	Like YG8R, but with more GAA repeats and a more severe phenotype.	(Anjomani Virmouni, Ezzatizadeh et al. 2015)

Table 1 – Principal models that are used in FRDA research

In the table, for mammalian cell models, only models of neural lineage are shown. The most appropriate and "physiological" cell models are, clearly, the ones deriving from patients, containing the GAA expansion along with the complete frataxin locus. Unfortunately, the most common patient cell models used in FRDA research are not of neural lineage and this is why, more recently, fibroblasts are being reprogrammed into induced pluripotent stem cells (iPS) and then into neurons or, directly into neurons (iN cells) in order to have a more disease-relevant cell model to investigate. Hick et al. have shown that iPS differentiated into neurons maintain low frataxin levels and have proper morphology, but possess a weak biochemical phenotype compared to patient cells. This makes this model an optimal one to study potential therapies focused on rising frataxin levels, but probably it would be best to use another one to study the molecular mechanisms triggered by frataxin deficiency.

Apart from cellular *in vitro* models, animal models have a big impact on FRDA research, allowing to study *in vivo* the effects of frataxin deficiency. We have to say that a complete frataxin knockout is lethal and unviable (Cossee, Puccio et al. 2000), so, at first, conditional models in

which frataxin could be silenced from the tissue of interest via Cre recombinase, leading to a severe phenotype, even harsher than the one seen in patients, since FRDA is developed slowly and gradually over the years. That is why other mouse models have been developed, for example the KIKI/KIKO in which there is a double or single knock-in of the GAA expansion in the murine frataxin gene (Miranda, Santos et al. 2002) or the YG8R/sR in which murine frataxin has been replaced with a single copy of human frataxin containing the GAA expansion. The "sR" version of this model, includes a contracted version of human frataxin with more repeats, giving a stronger phenotype compared to the YG8R version. Recently, another model is being characterized, called YG8LR (not yet available for purchase) containing even more repeats than the sR and resulting, in general, more stable as a model (M. Pook, personal communication).

5. Regulation of frataxin expression

After a brief overview of FRDA and the status of its research, it appears clear that Frataxin is involved in so many processes of the utmost importance for the cell and its physiology. For this reason, we decided to focus this thesis on its regulation, being it a field with many aspects yet to clarify. Frataxin regulation is a multi-layered area in which a network of various factors is taking part. We decided to point our attention on several "sub-fields" in several of the models we examined earlier, with the goal of reaching a better understanding on frataxin expression mechanisms which could be useful in gaining new knowledge on FRDA itself and, hopefully, in the design of potential new treatments.

5.1. Frataxin isoforms

Little is known about frataxin isoforms which have been recently described by Xia (Xia, Cao et al. 2012). Aside from what we have described before, the three isoforms only differ in the first exon, while exon 2, 3, 4 and 5 are the same for the three of them (Fig.1). In this work we have tried to characterize these isoforms, evaluating their localization inside the cell and trying to gain insight into the functions they could be involved into. In order to do this, we have used lentiviral vectors carrying the sequence codifying for the different isoforms to transduce the cells and study, in detail, the specific isoform delivered.

5.2. Erythropoietin-derived peptides

As mentioned earlier in this introduction, one of the approaches for FRDA treatment consists of using recombinant human erythropoietin-derived peptides which are able to elicit a neuroprotective effect and, specifically, to increment frataxin levels binding to an alternative EPO receptor (Brines and Cerami 2005; Siren, Fasshauer et al. 2009; Miller, Rai et al. 2017), apart from the classical one. Erythropoietin has been known as a modulator of erythropoiesis and, as such, was shown to produce some side-effects like an increment in hematocrit which, unfortunately, represents a serious obstacle in the clinical use of EPO as a therapeutic drug for the treatment of patients. Studies with recombinant-human EPO in lymphocytes and cardiac myoblasts from FRDA patients, demonstrated that the peptide is able to induce increments in frataxin protein levels up to 2.5 fold in a dose-dependent manner: this increase can be observed just after a few hours after the treatments. Previous work from our lab has shown that alternative forms of erythropoietin, such as the carbamylated form (CEPO) and a synthetic peptide produced from the aminoacids composing the soluble part of the B-Helix of EPO (Helix B Small Peptide, HBSP) are able to produce an increment in frataxin protein levels in neuroblastoma SH-SY5Y cells (both in proliferation or differentiated in "neuron-like" cells) and in olfactory mesenchymal stem cells from FRDA patients (Thesis Yurika Katsu-Jiménez, 2013). Based on these results, even more studies are currently ongoing using these peptides or synthetic derivatives with several advantages, which has been one of the focuses of this work and has been debated extensively in later parts of this thesis. It must be noted that while both rhEPO and the carbamylated form CEPO have reached the stage of clinical trial (Sacca, Piro et al. 2011; Mariotti, Fancellu et al. 2012; Boesch, Nachbauer et al. 2014), few data are available in animal models: recently other groups have shown that following treatment with rhEPO in KIKO mice, while there were no significant results in brain tissue, the peptide was able to induce an increase in frataxin mRNA levels in hearth, not followed by changes in frataxin protein levels (Miller, Rai et al. 2017). Unfortunately, no one has ever examined in depth the molecular mechanisms underlying frataxin (protein or mRNA) increases after the treatment with these compounds.

5.3. Physical activity and Neurotrophic Factors

Physical activity is known to play a fundamental role in maintaining a healthy organism, bolstering the cardiovascular, endocrine and immune systems while providing also positive effects and benefits on the nervous system of an individual, promoting for example survival and maturation of cells of dentate gyrus and contributing to hippocampal neurogenesis in adult rodent models (Kempermann, Brandon et al. 1998; van Praag, Shubert et al. 2005). Even in humans,

adults of over 60 years participating in regular moderate physical exercise protocols showed less risks of dementia and performed better in common memory tests (Colcombe and Kramer 2003; Kramer and Colcombe 2018) and, furthermore, exercise has been shown to have positive effects even on people affected by early stages of dementia (de Assis and de Almondes 2017). For these reasons, physical exercise is gaining constantly more importance even in neurodegenerative diseases since it could provide an effective strategy to prevent, or at least slow down, the deterioration of the nervous system. Much is known about the benefits of physical exercise and its relation to neurotrophic factors in hippocampus, while little endeavors have been done regarding cerebellum. Furthermore, nothing is known about any kind of link between physical activity and FRDA. As described previously, an important approach when dealing with FRDA is trying to understand the mechanisms behind frataxin expression regulation in order to increment the levels of frataxin from dangerous pathological amounts to physiological ones. Indeed, recent studies from our laboratory have shown that the gene delivery of neurotrophic factors, such as the Brain-derived neurotrophic factor (BDNF) or Neurotrophin 3 (NT-3), protect from the neurodegeneration induced by low levels of frataxin protein both *in vivo* and *in vitro* (Katsu-Jimenez, Loria et al. 2016).

Interestingly, it has been demonstrated by other groups that physical activity induces neuroprotective effects by increasing the expression of several trophic factors, mostly in the hippocampus [eg. BDNF (Marlatt, Potter et al. 2012), Nerve Growth Factor (NGF) (Ang, Wong et al. 2003), Insulin-like Growth Factor 1 (IGF-1) and Vascular Endothelial Growth Factor (VEGF) (Ding, Vaynman et al. 2006), Glial-cell Derived Neurotrophic Factor (GDNF) (Campos, Rocha et al. 2016)]. Some studies have shown that the effects of physical activity on BDNF expression are mediated by the PGC-1α protein, a transcriptional coactivator involved in mitochondrial biogenesis and energy metabolism through activation of PPAR□□that, in turn, leads to the activation of a series of transcription factors like the cAMP response element-binding (CREB) protein or the Nuclear Respiratory Factor proteins (NRF 1 and 2) (Wu, Puigserver et al. 1999; Wrann, White et al. 2013). As mentioned before, previous studies have indicated a direct correlation between the levels of PGC-1α, PPAR-γ activation and Frataxin levels (Coppola, Marmolino et al. 2009). However, the effects of physical exercise on frataxin expression, and the feasibility of physical exercise, or its effects at the molecular level, as a therapeutic avenue to treat Friedreich's Ataxia, have not been investigated up to now.

6. FRDA: Therapeutic approaches

Unfortunately, there still is no effective cure for FRDA. Nonetheless, many researchers are trying their best to dissect every mechanism of the disease in order to intervene at different stages of the disease itself, as visible in this picture taken from a recent review (Zhang, Napierala et al. 2019) (Fig. 4).

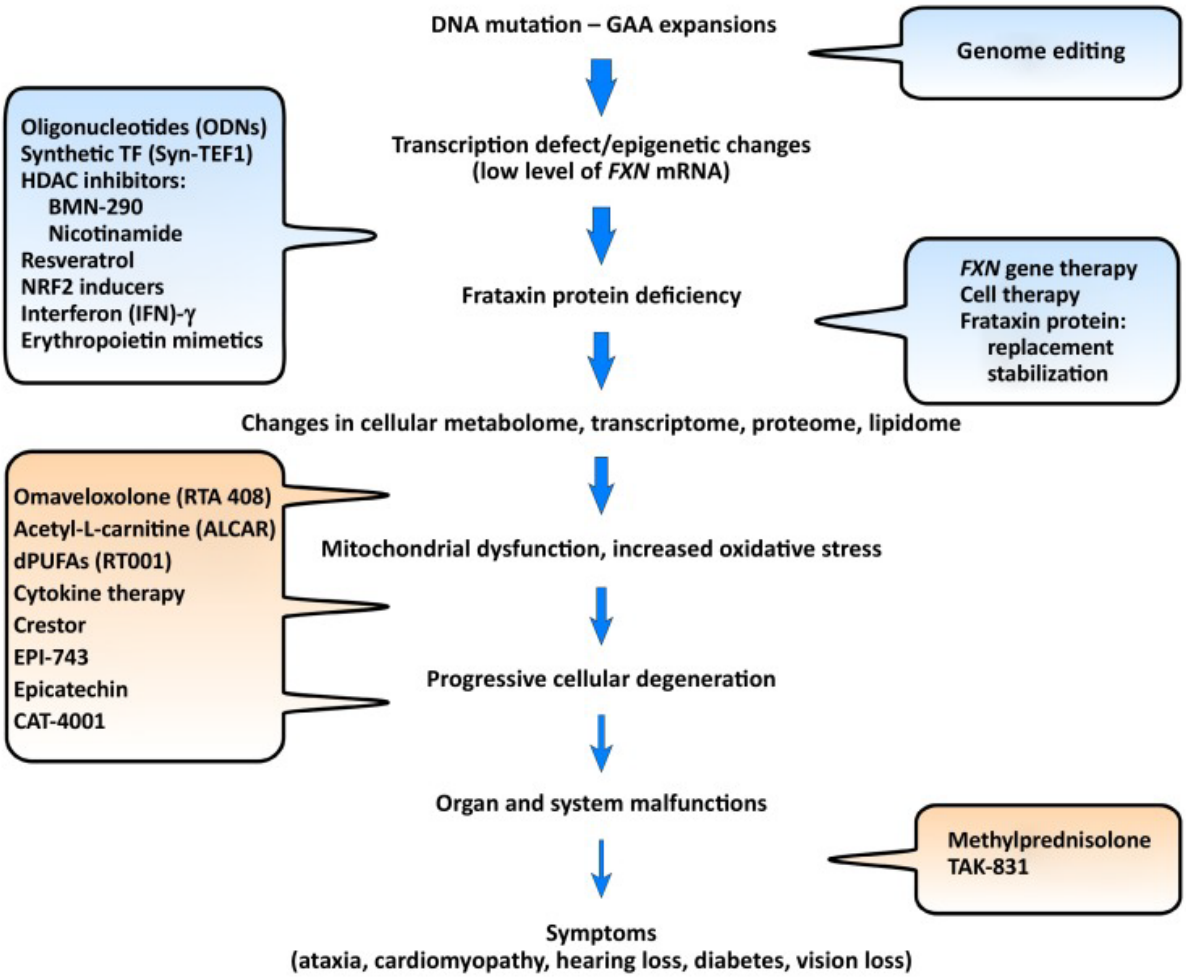

Figure 4 - Diagram showing current situation in FRDA research taken from Zhang et al., 2019

As clearly visible in the picture, many groups tried to improve mitochondrial function or to compensate for frataxin low levels through the use of some drugs capable to modulate its expression or to stabilize the protein itself.

One of the first approaches has been to use antioxidant compounds to ameliorate the symptoms observed in patients due to excessive oxidative damage (vitamin E or coenzyme Q10,

along with various analogs) (Jauslin, Vertuani et al. 2007), but their therapeutic efficacy remains doubtful (Kearney, Orrell et al. 2016).

Another possible strategy is focused on compounds chelating iron, since in FRDA iron is accumulating inside the mitochondria. For this reason, iron-chelating compounds able to enter mitochondria are the most interesting: one of the most studied is Deferiprone, which is also used in thalassemia treatment. The problem with Deferiprone is that leads to secondary effects which can be quite troubling, as pointed out by Dr. Nancy Olivieri whose data suggests that this drug can lead to progressive hepatic fibrosis (Brittenham, Nathan et al. 2003). Even *in vitro* this drug is controversial, since the results obtained vary depending on the cell type used and the concentration, leading to improvements in mitochondrial functions in one case (Kakhlon, Manning et al. 2008) or to impairments in aconitase activity and decreased cell proliferation in another one (Goncalves, Paupe et al. 2008).

Other approaches have tried to improve the impaired mitochondrial function, and the consequent oxidative stress, due to frataxin deficiency by intervening at different cellular events: this is the case of Omaveloxone, a drug stabilizing the transcription factor NF-E2-related factor 2 (NRF2), which is involved in the antioxidant defense response. Omaveloxone inhibits NRF2 ubiquitination, thus keeping it active to counteract the oxidative stress provoked by frataxin low levels (Abeti, Baccaro et al. 2018).

Other groups focused their efforts in trying to resolve the issue entirely, through gene therapy, thus replacing the faulty gene with a correct one (Fleming, Spinoulas et al. 2005; Lim, Palomo et al. 2007), being this one of the most promising approaches. Being FRDA a monogenic disease, the substitution of the gene containing the GAA expansion with a healthy one would rescue the phenotype of the disease (Gomez-Sebastian, Gimenez-Cassina et al. 2007; Lim, Palomo et al. 2007; Perdomini, Belbellaa et al. 2014; Piguet, de Montigny et al. 2018). There are some issues with this kind of approach since, to deliver the gene, the main limitation is the vector for the delivery itself., since viral vectors could provoke safety issues. To overcome these issues, a promising new alternative is represented by the use of synthetic nanoparticles carrying frataxin mRNA. A recent *in vivo* study demonstrated that, after intrathecal injections of these synthetic nanoparticles, frataxin expression was detected massively in dorsal root ganglia (Nabhan, Wood et al. 2016).

Other possible treatments aim to enhance *FXN* gene expression through the use of several compounds that overcome the transcriptional deficit due to heterochromatization. In this group, the Hystone Deacetylase (HDAC) inhibitors can be found. HDAC molecules are able to counteract the huge heterochromatization induced by the GAA expansion, as described earlier, by incrementing the acetylation of hystones, which in turn leads to the DNA being more

accessible by the polymerase, leading to an increment in Fxn levels. The most promising in this class of compounds is the N-phenyl-N'-(2-Aminophenyl) hexamethylenediamide (BML-210), which reverted frataxin gene silencing in primary lymphoblasts of FRDA patients (Herman, Jenssen et al. 2006). The drawback of these class of compounds is that there is no way to specifically direct them on Frataxin gene, so adverse epigenetic effects might occur.

Some studies with recombinant human (rhu)-EPO compounds have pointed at an increment in frataxin protein levels without rising mRNA levels, thus suggesting a post-translational regulatory mechanism of EPO on frataxin (Acquaviva, Castaldo et al. 2008), with the mechanism itself being still not very clear yet. After EPO treatments, frataxin levels seem to be incremented for about 30% and oxidative stress seems to be reduced, but hematocrit problems incurred after the chronic treatment (Boesch, Sturm et al. 2008) and that is precisely why alternative versions of the EPO peptide are gaining interest, lacking the erythropoietic functions in order to avoid undesired effects: this is the case of the carbamylated form of erythropoietin (CEPO), which is unable to bind classical EPO receptor, thus having no erythropoietic effects, but still able to increment frataxin levels in FRDA patient primary lymphocytes (Sturm, Helminger et al. 2010).

Recently, several studies have shown also the potential effect of trophic factors in the regulation of frataxin expression or in the prevention of the negative effects induced by frataxin deficiency, being this yet another therapeutic approach for the disease. Trophic factors have been shown either to upregulate frataxin levels in YG8R transgenic mice (Calatrava-Ferreras, Gonzalo-Gobernado et al. 2016) and, in our group, that the neurodegeneration elicited by frataxin deficiency in a mouse model is significantly reduced when the mice were injected with a viral vector carrying the Brain-Derived Neurotrophic Factor (BDNF) gene (Katsu-Jimenez, Loria et al. 2016).

Another important molecule involved in the regulation of frataxin expression is the peroxisome proliferator-activated receptor gamma (PPARγ), which seems to be a new promising therapeutic approach for the disease. A study using an agonist of PPARγ, Azelaoyl PAF, has shown that the treatment with this agonist is responsible of the direct upregulation of frataxin protein levels and mRNA levels (Marmolino, Acquaviva et al. 2009) and it has been confirmed that both PPARγ and its coactivator PGC-1α are downregulated in FRDA (Coppola, Marmolino et al. 2009), thus opening the way for new avenues for FRDA treatment.

All therapeutic approaches involve some safety concerns, either for the possible toxicity of the drugs used or for the viral vectors related to gene therapy approaches.

Objectives

In this work, we have focused on some aspects about the regulation of frataxin both in cell models and *in vivo*, with the specific aims of:

1. Characterizing the extra mitochondrial Frataxin isoforms.

2. Studying the effects of erythropoietic-derived synthetic peptides on Frataxin expression.

3. Exploring the regulation of Frataxin expression *in vivo* in mouse cerebellum after spontaneous physical exercise.

Materials and methods

1. Cell Cultures

Cell lines **HEK 293T** containing the SV40 Large T-antigen (derived from human embryonic kidney) and **SHSY-5Y** (derived from human neuroblastoma) and were cultivated in Dulbecco's modified Eagle medium (DMEM, Table 1), supplemented with 10% Fetal Bovine Serum (FBS), 2mM L-Glutamine and Streptomycin/Penicillin mix (100 μg/ml, 100 U/ml). All the cell cultures were maintained at 37º with 95% humidity, in an incubator and a list of all media and supplements used is provided in Table 1.

1.1. Olfactory Mesenchymal stem cells

Olfactory mesenchymal stem cells (**OMSCs**) were obtained from voluntary donors both affected with FRDA or healthy. Biopsies were performed at the "*Gregorio Marañon*" Hospital, following the described protocols (Lanza et al., 1993). All the donors signed an informed consent and procedures were approved by the ethics committee of the hospital. OMSCs were plated in plates previously treated with Matrigel for 30 minutes at RT, and then cultivated in DMEM/F12 supplemented with GlutaMAX, Albumax I 0,5% (w/v), 4-(2-hydroxyethyl)-1-piperazineethanesulfonic acid (HEPES) 10mM, glucose 0,6% (w/v), non-essential Amino Acids (NEAA, L-Ala 44mM, L-Asn 45mM, L-Asp 40mM, L-Glu 40mM, L-Pro 30mM), 2% FBS, 1% N2 Supplement, Streptomycin/Penicillin mix (100 μg/ml, 100 U/ml). 8 ng/ml human-recombinant Fibroblast Growth Factor 2 (hrFGF-2) and 50ng/ml Nerve Growth Factor (NGF) were added freshly each time cells were passaged.

1.2. FRDA Fibroblasts

Human fibroblasts taken from FRDA patients and healthy subjects (**GM08402, GM01652, GM08399** known as Ctrl1, Ctrl2 and Ctrl3 in order and **GM0478, GM03816**, **GM03665,** called FRDA1, FRDA2 and FRDA3 respectively, were obtained from Coriell Repository) and cultured in DMEM containing 10% FBS, 0,1mM Non Essential Amino Acids (NEAA) and supplemented with hrFGF-2 10ng/ml and Epidermal Growth Factor (EGF) 10ng/ml following an established protocol (Jauslin, Schoumacher, 2002).

1.3. Primary cultures of mouse cortical neurons

Cortical Neurons were obtained from C57BL/6J mouse fetuses at E17-18, following described protocols (Bartlett & Banker, 1984). The dissection was performed in complete Hank's Balanced Salt Solution (HBSS), after which the resulting cortexes were washed three times in HBSS deprived of Ca and Mg cations. A 15' digestion with HBSS Ca^{2+} Mg^{2+} -/- containing 2,5mg/ml Trypsin and 1mg/ml pancreatic bovine DNAse I was then performed at 37º, mixing every 5'. After the digestion, an accurate serie of washes with HBSS Ca^{2+} Mg^{2+} -/- was carried out to remove traces of trypsin and DNAse. Then, through a mechanical resuspension with a glass Pasteur pipette narrowed with fire, the cortexes were broken apart and the resulting cell suspension was plated on plates previously treated with 500µg/ml poly-L-Lysine in Neurobasal medium supplemented with B27, GlutaMAX I and streptomycin/penicillin mix. Cells were maintained in this medium for at least 3 days before starting the experiments.

2. SHSY-5Y differentiation

Human neuroblastoma cells were differentiated in neuron-like cells following two different protocols, one already tested in our lab (Gimenez-Cassina, Lim et al. 2006) and one recently published (Chiocchetti, Haslinger et al. 2016), which allows for SHSY cells to reach a more "mature" neuron-like phenotype.

2.1. New differentiation protocol

Cells were plated in plated treated with Matrigel at the same density as for the old protocol and maintained for one day in DMEM 10% FBS. The next day the medium is changed for Neurobasal-A supplemented with GlutaMAX I, B27, 10µM Retinoic Acid, 20mM KCl, 2mM Bucladesine (dbcAMP), 50ng/ml BDNF. Cells are cultivated with this medium for 11 days and the medium is changed every 2 days, adding BDNF, dbcAMP and Retinoic acid freshly each time. By the end of the differentiation, the cells were then ready to be used for different experiments.

3. Treatments

During the development of this thesis, many compounds were used and tested at the concentrations and times indicated for each experiment. The compounds were always added dissolved in medium and a control with just the medium used with the drug was always maintained to avoid non-specific results.

Table 2 – List of media and supplements used in cell culture

Product	Commercial Brand
Albumax	Invitrogen, Life Technologies
B27	Invitrogen, Life Technologies
BDNF	Alomone Labs
dbcAMP	Sigma
DMEM	CBMSO Culture Service
DMEM/F12	Gibco, Life Technologies
DNAse I	Roche
EGF	Sigma
FBS	Invitrogen, Life Technologies
Glucose	Sigma
GlutaMAX	Invitrogen, Life Technologies
HBSS Ca^{2+} Mg^{2+} -/-	Gibco, Life Technologies
HBSS Ca^{2+} Mg^{2+} +/+	Gibco, Life Technologies
HEPES	CBMSO Culture Service
hrFGF-2	PeproTech
L-Glutamine	CBMSO Culture Service
Matrigel	BD Biosciences
NEAA	CBMSO Culture Service

Neurobasal	Gibco, Life Technologies
NGF	Sigma
Retinoic Acid	Sigma
Streptomycin/Penicillin Mix	CBMSO Culture Service
Trypsin	Sigma

4. Animal models

4.1. C57BL/6 and YG8r mice

All the work with mice employed for the experiments has been done following strictly the current regulations established by the Bioethics committee of the Autonomous University of Madrid. Two strains have been used: wild type C57BL6/J and a contracted human FXN transgenic mouse model with murine Frataxin knockout called YG8r. The mice were maintained in the animal facility of the CBMSO with proper light/dark cycles of 12hours each and at a constant temperature of 20º C. Food and water have been administered freely to the animals while the experiments were conducted.

For the *in vivo* assays, C57BL6/J mice were intraperitoneally injected with 500µl NaCl 0,9% with or without compounds. The injections have been performed by the animal facility staff with a 0,3mm needle. For the genotyping process of the YG8r mice, DNA was extracted from the tail of the animal following standard protocols and then a PCR has been performed to determine the genotype: for the $Fxn^{-/-}$ genotype, a common forward primer (P3: *5'-TGTTTACCATGGCTGAGATCTC-3'*) was used along a primer specific for the wild type allele (MOF: *5'-AACGTTACTCTTAGGGTCAG-3'*) or one specific for the KO allele (P2-Neo: *5-CGCCTCCCCTACCCGGTAGAATTC-3'*), giving a PCR product of, respectively, 350bp and 240bp, visualized in a 2% agarose gel in TAE buffer (containing Tris base, acetic acid and EDTA). The PCR reaction was set up with the GoTaq G2 Flexi DNA Polymerase (Promega) supplemented with 5% DMSO, 25mM $MgCl_2$, 10mM dNTPs and 0,4uM of the primers. Reaction conditions are described in the following table. For the FXN knock-in two primers amplifying the left and right tail of the yeast artificial chromosome (YAC) containing human FXN transgene were used.

Table 3 – Genotyping PCR conditions

Temperature	Time	Process	
94º	2 minutes	Activation	
94º	20 seconds	Denaturation	35 cycles
54º	20 seconds	Annealing	35 cycles
72º	20 seconds	Elongation	35 cycles
72º	7 minutes	Final elongation	

Furthermore, for the mice to reach pathological levels of human frataxin expression, fxn allele needs to be in hemizygosity, so qPCRs were needed to determine copy number. Different concentrations of DNA (5ng and 10ng) were tested by qPCR using the following primers for frataxin and a housekeeping of our choice:

- Fxn Forward: *5'-CCCCTGATTTGCTGTATGCT-3'*
- Fxn Reverse: *5'-CTCAAGGTCTCCGGACTTG-3'*
- GAPDH Forward: *5'-CCCCTGGCCAAGGTCATCCATG-3'*
- GAPDH Reverse: *5'-CAGTGAGCTTCCCGTTCAGCTC-3'*

The reaction was set up with the "Fast SYBR-Green Master Mix" (Applied Biosystem), containing both the enzyme and the fluorescent dye, using the ABI PRISM 7900HT Fast. The results were analyzed by measuring fluorescence given by the intercalating agent SYBR-green, which is directly proportional to the amount of product generated though the cycles. We used the following conditions:

1. Stage 1⟶ 20'', 95º C
2. Stage 2⟶ 1'', 95ºC – 20'', 60º C (40 repeats)
3. Stage 3⟶ 15'', 95ºC – 15'', 60ºC – 15'', 95ºC

Dissociation curves of the analyzed DNA samples were studied in order to prove that no no-specific product was obtained. Cycle quantification numbers (Ct) were analyzed to determine frataxin allele copy number and, thus, the genotype of YG8r mice.

4.2. Protocol to monitor physical exercise in mice

All the work regarding the impact of physical exercise in mouse cerebellum has been done on a C57BL6/J strain at the Department of Physiology and Pharmacology (FYFA) of Karolinska Institutet (Stockholm, Sweden). All studies were performed with approval from the regional animal ethics committee of Northern Stockholm, Sweden (granted to Dr. Jorge L. Ruas), according to institutional and European guidelines for animal handling and research. All efforts were made to minimize the number and suffering of used animals. The protocol lasted 8 weeks, where the mice were subjected to spontaneous physical activity being able to mount, at discretion, on a treadmill connected to a laptop measuring the meters corresponding to the amount of exercise, except those used as control, which were not provided with any treadmill in their cages. After eight weeks all mice were sacrificed, and the cerebella were extracted to proceed with further analysis.

5. Plasmid obtention, Viral production and titration

5.1. Obtention of plasmids encoding for FXN isoforms

The plasmid containing the cDNA for human frataxin was a kind gift of Dr Alexander and Dr Fleming (Fleming, Spinoulas et al. 2005) and is the one referred as pLv-Frat (or pLv-IsoI). The plasmids encoding for the cDNA of the different isoforms of frataxin were obtained, during this work, from the backbone of the pLv-Frat. The original plasmids containing cDNA for the isoforms (PET-II and PET-III) were a kind gift from Dr Xia and Dr Li (Xia, Cao et al. 2012). Since the only difference between the isoforms is in the first exon, we decided to clone and substitute the first exon of Iso II and Iso III contained in the PET plasmids donated by Xia et al in the pLv Frat previously used in the lab. To achieve this, we cut pLv-Frat with *XbaI* and *BclI*, which removes the first exon leaving the rest of the plasmid intact. The band containing the DNA was cut from the gel and purified with the Qiagen QIAquick Gel Extraction Kit. PET-II and PET-III were partially digested with *XbaI* and *BclI* since the cDNAs of isoforms contained a *XbaI* sequence inside that needed to be left intact. Bands corresponding to the first exon of Iso II and Iso III were purified with the same kit described before. We then proceeded with the ligation between inserts and vector, respecting the molar ratio between them to ensure a proper ligation process. The resulting products were sequenced and aligned to ensure that no errors were done during the whole process. An E. coli bacterial strain (Stbl3) were then transformed and the colonies were checked by through a Mini Kit (Wizard Plus SV Minipreps DNA Purification System, Promega) before proceeding with the amplification of the plasmidic DNA through a Maxi system (Qiagen).

5.2. HIV-1 derived lentiviral vectors production

Three plasmids were used in the lentiviral vector production (2nd generation):

- Packaging plasmid **pCMV dR8.74** (5 µg) containing the viral genes *gag*, *rev*, *pol* and *tat* mandatory for producing viral particles
- Envelope plasmid **pMD2.G** (2 µg) containing the *env* gene needed to pseudotype viral vectors with VSV-G protein
- Plasmid containing the **gene of interest** (5 µg), described in table 2

Table 4 – Plasmids used in lentiviral packaging and diagram showing them

Product	Commercial Brand
MISSION pLK0.1 shRNA37	Sigma
pRRL hCMV/eGFP WPRE	Naldini lab
pLVFRAT (or pLV-IsoI)	Fleming and Alexander
pLV-IsoII	This thesis
pLV-IsoIII	This thesis

These plasmids were added to 293T cells cultivated in p100 plates at 80% confluence along with the transfecting reagent, Lipotransfectin (Solmeglas), following manufacturer instructions. After 48 h post transfection, the supernatant was taken and filtered with a low-binding 0.45 µm filter, aliquoted and stored at -80ºC until further use.

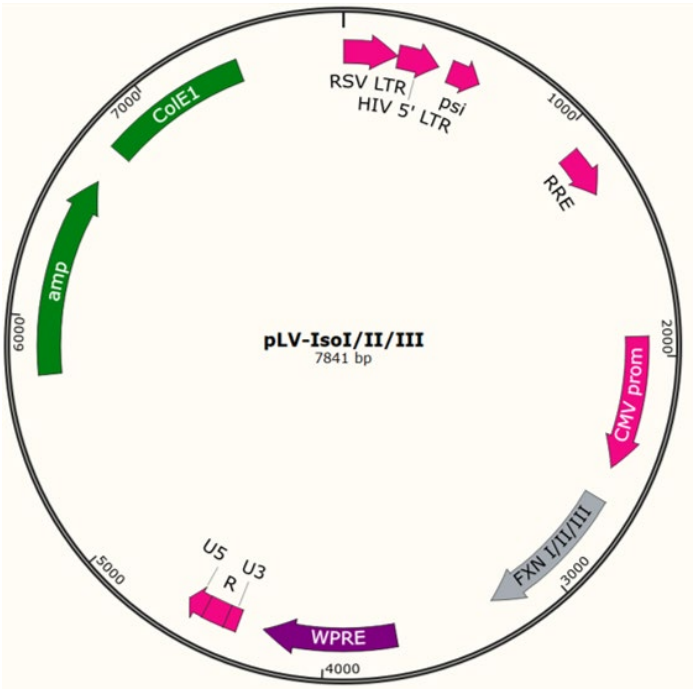

5.3. Titration and transduction of target cells

Virus expressing the green fluorescent protein (GFP) were titrated by cytometry: 293T cells were plated in M6 plates (200.000/w) and then infected with different amount of virus. After 48 h cells were suspended in a fix buffer (Phosphate Saline Buffer (PBS), 2% FBS, 1% paraformaldehyde (PFA)) and analyzed at the cytometer (FACSCalibur), calculating the percentage of GFP positive cells in 10000 events in order to estimate the viral titration of the starting aliquot. Since the whole process was done in parallel for GFP or other genes of interest, we approximated that the titer obtained for GFP was the same as the other genes. To realize the experimental procedures, a multiplicity of infection (MOI) of 5-10 was used depending on cell type, with the general guidance that minimum of 70-80% of the cells had to be transfected. When appropriate, an extra control of the transduction was used to remove any non-specific effects.

6. Analysis of Protein Extracts

6.1. Western Blot

Two different buffers were used considering the starting samples: cells or organs. Cells, after removing the medium and washing with ice cold PBS, were frozen at -80º for at least 24 h. Following this step, cells were lysed with a cell scraper on ice with a buffer containing:

- HEPES 20 mM pH 7,4
- Sodium Chloride (NaCl) 100 mM
- Sodium Fluoride (NaF) 100 mM
- Sodium Orthovanadate ($NaVO_4$) 1 mM
- EDTA pH8 5 mM
- Triton X-100 1%
- Okadaic acid 1 µM
- Protease Inhibitor Cocktail (Roche, cOmplete)

For tissue extracts, the buffer used was a RIPA containing:

- Tris HCl 25mM pH 7,6
- NaCl 150mM
- NP-40 1%
- Sodium Deoxycholate 1%
- SDS 0,1%
- Protease Inhibitor Cocktail (Roche, cOmplete)

Protein concentration, in both cases, was determined through Bradford assay following manufacturer instructions (BioRad) and read at a wavelength of 630 nm. After quantifying protein concentration, samples were mixed with loading buffer containing sodium dodecyl sulfate (SDS), boiled for 5 minutes and separated through polyacrylamide gel electrophoresis run in 15% acrylamide-bis-acrylamide gels or in 4-12% bis-tris plus gels (Invitrogen). The 15% gels were run in a Tris-Glycine buffer containing 10% SDS, while for the 4-12% we used the commercial buffer suggested by the manufacturer (MES Buffer, Invitrogen). Proteins were transferred on a nitrocellulose membrane (iBlot 2 NC Stack, Invitrogen) through the use of iBlot2 transfer device and then blocked with a 5-10% milk powder solution dissolved in PBS-Tween 20 0,2%. Blocked membranes were incubated overnight with the primary antibody (described in Table 3, following the suggested dilutions indicated by the datasheets) diluted in blocking solution at the concentration recommended by the manufacturer; after the primary antibody incubation, membranes were washed 3 times for 5' each with PBS-T and then incubated with the Horse Radish Peroxidase (HRP)-conjugated secondary antibody of the appropriated host for 1h at room temperature following manufacturer instructions (Southern BioTech). After this, membranes were washed 3 times for 5' each with PBS and then incubated 1' with an Enhanced ChemiLuminescence (ECL) solution. The data were analyzed either by a Kodak X-Omat 2000 processor or by the biomolecular imager ImageQuant LAS 4000 Mini (GE Healthcare). The resulting densitometry data were normalized for a control antibody versus a housekeeping protein (β-actin, GAPDH, β-Tubulin) in order to reduce the variation derived from the difference between loaded samples. The following table contains a list of the antibodies used in this work.

Table 5 - List of antibodies used in western blots

Product	Dilution	Commercial Brand
Aconitase 1	1:1000	Abcam (#ab126595)
Aconitase 2	1:1000	Abcam (#ab71440)
Frataxin	1:1000	Abcam (#ab110328)
Frataxin	1:500	Merck (#ab15080)
Frataxin (H-155)	1:1000	Santa Cruz (#sc-25820)
GAPDH	1:2000	Abcam (#AB8245)

IscU1/2 (D-6)	1:500	Santa Cruz (#sc-373694)
Lamin B1 (S-20)	1:1000	Santa Cruz (#sc-30264)
NDUFS3	1:1000	Thermo Fisher (#PA5-29747)
VDAC	1:1000	Abcam (#ab14734)
β -Tubulin	1:5000	Sigma (#T4026)

6.2.Cell Fractionation

To separate different cellular compartments before analyze protein expression, a commercial kit available from MitoSciences was used (Cell Fractionation Kit Standard, #MS861, (Chattaragada, Riganti et al. 2018; Paredes, Sheldon et al. 2018). Cells were plated and grown until semi-confluence. Cells then were trypsinized and centrifuged along with their supernatant. The resulting pellet was resuspended in the buffer A provided with the kit to have cells at a concentration of $6{,}6x10^6$ cells/ml. This volume of cells in buffer A was mixed with an identical volume of buffer B, containing a special detergent able to break cell membranes and then centrifuged at 10000g. The resulting supernatant contained the cytosolic fractions. The pellets were resuspended in buffer A to be then mixed with buffer C, containing another detergent and then centrifuged at 10000g again. The supernatants, containing the mitochondrial fractions, were isolated and the pellets, composed by the nuclear fractions, were resuspended in buffer A. The samples were then added 5x SDS-containing loading buffer and boiled at 100º for 5'.

7. Immunocytochemistry

Cells for immunocytochemistry analysis were cultivated on glass coverslips at the optimal density depending on cell type. These cells were subjected to a sequential 4% PFA in PBS fixation protocol or an ice-cold methanol fixation protocol lasting 15' at room temperature (RT)for PFA or at -20º C for methanol. After this procedure, the cells were washed 3 times with PBS and blocked for 1h at RT with a PBS solution containing 1% Bovine Serum Albumin (BSA) and 0,1% Triton-X 100. After the blocking, cells were incubated with the primary antibody diluted in blocking solution at the concentration suggested by the datasheet for 2h at RT or, alternatively, O/N at 4ºC. After the primary antibody incubation, the coverslips were washed 3 times with PBS and then incubated with the secondary antibody (conjugated with Alexa-488, Alexa-555, Alexa-647) for 1h at RT, in darkness, and then washed again 3 times with PBS and then incubated with the nuclear counterstain DAPI (4', 6-Diamidine-2'-phenylindole dihydrochloride) at the

concentration of 1 µg/ml for 10'. After this, the coverslips were mounted with the aqueous-based mounting medium Fluoromount-G (Southern Biotech) and analyzed at the *Zeiss Axiovert 200* or at the *LSM710* confocal scanning microscopes.

Table 6 - List of antibodies used in immunocytochemistry

Product	Dilution	Commercial Brand
Frataxin	1:200	Abcam (#ab110328)
Frataxin (H-155)	1:200	Santa Cruz (#sc-25820)
GFP	1:200	Roche
p-53	1:100	BD Pharmingen (#556534)
β-III Tubulin	1:500	Sigma (#T4026)

8. Aconitase assays

Aconitase activity was measured with two different methods, one qualitative (in-gel) and one more quantitative (microplate):

8.1. *In gel* assay for Aconitase Enzyme Activity

This assay allows to visualize directly in the gel aconitase activity. The protocol was adapted from a published one (Shulman, Belakhov et al. 2014). Cells were harvested from plate with a lysis buffer containing:

- KCl 40 mM
- Tris-HCl 25 mM pH 7,5
- Triton X-100 1%
- 4-(2-aminoethyl)benzenesulfonyl fluoride hydrochloride (AEBSF) 0,21 mM
- Dithiothreitol (DTT) 1 mM
- Sodium citrate 2 mM
- $MnCl_2$ 0,6 mM
- Protease Inhibitor Cocktail (Roche)

After a brief centrifugation at 13.000 rpm for 5' at 4º, the supernatant was used to quantify protein concentration by a Bradford assay. Once proteins were quantified, loading buffer 4x (Tris-HCl 10 mM ph8, Glycerol 34,8%, Bromophenol blue 0,1%) was added.

Samples were separated through an electrophoresis in native conditions at 4º in a 4-8% acrylamide gel prepared with borate buffer and sodium citrate. The electrophoresis was run at 4º at 170V for 2-2,5 h with a running buffer containing Tris-Glycine and sodium citrate 3,6 mM.

Once the electrophoresis was over, the gel was incubated in a staining solution for 30-60 minutes at 37º in darkness.

The staining solution is made of:

- Tris 100 mM
- Nicotinamide adenine dinucleotide phosphate (NADP) 1 mM
- Cis-Aconitate 2,5 mM
- $MgCl_2$ 5 mM
- 3-(4,5-Dimethylthiazol-2-Yl)-2,5-Diphenyltetrazolium Bromide (MTT) 1,2 mM
- Phenazine Methosulfate (PMS) 0,3 mM
- IDH (Isocitrate Dehydrogenase) 5U/ml

After the staining, the gel was washed with deionized water for 5min for approximately 3 times and then bands were visualized and scanned.

8.2. Microplate assay for Aconitase Enzyme Activity

For this assay, the commercial kit Aconitase Activity Assay Kit #ab109712 available from Abcam was used (Kauppila, Bonekamp et al. 2018; Vannocci, Notario Manzano et al. 2018). This kit allows to determine the amount of total aconitase activity from tissue or cultured cells by monitoring the formation of cis-aconitate, proportional to aconitase activity. The protocol was adapted and scaled down for our OMSc cell type. Results are expressed as the variation of absorbance per minute measured at 240nm in fixed time interval, compared to control group. At least five points for experimental condition were analyzed in at least three independent experiments.

9. Enzyme-linked Immunosorbent assay (ELISA)

The levels of Frataxin, BDNF and NT-3 in different experiments were evaluated through commercial immunosorbent assay kits available from different providers.

For our experiments, we used the #ab199078 and #ab176112 from Abcam (Kemp, Cerminara et al. 2017; Khdour, Bandyopadhyay et al. 2018) to measure frataxin levels in mouse and human, respectively; the #CYT306 (Merck) for BDNF and the #LS-F5159 (LS-Bio) for Neurotrophin 3. In each case, the protocol from the manufacturer was strictly followed. The procedure, in all cases, involved a M96 plate pre-coated with the antibody against the selected protein (frataxin, BDNF or NT-3) to which samples are added. After this, a mix of secondary antibodies conjugated to streptavidin-HRP. These are used for the oxidation of 3,3', 5,5' – tetramethylbenzidine (TMB), which product can be detected at a wavelength of 450 nm. The values for the samples were interpolated from a standard curve prepared with known concentrations of the sample protein (frataxin, BDNF, NT-3), depending on the kit used.

10. RT-PCR

In order to search for gene expression changes, reverse transcription-polymerase chain reaction (rt-PCR) analysis were performed. First, RNA was isolated from tissue (cerebellum) using a *Direct-zol RNA kit* (Zymo Research) following manufacturer instructions. Yield and purity of the obtained RNA was measured through a *Nanodrop* spectrophotometer. The RNA (1 µg in 20 µl) was reverse transcribed into cDNA (50 ng/µl final concentration) using the *Maxima First Strand cDNA Synthesis Kit for rt-qPCR* (Thermo Fisher Scientific). The qPCR was performed starting from 10 ng of cDNA with the *Luminaris Color HiGreen qPCR Master Mix* (Thermo Fisher) with 600 nM primers and using the *PikoReal Real-Time PCR System* (Thermo Fisher) with the following cycling conditions: 50ºC for 120s, 95ºC for 120s, 40 cycles of 95ºC for 15s + 55ºC for 60s and 60º for 30s. The expression ratio was calculated using the $^{\Delta\Delta}$CT method. To normalize data, β-Actin expression was used to obtain relative expression values with the comparative Ct method. Specificity of the PCR reaction was validated by melting curve analysis. For all the experiments, primers were designed to span from intron-exon boundaries. Results are expressed as fold-change between control and samples group. In the following table, a list of the primers used can be found.

Table 7 - List of primers used in RT-qPCR

Primer	Sequence
Actin Forward	*5'-AACTCCATCATGAAGTGTGACG-3'*
Actin Reverse	*5'-GATCCACATCTGCTGGAAGG-3'*
BDNF Forward	*5'-TGGCCCTGCGGAGGCTAAGT-3'*
BDNF Reverse	*5'-AGGGTGCTTCCGAGCCTTCCT-3'*
CSF3 Forward	*5'-AGTCCCTGGAGCAAGTGAGG-3'*
CSF3 Reverse	*5'-AGAGCCTGCAGGAGACCTTG-3'*
Frataxin Forward	*5'-CCTGGCCGAGTTCTTTGAAG-3'*
Frataxin Reverse	*5'- GCCAGATTTGCTTGTTTGG-3'*
Interferon-γ Forward	*5'-GCTTTGCAGCTCTTCCTCA-3'*
Interferon-γ Reverse	*5'-CTTTTGCCAGTTCCTCCAG-3'*
Interleukin 6 Forward	*5'-TAGCTACCTGGAGTACATGAACA-3'*
Interleukin 6 Reverse	*5'-TGGTCCTTAGCCACTCCTTCT-3'*
MIP-1α Forward	*5'-AAGATTCCACGCCAATTCATC-3'*
MIP-1α Reverse	*5'-CAGGCATTCAGTTCCAGGTCAGT-3'*
Neurotrophin 3 Forward	*5'-CCGGTGGTAGCCAATAGAACC-3'*
Neurotrophin 3 Reverse	*5'-GCTGAGGACTTGTCGGTCAC-3'*
Sonic Hedgehog Reverse	*5'-GGGACGTAAGTCCTTCACCA-3'*
Sonic Hedgehog Forward	*5'-TTCTGTGAAAGCAGAGAACTCC-3'*

11. Cytokine Array

To search for possible candidates in the study of the regulation of frataxin gene expression after physical exercise, we decided to perform two cytokine array tests, the *Mouse Neuro Discovery Array* and the *Mouse Cytokine Array C1* (both from RayBiotech), able to detect simultaneously a wide range of 37 cytokines. The procedure consists in incubating 50-100 µg tissue protein extracts on a membrane pre-printed with antibodies directed versus the selected cytokines. All the incubations steps were done overnight at 4º with gentle shaking, as suggested by the protocol, to obtain a stronger signal. Results were analyzed with *ImageQuant 8.1* (GE Healthcare) software and results are expressed as fold changes between groups.

12. Cellular Bioenergetic analysis

Mitochondrial respiration was analyzed through the SeaHorse XF24 Extracellular Flux Analyzer (Agilent) with a protocol adapted from Dr, Ribeiro and Dr. Giménez-Cassina (Ribeiro, Gimenez-Cassina et al. 2015), measuring the oxygen consumption rate (OCR) per minute in cell cultures subjected to different modulators of respiration: 0,5 µM oligomycin, 0,75 µM Carbonyl cyanide 4-(trifluoromethoxy) phenylhydrazone (FCCP) and 4µM antimycin A, for OMScs and FRDA fibroblasts, while for cortical neurons, FCCP 0,25 µM was used. OMScs were plated at a density of $2{,}5x10^4$/well in 150 µl of CSC medium, while neurons were plated at a density of $1{,}5x10^5$ in 100 µl of NB-B27. For the experiments, the medium was changed to a special DMEM without Glucose, Pyruvate and sodium bicarbonate $NaHCO_3$ to which the nutrients to be consumed in the assay are added: Pyruvate 1 mM and Glucose 5 mM. OCR values are used to calculate different parameters of mitochondrial respiration, including basal respiratory capacity, maximal respiratory capacity, store respiratory capacity, proton leak and ATP-coupled respiration.

13. Statistical Analysis

As described in the figures, data were represented as mean ± SEM of at least three independent experiments from independent samples. When it was not possible reproduce the experiment three times, data were represented as mean ± SD. For the statistical analysis, GraphPad™ program was used and the most appropriate statistical test was used with the most appropriate correction, always indicated in figure legends. Statistical significance obtained after the analysis performed by the program, was indicated for the results that obtained a *p value* inferior at least to 0.05.

Results

1. Characterization of Extramitochondrial Frataxin Isoforms

With the aim of characterizing the functional relevance of the novel extramitochondrial FXN isoforms described by Xia et al. (Xia, Cao et al. 2012), we built lentiviral (LV) vectors carrying the cDNA encoding for FXN I, II and III. As a cell model we used OMSCs derived from both healthy subjects (henceforth C3c) and FRDA patients (AF6) and frataxin levels were then analyzed and quantified (Fig. 5).

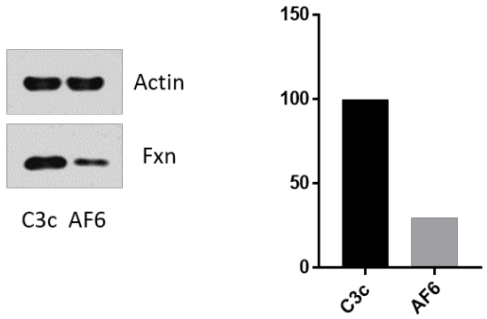

Figure 5 - OMScs cellular model obtention and frataxin levels quantification. Frataxin levels in healthy and patient OMSCs with relative quantification after densitometric analysis, where patients possess ~30% of fxn when compared to healthy controls (n=1).

1.1. Subcellular localization of Isoform I, II and III in OMSc patient cells

To confirm Xia et al claims about the different cellular compartments in which isoforms are present, we decided to perform a subcellular fractionation in OMSc patient cells after having transduced them with the Lv-Iso I, Lv-Iso II and Lv-Iso III for 48h. Compartment markers were used in order to prove that they were separated properly. Lamin B1 as nuclear marker, ATP Synthase (Complex V) for mitochondria and β-Tubulin as the cytosolic one (Fig. 6).

Due to the strong expression of frataxin obtained after lentiviral transduction with LV-Iso I, some frataxin contamination can be seen in the nuclear compartment of the picture in panel A, while no housekeeping contamination can be detected.

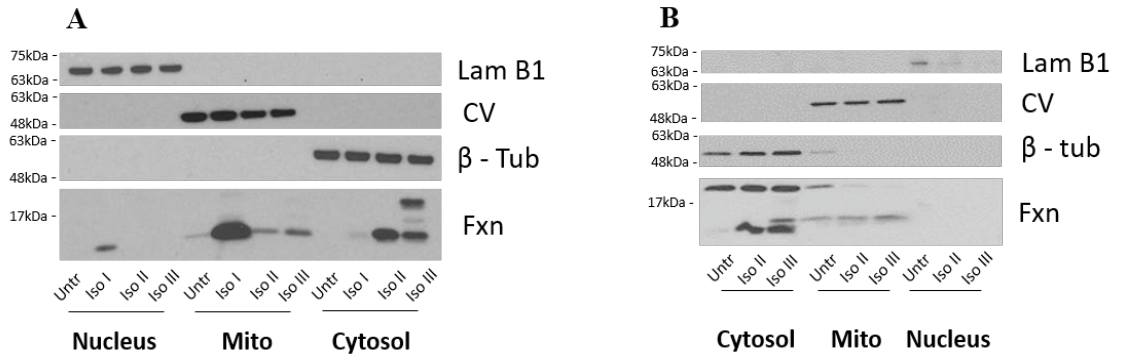

Figure 6 - Cellular Subfractionation of Olfactory Mesenchymal Stem Cells. Cells from FRDA patient were transduced for 48h before the fractionation was performed with the protocol described previously in this thesis. The transduction was performed either with the lentivirus carrying the sequence of canonical frataxin (Iso I), or the different isoforms Iso II and III All results are in comparison with the Untreated condition (Untr). **A)** OMSC patient cells in which nuclear and mitochondrial compartment are clearly separated. Frataxin Isoform I is detected in mitochondria and Isoform II and III are detected in cytosol. **B)** Western blot showing OMSC patient cells results just for isoform II and. Frataxin isoform pattern is clear, with Iso II and III expressing themselves in cytosolic compartment. No nuclear frataxin can be detected.

Thus, we were able to confirm the cytosolic localization for isoform II in OMSc patient cells, along with the difference in molecular weight when compared to canonical Isoform I; but we did not confirm that Iso III is present in nucleus, in contrast to the previous results from Xia et al. (Xia, Cao et al. 2012). To have a better understanding about isoforms localization, we decided to perform immunocytochemistry experiments in OMSc patient cells (Fig. 7).

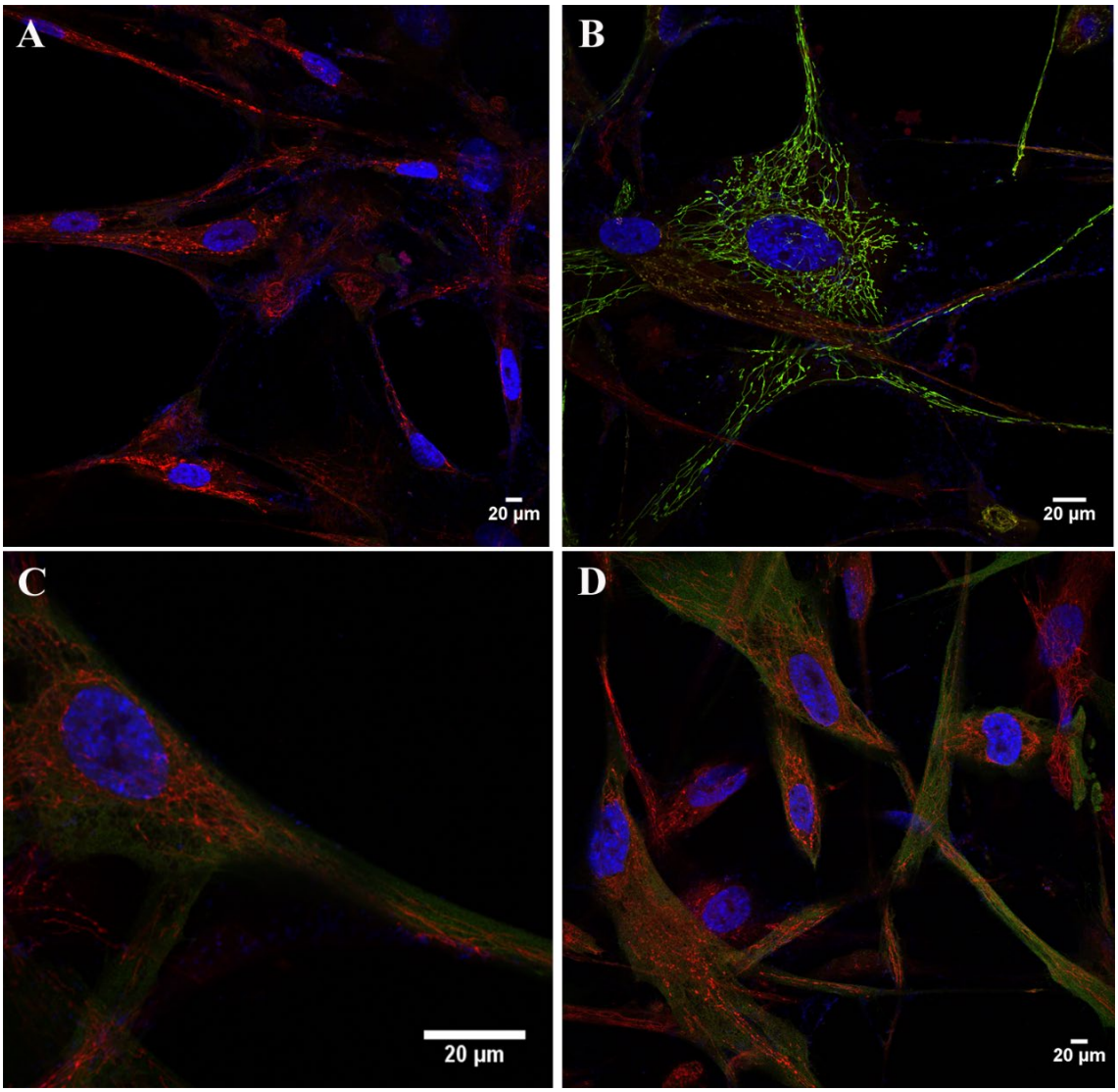

Figure 7 - Immunocytochemistry of OMSC patient cells transduced with Lv enconding for Fxn Isoforms. Cells were stained against anti-frataxin H155 antibody (green), while mitochondria were stained with Mitotracker Red and DAPI (blue) was used to stain nuclei. **A)** Untransduced OMSc patient cells with very low endogenous frataxin levels (40x). **B)** OMSc patient cells transduced with canonical frataxin isoform I (100x). **C)** OMSc patient cells transduced with lentiviral expressing cytosolic Isoform II (100x). **D)** OMSc patient cells transduced with Isoform III (40x).

As the picture shows, canonical isoform I co-localizes clearly with the mitochondrial network of the cells, while isoform II show a cytosolic pattern. We did not detect isoform III in the nucleus of the cells, as described by Xia et al (Xia, Cao et al. 2012). For this reason, we decided to perform another immunocytochemistry experiment analyzing the samples at the confocal microscope, which allowed us to perform a "z-stack" in order to check for presence of Isoform III in different planes of the nucleus (Fig. 8 – A). Furthermore, in the chance that Isoform III was somehow exported out of the nucleus during the process, we decided to treat the cells with Leptomycin B 100 nM (Fig. 8 – B). Leptomycin B allows to inhibit nuclear exporting by blocking Exportin 1, thus blocking the translocation of proteins from the nucleus to the cytoplasm (Kudo, Matsumori et al. 1999).

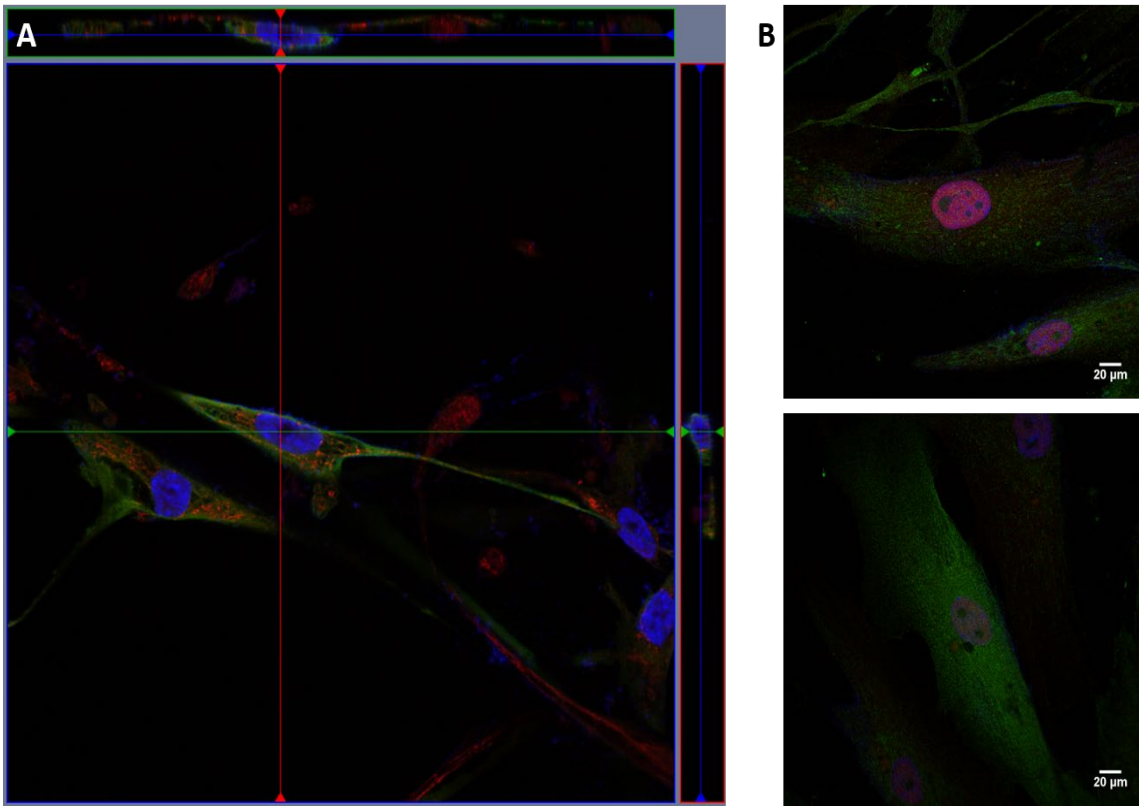

Figure 8 - Immunocytochemestry in OMScs transduced with Iso III. **A)** Z-stack of cells stained against Frataxin (green), Mitotracker (red) and DAPI (blue). **B)** OMSCs transduced with Lv-IsoIII and treated with 100nm Leptomycin B. Cells stained against Frataxin (green), p53 (Red) and DAPI (blue) (40x).

After treating cells with Leptomycin B, we can see that p53 (shown in red) present in the nucleus, while Isoform III is still present in the cytoplasm of the cells, meaning that it is not exported from the nucleus to the cytosol, but that it was never in it. To check if Isoform II could possibly be located in the nucleus before being translocated to cytosol, we decided to perform the same Leptomycin experiment after transducing cells with Lv-Iso II (Fig. 9)

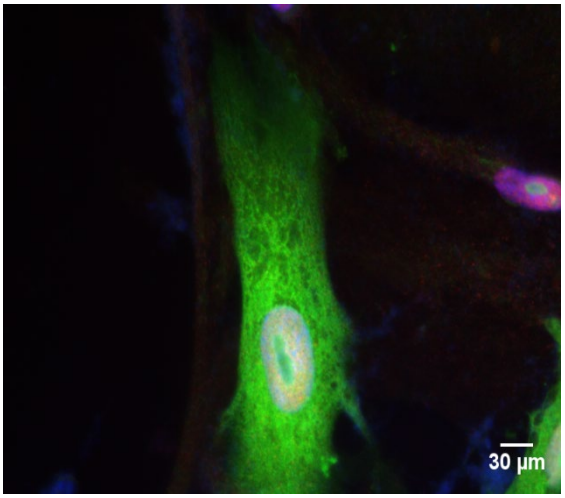

Figure 9 - OMScs patient cells transduced with Lv-IsoII treated with Leptomycin B. Stained against frataxin (green), p53 (red) and DAPI (blue) (63x).

The results from this experiment clearly clarify that isoform II is strictly cytosolic and it does not seem to be present in the nucleus. In view of the lack of confirmation of the nuclear localization of FXN III, as previously reported by

Xia et al. (Xia, Cao et al. 2012), we decided to focus our work on the canonical mitochondrial FXN I and the cytosolic FXN II isoforms.

1.2. Subcellular localization of isoforms I and II in primary cultures of mouse cortical neurons

We wanted to check if what we observed in human OMSc patient cells was also valid in neurons, for this reason we performed a subcellular fractionation of mouse cortical neurons transduced with lentivectors carrying Iso I and Iso II, performing also an immunocytochemistry (Fig. 10 – A, B, C, D).

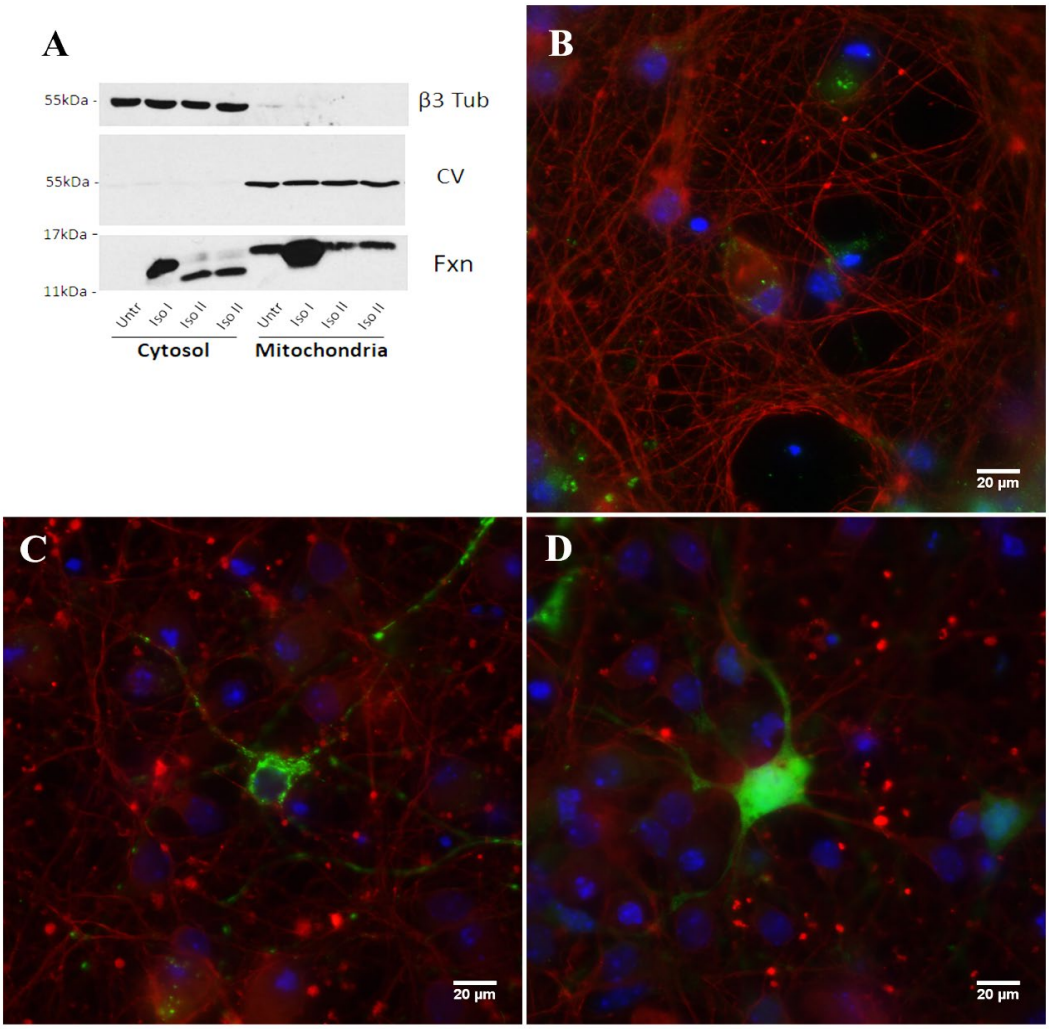

Figure 10 - Isoform I and II in E16 cortical neurons. **A)** Subcellular fractionation of E16 neurons. β3 Tubulin was used as cytosolic marker and ATP synthase for mitochondria. Isoform I cytosolic contamination is present due to its high expression. **B)** Untreated cortical neurons stained against frataxin (green), β3-tubulin (red) and DAPI (blue) (40x). **C)** Cortical neurons transduced with Lv-Iso I (40x). **D)** Cortical neurons transduced with Lv-Iso II (40x).

The results show that the same conclusion can be drawn for cortical neurons. The presence of canonical frataxin in the cytosol in the western blot is due to the high fxn expression achieved after the transduction with the lentiviral vector, which allows for an easy contamination, even though we did not detect Complex V (CV) signal in the cytosolic compartment. Another possible interpretation is that this strong cytosolic signal could be due to an alternative processing of the overexpressed FXN I precursor to the mature form.

1.3. Time-course of Isoform I/II transduction

Once we confirmed the results described by Xia, at least for isoform II, we decided to study how isoforms are expressed in cells over time after lentiviral transduction. For that reason, we decided to check in both models of OMSCs, the healthy and patient ones, to determine the appropriate time for future experiments (Fig. 11 A-B). As showed in Fig. 5 in panel B, patient cells express endogenously low levels of frataxin protein, around ~20-30% of the levels expressed in healthy subject cells, which are the levels we consider to be pathologic since the cells come directly from patients.

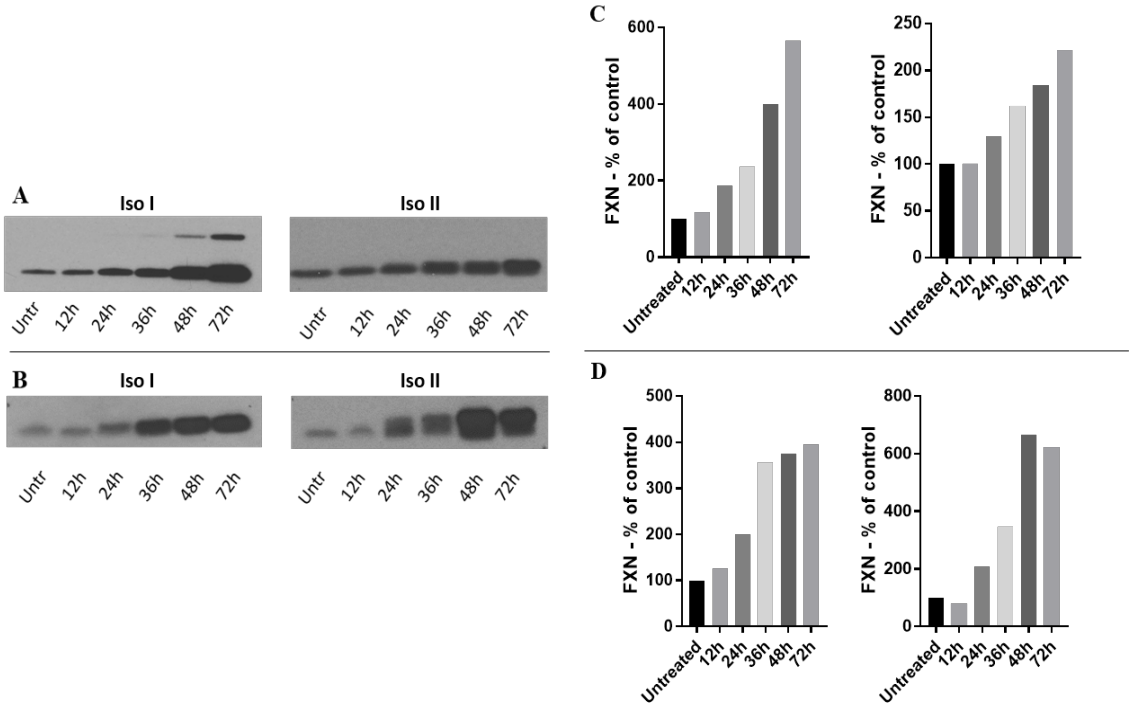

Figure 11 - Frataxin levels in OMSCs. **A)** Time-course after transduction with Lv-IsoI (left) and Lv-IsoII (right) in healthy OMScs. **B)** Time-course after transduction with Lv-IsoI (left) and Lv-IsoII (right) in patient OMScs. **C)** Relative quantification of Frataxin overexpression with Lv-IsoI (left) and Lv-IsoII (right) in healthy OMScs. **D)** Relative quantification of Frataxin overexpression with Lv-IsoI (left) and Lv-IsoII (right) in patient OMScs.

Based on the results of our time-courses, we decided to use 48 h as a final time point for our future experiments, where frataxin is able to reach, in the case of healthy OMSc cells, around 200% of basal levels.

1.4. Mitochondrial network analysis in patient cells overexpressing frataxin isoforms

Since, as it has been described in the introduction, we know frataxin plays a crucial role in maintaining mitochondria proper homeostasis, we wanted to check if the expression of isoform I and II could affect the mitochondrial network of the cell, focusing on their structure, networks, branches and length of the branches. For this reason, we decided to transduce OMSc patient cells with Lv-IsoI and II and then stain mitochondria with mitotracker red (1 μM, 30') (Fig. 12 A-B-C).

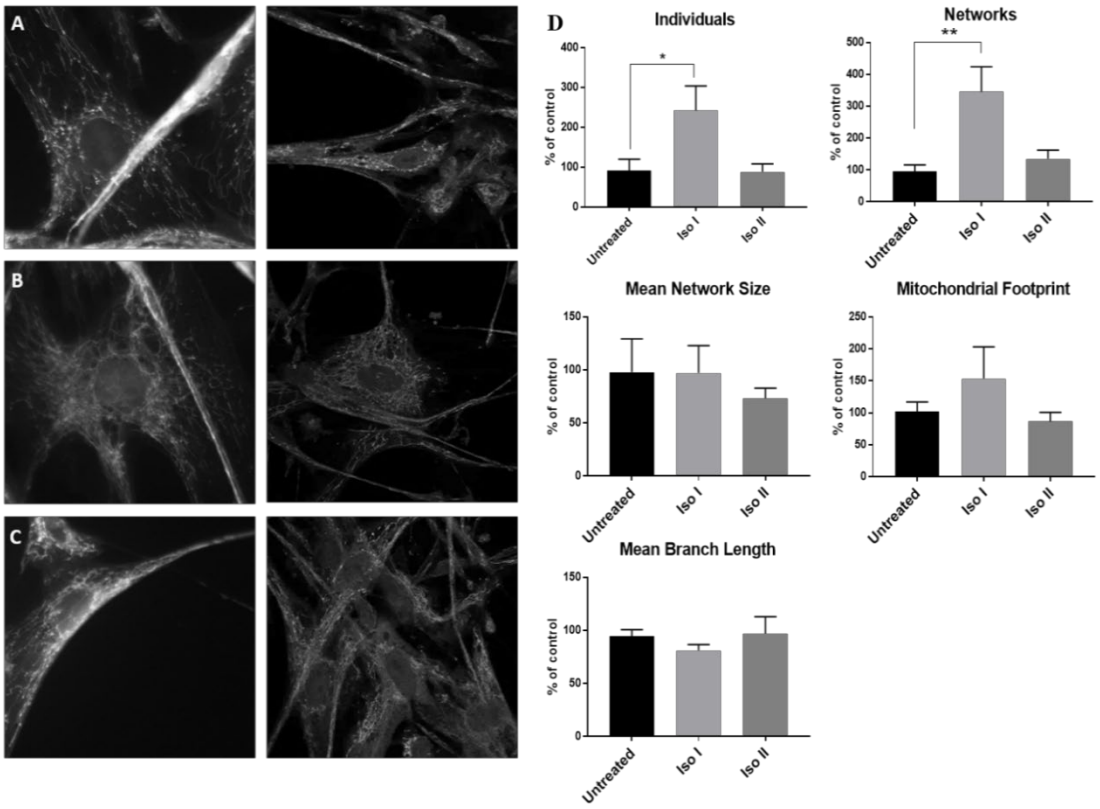

Figure 12 - Mitotracker-stained OMSc patient cells to be processed with MiNA. **A)** Untransduced untreated patient cells. **B)** Lv-IsoI transduced patient cells. **C)** Lv-IsoII transduced cells. **D)** MiNA plugin allows to convert the images to binary and then elaborates a skeleton which is further analyzed to provide the parameters that characterize mitochondrial network, such as individual mitochondria number, networked mitochondria number, size of the networks, length of the branches and total mitochondrial footprint. Data were represented as mean ± SEM and were analyzed with a two-tailed Welch's t test with an n=6.

We then took pictures of mitochondrial structures at the microscope and analyzed the data with the ImageJ plugin "**Mi**tochondrial **N**etwork **A**nalysis" (MiNA, (Valente, Maddalena et al. 2017) that allows us to examine deeper the morphology of mitochondrial network, number of punctate individual mitochondria, number of mitochondria forming networked structures, span of the network formed by mitochondrial net, length of the branches obtained in network junction points, along with total mitochondrial footprint, indicating the total area in the image consumed by signal separated from background (Fig. 12 D).

Transduction with Lv-IsoI, as could be predicted, greatly improves the number of isolated and networked mitochondria, while no changes can be seen in regard to network sizes or length of branches with Isoform I or II. Cytosolic isoform II, in the specific, does not seem to modify the mitochondrial network.

1.5. Mitochondrial bioenergetic analysis in OMScs

We also checked if the mitochondrial metabolism was also affected by the overexpression of FXN isoforms. For this reason, we investigated what was happening at the respiratory chain level through Seahorse assays. With this technique, we can see how the respiratory chain is working by measuring oxygen consumption rate, ATP production, respiratory capacity and membrane integrity, all at once, giving insight on any kind of disfunction impairing mitochondria. During the assay, we measure Oxygen Consumption Rate (OCR) expressed as pico moles per minute.

We used several compounds that interfered with different components of the respiratory chain, to elicit specific reactions. After measuring the "basal" OCR levels, we added oligomycin, an inhibitor of the F_0 subunit of ATP synthase, causing a fall in the OCR which is associated with ATP production. Then, we added FCCP which acts as an uncoupling agent, transporting hydrogen ions through mitochondrial membrane disrupting the inner membrane gradient and "enhancing" the electron transport chain (ETC). This causes a sudden increase in the OCR, which gives us an idea of the maximal respiratory capacity of the mitochondria. Lastly, we added Antimycin A that blocks complex III, shutting down completely the entire electron transport chain process, thus also decreasing dramatically the OCR levels to the non-mitochondrial respiration (Fig. 13).

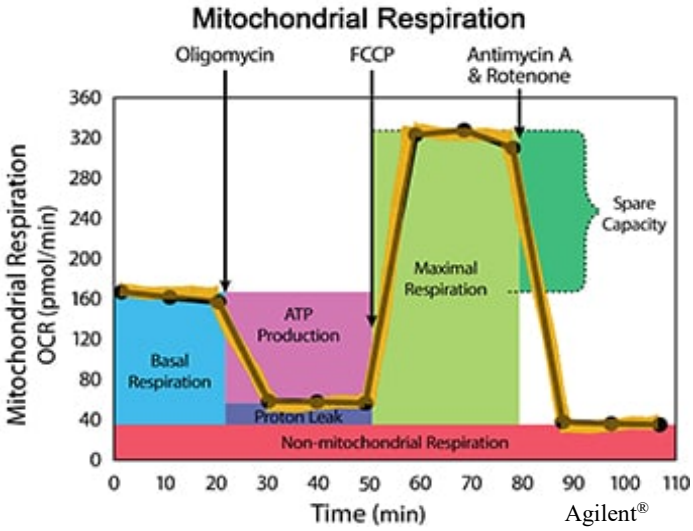

Figure 13 - Diagram showing the theorical principles behind Seahorse assay. The modulators Oligomycin, FCCP and Antimycin A are gradually added to alter the electron transport chain and to permit to measure several parameters useful to assess mitochondrial metabolism.

The difference between Maximal and ATP-coupled respiration values, represents the so called "Spare capacity", responsible of avoiding ATP deficits in critical energetic-demanding situations. The difference between respiration levels when adding Oligomycin and Antimycin A indicates the so called "Proton Leak": H^+ ions escape through the inner membrane, representing inner membrane integrity. All the modulators were added at the concentration described in the previous section of this thesis.

We started by plating 25.000 OMSc cells in 100 µl of CSC medium, comparing the bioenergetics of healthy and patient cells by Seahorse assay (Fig. 14). We observed a non-significant tendency of the healthy cells to show increased ATP-coupled respiration levels when

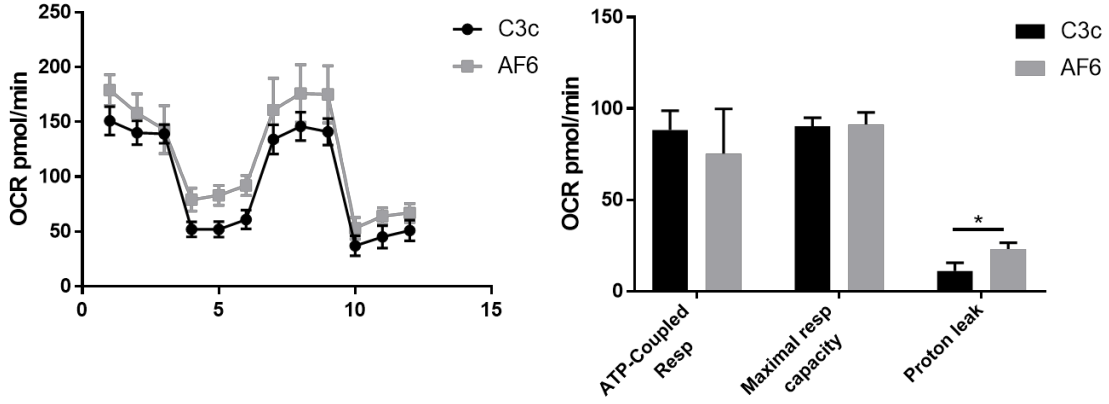

Figure 14 - Seahorse assay in OMSCs in untreated conditions. Patient cells show a little tendency to have diminished levels of ATP-Coupled respiration rates while showing an increase in proton leak. Left panel: OCR variation in the different time points. Right panel: normalization of the results obtained in the experiment. Data were represented as mean ± SD and were analyzed with an unpaired two-tailed t test with n=3.

compared to patient cells, which are, in turn, characterized by a significant level of proton leak, suggesting that their mitochondrial membrane is somewhat more damaged than in healthy cells.

We, then, analyzed separately C3c healthy cells and AF6 patient ones after transducing them with lentivectors carrying GFP, Iso I and Iso II (Fig.15 A-B). We did not detect any significant change for maximal respiratory capacity or for ATP-coupled respiration (data not shown), while we saw an increment in basal respiration rate in both cell types after transducing with the lentiviruses carrying Isoform I and II (Fig. 15, lower panels). The basal mitochondrial respiratory capacity is calculated by subtracting the non-mitochondrial respiration (when Antimycin A is added) to the OCR values obtained before the addiction of oligomycin.

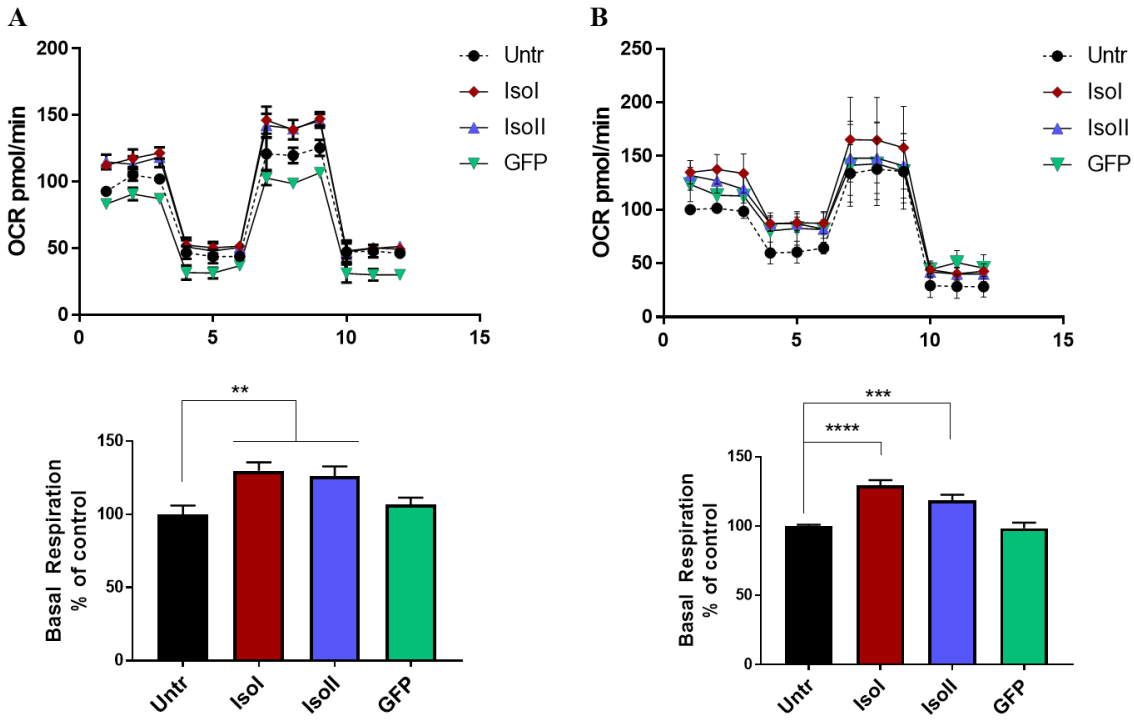

Figure 15 - Seahorse analysis in OMScs from healthy and patient subjects. After transducing separately cells with the lentiviral vectors carrying Isoform I, II and GFP. **A)** Results for healthy OMScs with normalized basal respiration shown below. **B)** Results for patient OMScs with normalized basal respiration shown below. Data were represented as mean ± SEM and were analyzed with a two-tailed Welch's t test with n=3.

1.6. Mitochondrial bioenergetic analysis in FRDA Fibroblasts

In addition to OMSCs, we also analyzed the mitochondrial bioenergetics in another cell type: fibroblasts, from FRDA patients and from healthy donors. We plated 25.000 cells for well of Seahorse plate in the same medium amount and cells were transduced with Lv-GFP, Iso I and Iso II and then the experiment was performed (Fig. 16). We compared two different patient cells versus a healthy (control) fibroblast line.

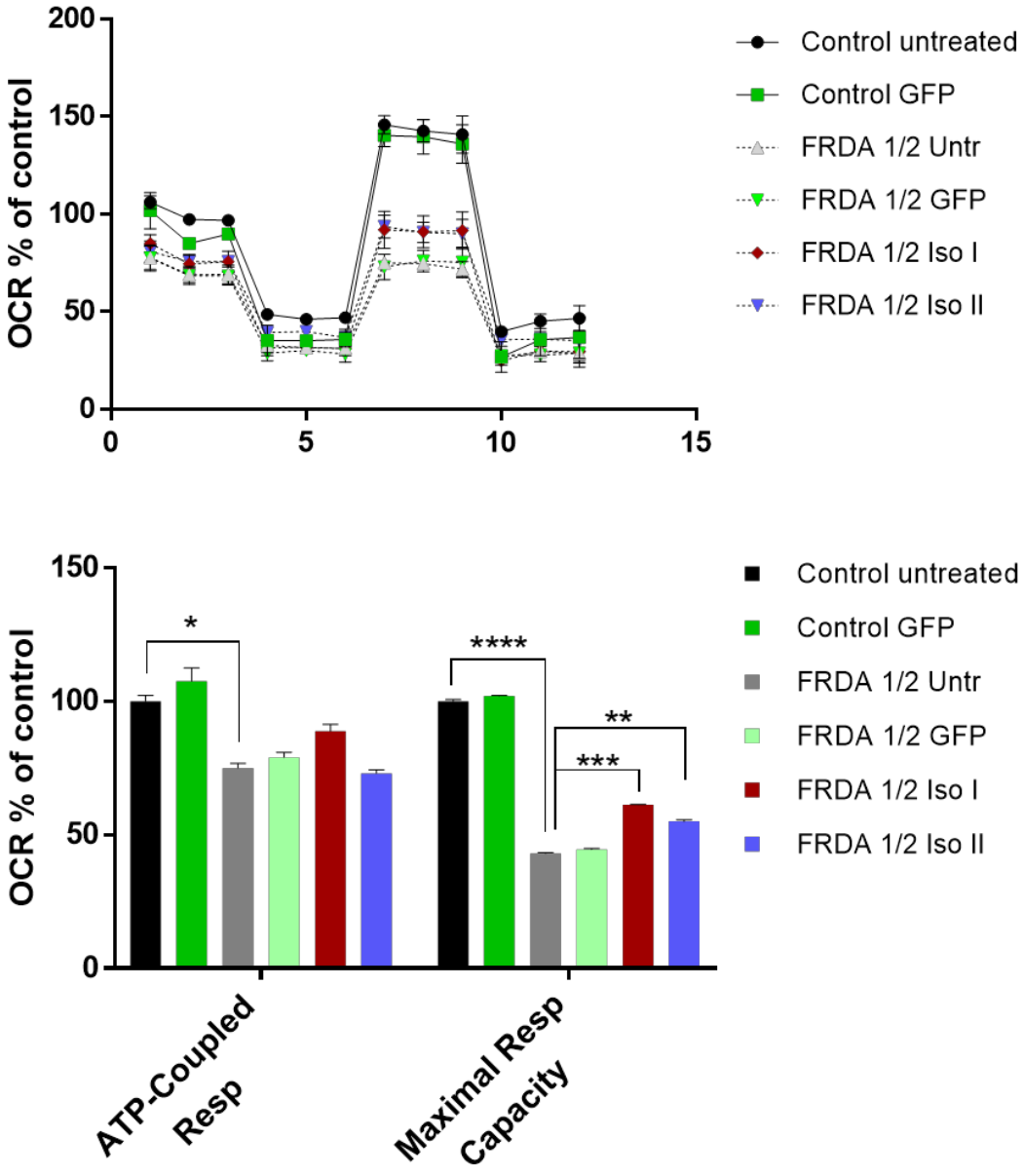

Figure 16 - Seahorse assay in fibroblast isolated from FRDA patients and healthy control subjects. Patient cells transduced with frataxin isoforms seem to perform better on the assay, getting closer to the healthy cells OCR values. Data were represented as mean ± SEM and were analyzed with multiples two-tailed t-tests with a n=3.

For these cells, there is a clear separation between the different populations: FRDA patient cells visibly show less-performing mitochondria, translating in lower OCR values than healthy ones. When transduced with frataxin isoforms, they seem to recover mitochondrial function, even though not at the levels of healthy cells, probably because the transduction of lentiviral vectors in fibroblast is not as efficient as in other cell types.

Maximal respiratory capacity appears to recover especially when cells were transduced with Isoform I, thus showing that frataxin is involved in supervising and maintaining mitochondrial homeostasis. No changes were detected between the two cell lines with or without isoforms in regard to proton leak or basal respiration rate (data not shown).

1.7. Frataxin mediated regulation of mitochondrial related proteins

With the deduction that frataxin expression is able to somewhat rescue mitochondrial function and reestablishing a correct functioning of the ETC, we then wanted to check if the over-expression of the different isoforms was related to the regulation of a series of proteins crucial for the correct homeostasis of the organelle.

After transducing OMSC cells with the different isoforms, we examined the protein levels of several factors involved in mitochondrial metabolism, like the Iron-Sulfur Cluster assembly scaffold protein 1 (ISCU1), Voltage-Dependent Anion Channel (VDAC) proteins, mitochondrial Aconitase 2, cytosolic Aconitase 1 and NADH Dehydrogenase Ubiquinone Iron-Sulfur protein 3 (NDUFS3).

While we did not detect significant changes in ISCU1, NDUFS3 or Aconitase 2 levels (data not shown), we saw an isoform-related response in the levels of VDAC and Aconitase 1 (Fig. 17).

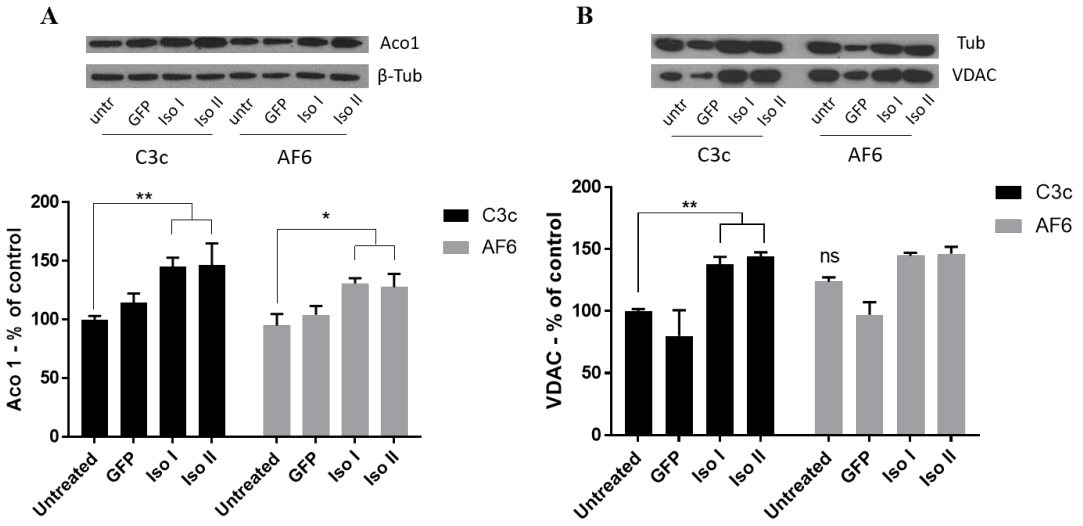

Figure 17 - Expression of mitochondrial-related proteins after transduction with frataxin isoforms in healthy and affected OMScs. **A)** Aconitase 1 expression modulated by lentiviral vectors carrying GFP, Isoform I or II. **B)** VDAC expression modulated by lentiviral vectors carrying GFP Isoform I or II. Data were normalized versus the untreated healthy control and represented as mean ± SEM and were analyzed with multiplestwo-tailed t-tests with a n=3.

1.8. Aconitase activity modulation by frataxin isoforms

Being both aconitases a candidate for interactions with frataxin (Condo, Malisan et al. 2010), we checked whether the different isoforms of frataxin were modulating aconitase activity. We know that Isoform I is surely capable of upregulating both the mitochondrial and the cytosolic aconitase (Bulteau, O'Neill et al. 2004) which was also demonstrated through an *in-gel* aconitase activity assay (Fig. 18).

For this reason, we checked what happened when cells were also transduced with the lentiviral vector carrying Isoform II through a more sensitive and accurate kit for measuring aconitase activity assay, checking optical density (OD) variation during a fixed time of 40 minutes, even though not able to distinguish between the two different aconitase isoforms (Fig. 19).

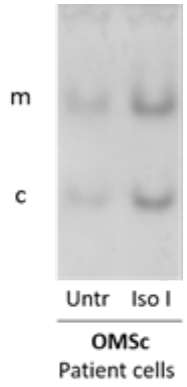

Figure 18 - In-gel Aconitase activity assay in OMSc patient cells. Cells were either left untreated or transduced with the lentiviral vector carrying Isoform I. Both the mitochondrial aconitase (**m**) and the cytosolic one (**c**) appear to be upregulated.

Apart from the results obtained with this protocol in OMScs (Fig. 19 A-B), since the protocol itself was incompatible with this cellular model and was, thus giving unreliable results, we decided to perform the experiments also in neuroblastoma SH-SY5Y cells, transduced, besides GFP, Isoform I and II, also with the lentiviral vector carrying the sequence for a short-hairpin RNA used to reduce frataxin level to ~30% of healthy cells, thus mimicking patient conditions (Fig. 19 C). Nevertheless, no significant reduction in aconitase activity levels was detected with the shRNA, due probably to the fact that in 48h (our standard transduction time identified with the time course indicated in figure 11) Fxn levels were not low enough (around ~ 35-40% of untreated cells, data not shown) to be reflected on aconitase activity. SH-SY5Y were easier to adapt to the assay, giving us an enormous advantage during these experiments. While we did not detect any significant change between Aconitase activity levels between untreated healthy versus patient OMS cells (data not shown), probably due to their adaptation to culture or the excessive enrichment of their medium, for all cell types the same conclusions can be achieved: that both isoform I and II are able to modulate positively aconitase activity.

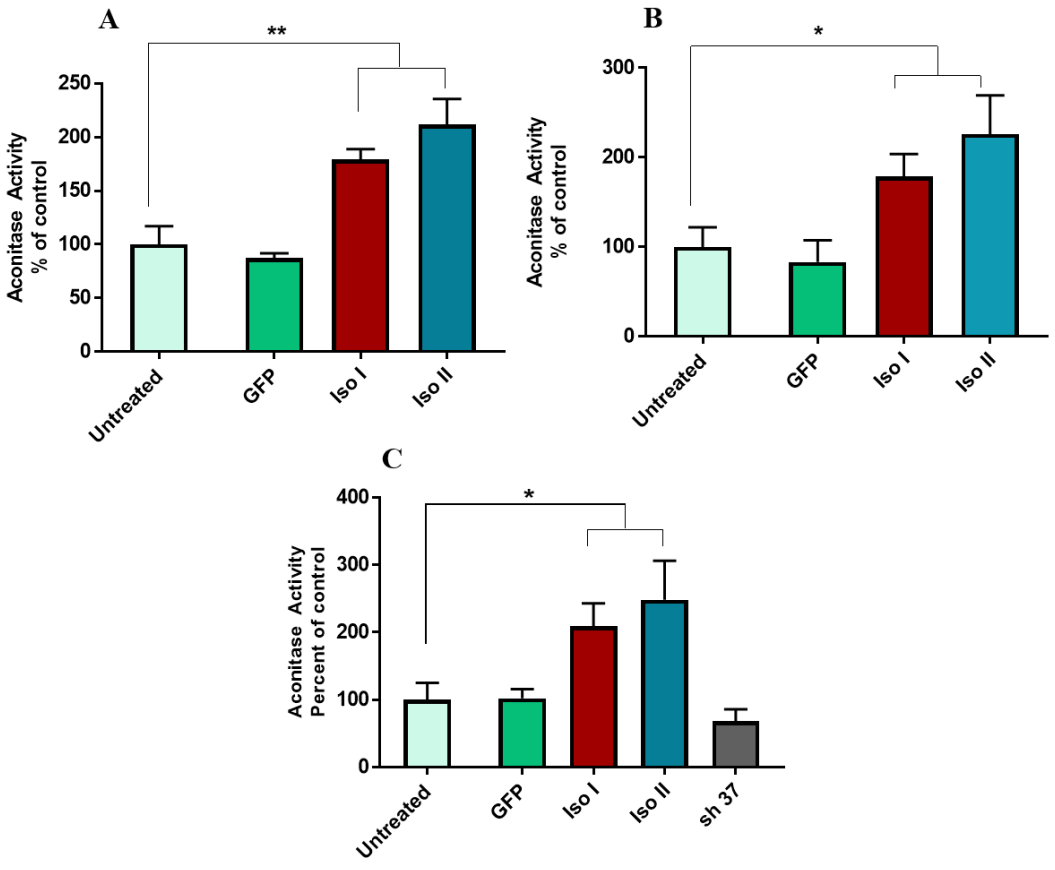

Figure 19 - Aconitase activity assay in different cell models. Results in OMScs and SH-SY5Y show the same conclusions, that both the overexpression of Isoform I and II can improve Aconitase activity. **A)** Aconitase activity assay in healthy OMScs. **B)** Aconitase assay in patient OMScs. **C)** Aconitase activity assay in proliferating neuroblastoma cells SH-SY5Y. Data were represented as mean ± SEM and were analyzed with a two-tailed Welch's t test with an n=3.

Since, as we mentioned previously, frataxin may be involved in protecting ISCs from oxidative damage (Bulteau, O'Neill et al. 2004), we checked whether, after exposing neuroblastoma SY5Y to oxidative stress (in this case induced by 2 h of 500 µM H_2O_2), isoform overexpression was able to rescue aconitase activity (Fig. 20).

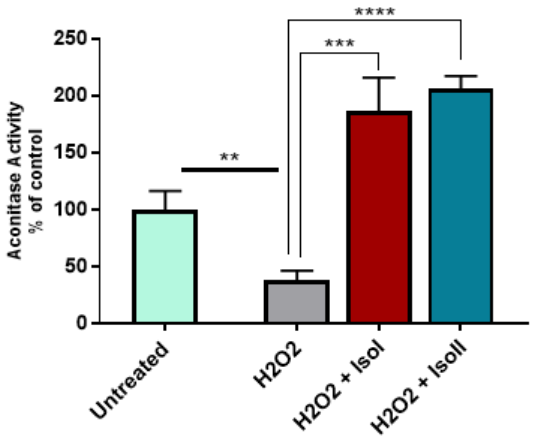

Figure 20 - Aconitase activity assay in SH-SY5Y exposed to oxidative stress. Cells were exposed for 2h to 500µM H_2O_2 before performing the assay. Hydrogen Peroxide effectively reduces aconitase activity when compared to untreated cells, while the presence of isoforms seems to totally rescue the reduction induced by oxidative stress. Data were represented as mean ± SEM and were analyzed with a two-tailed Welch's t test with an n=3.

As shown in the figure, after exposing neuroblastoma SH-SY5Y cells to H_2O_2 we can see a significant decrease in aconitase activity, probably due to the impairing of ISCs proper structure. After overexpression of the FXN isoforms, the impaired activity induced by the oxidative damage is completely rescued to values even higher than the untreated control, thus confirming that both FXN isoforms are able to protect and stabilize aconitase.

2. Regulation of Frataxin expression by Erythropoietic-derived peptides

As described previously, another focus of this work has been the study of frataxin expression levels in response to erythropoietic-derivative peptides, not binding to the classical EPO receptor, but able to bind to the alternative one, promoting cellular growth and stimulating cell metabolism (Brines and Cerami 2005; Siren, Fasshauer et al. 2009). The results obtained for this part are in collaboration with the **I**nstitute for **R**esearch in **B**iomedicine (IRB) located in Barcelona (Spain), with the group of Dr. Ernest Giralt. Based on what we said previously, we synthetized 4 different versions of EPO-like peptides based on the retro-enantiomeric version of HBSP (ARA-290), having their sequence reversed and each residue in its alternative chiral form: the biggest advance of this is that these peptides are not recognized by peptidase enzymes, since they are able to recognize and bind L-aminoacids. In some cases, the biological activity of the original peptide may be retained in the retro-enantiomeric form (Nguyen, He et al. 2006).

We analyzed four different EPO-peptides, plus a scramble peptide, as described in the following table:

Table 8 - Different EPO-derivatives used in this work.

EPO Code	Sample	MW	Purity
HBSP	qeqleralnss	1257,3	95.9
EPO 1	H-ssnlarelqeq-NH2	1273,27	< 98
EPO 2	AC-ssnlarelqeq-NH2	1316,62	< 98
EPO 3	HOOC-(CH2)2-ssnlarelqeq-NH2	1373,44	< 98
EPO 4	NH2-ssnlarelqeq-COOH	1274,36	98
NC2	AC-NH-lsneaeqsrlq-COOH	1316,39	< 98

2.1. *In vitro* effect of Epomimetic peptides on frataxin levels in primary cultures of cortical neurons

At first, we decided to screen the different peptides *in vitro* in primary cultures of mouse neurons to gain insight on which one was the best candidate producing the strongest results in modulating frataxin expression.

Previous work from this lab demonstrated that the modulation induced by erythropoietic-like peptides seems to be mediated by several candidates, like the Tyrosine Receptor Kinase B (TrkB),

receptor of BDNF, or Sonic Hedgehog (SHH) (Thesis Dr. Yurika Katsu). For this reason, when evaluating the difference potential of the peptides we used, we treated the cells also with specific inhibitors of one pathway or the other, to prove their involvement in frataxin upregulation mediated by EPOs. We used Cyclopamine (cpm) that blocks SHH pathway through its binding to the receptor Smoothened. In normal conditions, SHH proteins are able to bind and inhibit surface membrane proteins called Patched, which in turn normally inhibits Smoothened.

Even if SHH levels rise in the cell, the presence of cpm binding to Smoothened blocks it from further proceed with the signaling cascade. The other inhibitor we used was K252a, an alkaloid able to block the signaling pathway of the Trk family receptors, thus blocking TrkB. In our assay, we wanted to check if the possible augment in frataxin levels after epomimetic treatment could be blocked by using either inhibitor (Fig. 22). Neurons were harvested from E16 mouse cortex and plated at a density of 500.000/ml in NB-B27. Epomimetic peptides at 500 ng/ml and drugs were added daily at the concentration indicated in the picture.

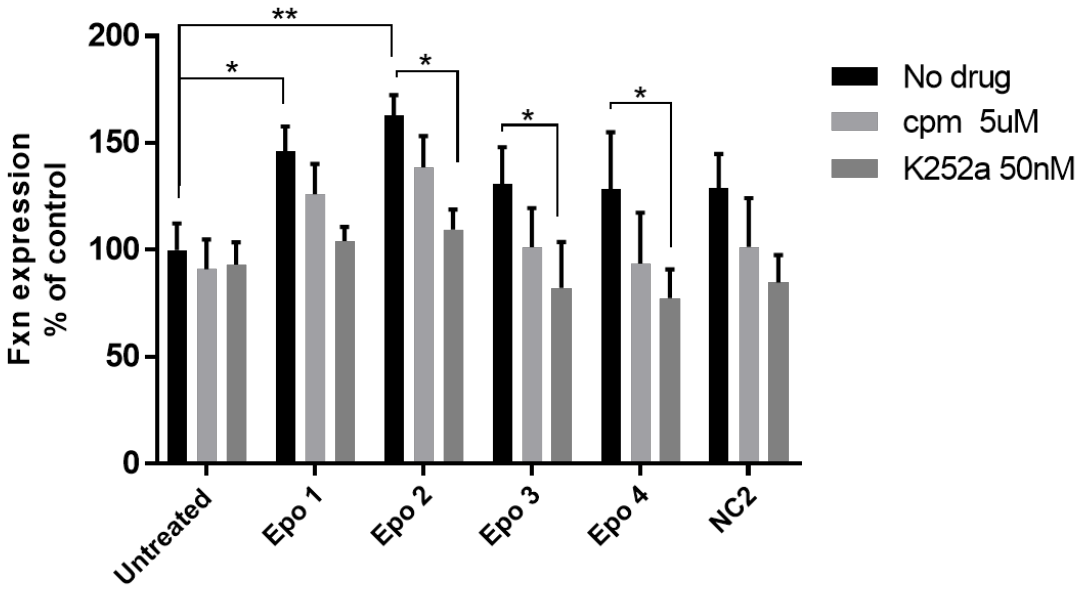

Figure 22 - Cortical neurons treated with different synthetic EPOs and drugs inhibiting the suspected mediators. Cells were cultivated for 5 days during which EPOs were added daily at 100nM along with the inhibitors Cpm (5uM) and K252a (50nM). The increment in frataxin levels obtained after EPOs treatment, appears to be hindered in conjunction with the drugs. Data were represented as mean ± SEM and were analyzed with multiples two-tailed t tests, with a n=5.

The increment in frataxin level that we can see with the different epomimetic peptides, seems to be reduced when treating cells in parallel with the inhibitors previously described, pointing to an involvement of those pathways we mentioned earlier. Based on the results obtained, we were able to detect a strong significant effect on frataxin expression exerted by both EPO1 and EPO2, reverted when using the inhibitors previously described, underlining that the increment in frataxin

detected was due to the activation of SHH and Trkβ pathway. We decided to focus our attention on the so-called EPO2, since it was the peptide that produced the most significant effect between the two.

As a very early preliminary result, we analyzed mRNA levels of frataxin and several hypothetic candidates involved in its upregulation after treating neurons with EPO2 or HBSP for five days. We performed a qRT-PCR in E16 cortical neurons using different concentration of peptides to check for amount specific modulation of frataxin and of several candidate mediators for its regulation (Fig. 23).

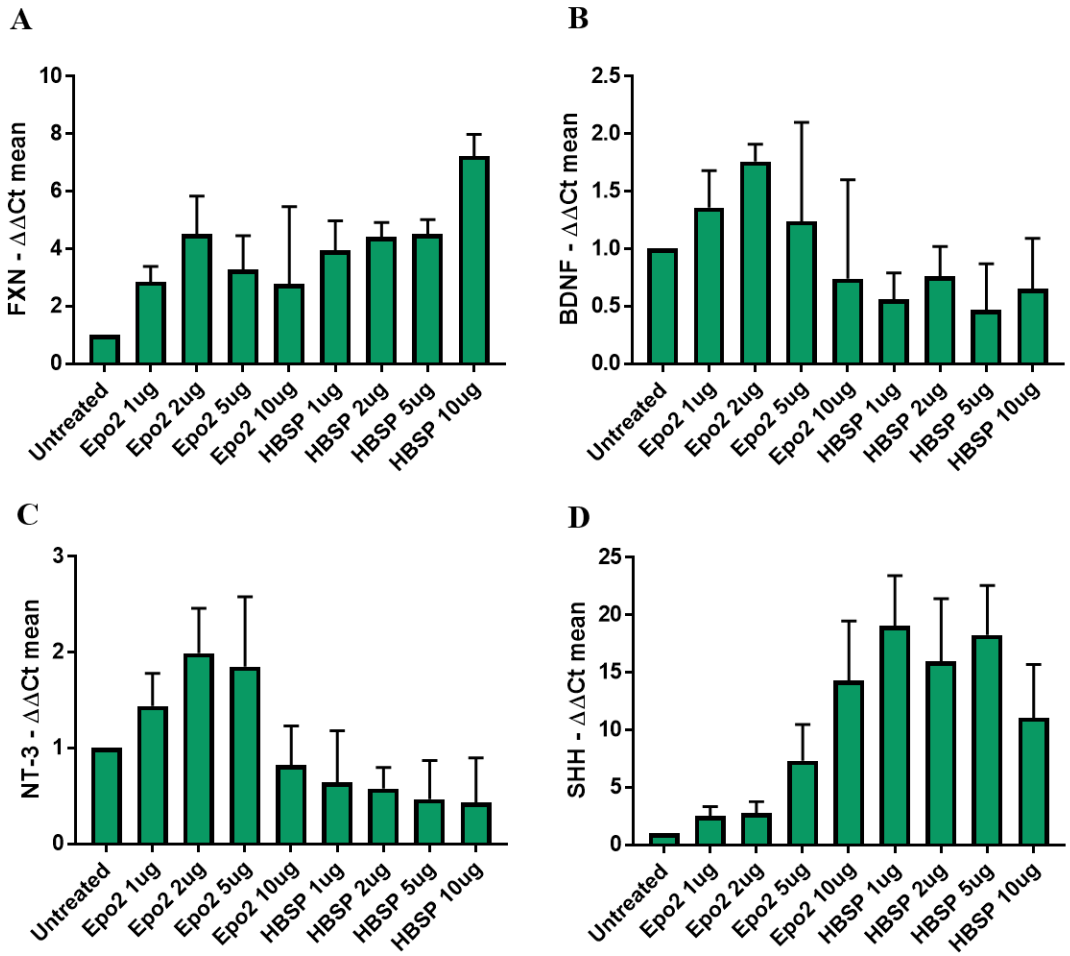

Figure 23 - qRT-PCR preliminary analysis of frataxin and its possible mediators in cortical neuron after EPO2/HBSP treatments. **A)** FXN mRNA levels in cortical neurons after five days EPO2/HBSP treatments. **B)** BDNF mRNA levels in cortical neurons after five days EPO2/HBSP treatment. **C)** NT-3 mRNA levels in cortical neurons after five days EPO2/HBSP treatments. **D)** SHH mRNA levels in cortical neurons after five days EPO2/HBSP treatments. Results were represented as ΔΔCt means ± SD, in two replicates coming from the same starting RNAs (n=1).

Both peptides seem to exert an equal effect on frataxin mRNA levels, while they seem to act differently on the mediators we have analyzed, with EPO2 causing a stronger effect on the

neurotrophic factors BDNF/NT-3 while HBSP seems to upregulate SHH. These results will be further examined in depth in the future.

2.2. *In vivo* effect of EPO2 in C57BL6/J mouse brain

We checked the effect of EPO2 on a wild type C57BL6/J mouse strain. For these experiments, we first analyzed different concentrations of peptide in order to establish the best parameters for our future experiments. Results with primary cultures of cortical neurons showed that 113 ng/ml HBSP was able to induce the same upregulation on frataxin levels as 500 ng/ml EPO. As Dr. Katsu performed her in vivo experiments with HBSP 33 µg/kg animal, we decided to maintain the proportion and use three different groups of four C57BL6/J mice that were then injected intraperitoneally daily for 5 days with either 200 µg/kg or 400 µg/kg of EPO2 and 0.9% NaCl as control (n=2). After the protocol, mice were sacrificed, and tissues were extracted to be further processed. We analyzed the expression of frataxin in total brain extracts of the different groups, as indicated below (Fig. 24)

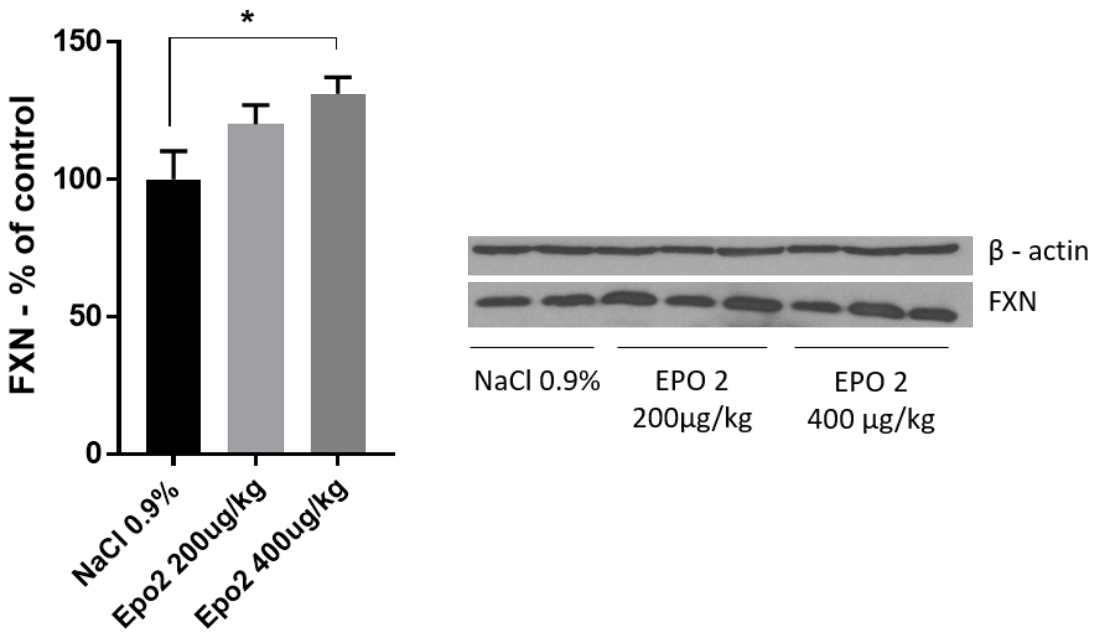

Figure 24 - Frataxin levels in C57BL6/J mouse brain after EPO2 treatment. Mice were injected daily for 5 days with two different EPO2 concentration to determine which one was more suitable for future experiments. Data were represented as mean ± SEM and were analyzed with an umpaired two-tailed t-test with n=4.

Taking into account the results from the experiment, we decided to use 400 µg/kg as the standard concentration for our future *in vivo* experiments.

Once we established the optimal concentration to produce a modulation upon frataxin expression, we analyzed the effects of the EPO2 peptide versus the original HBSP analogue, described previously. Three groups of C57BL67/J mice were injected intraperitoneally daily for 5 days either with 400 μg/kg EPO 2 or 33 μg/kg HBSP and 0.9% NaCl as control, maintaining the ratio described by Dr. Katsu integrated with our previous results from the *in vivo* experiments described earlier. After the protocol, mice were sacrificed, and tissues were isolated for analysis. We started analyzing total brain tissue, assessing frataxin expression through western blot (Fig. 25).

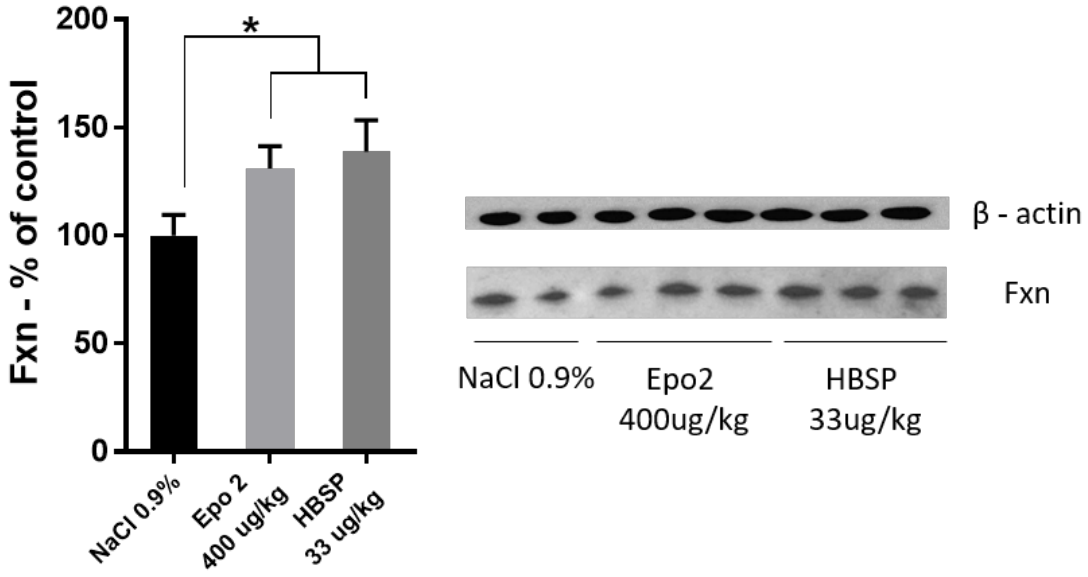

Figure 25 - Frataxin expression in C57BL6/J brain after EPO2 or HBSP treatments. Mice were injected daily for 5 days either with NaCl, EPO 2 or HBSP. Both treatments seem to produce a significant increment in frataxin levels in the cerebrum. Data were represented as mean ± SEM and were analyzed with an unpaired two-tailed t-test with n=3.

The results indicated that both peptides are able to increment frataxin levels for about 30% in the brain of C57BL6/J wild type mice. Being FRDA a disease that affects the whole spinocerebellar system, we decided to investigate the effects of the peptides in the cerebellum, to have a more comprehensive overview of the treatments with EPO2.

Cerebellar extracts were obtained and frataxin levels were evaluated with an ELISA Kit specific for murine frataxin, as described in the "Material and Methods" section (Fig. 26).

In cerebellum, both peptides provoked again an increment in frataxin levels, but unlike what we have seen in cerebrum, EPO 2 caused a significant stronger increase when compared to HBSP, while in brain the response induced on frataxin levels from both peptides was equivalent.

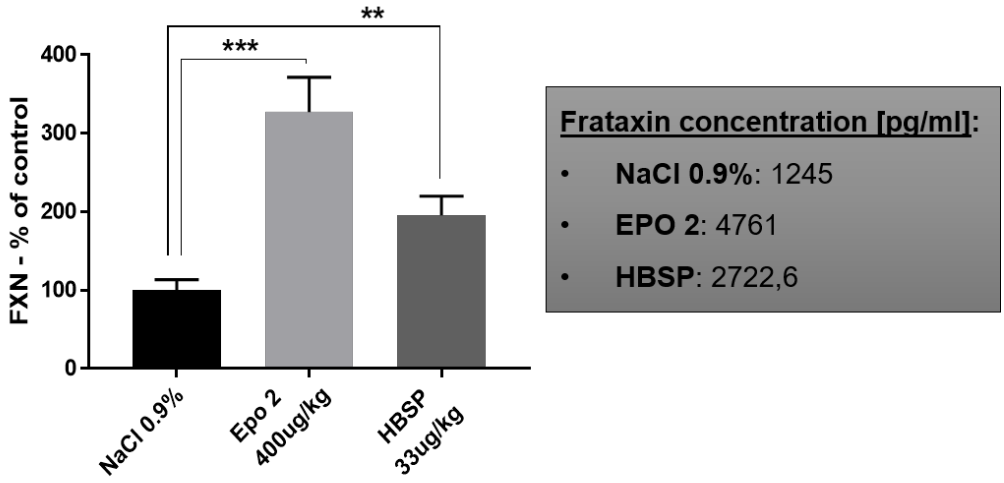

Figure 26 - Frataxin modulation in C57BL6/J cerebellum after Epo 2/HBSP treatments. Mice were injected daily for 5 days either with NaCl, EPO 2 or HBSP. Frataxin levels were analyzed with an ELISA kit. Both EPO 2 and HBSP seem to upregulate Frataxin significantly, with EPO 2 achieving a stronger upregulation. Data were represented as mean ± SEM and were analyzed with an unpaired two-tailed t-test with an n=3.

2.3. *In vitro* analysis of the effect of epomimetic peptides on frataxin levels in FRDA patient cells (OMScs and fibroblasts)

In addition to the results we obtained *in vivo* in mice, we examined the potential effects of the peptides in an *in vitro* cellular model for frataxin deficiency. Thus, we tested EPO 2 on healthy and affected OMS cells. Cells were cultivated at a density of 10^6/ml in a 6-Multiwell plate and treated daily with either EPO 2 or HBSP, both at 1 µg/ml. After 5 days, total protein extracts were obtained and analyzed through an ELISA kit specific for human frataxin (Fig. 27)

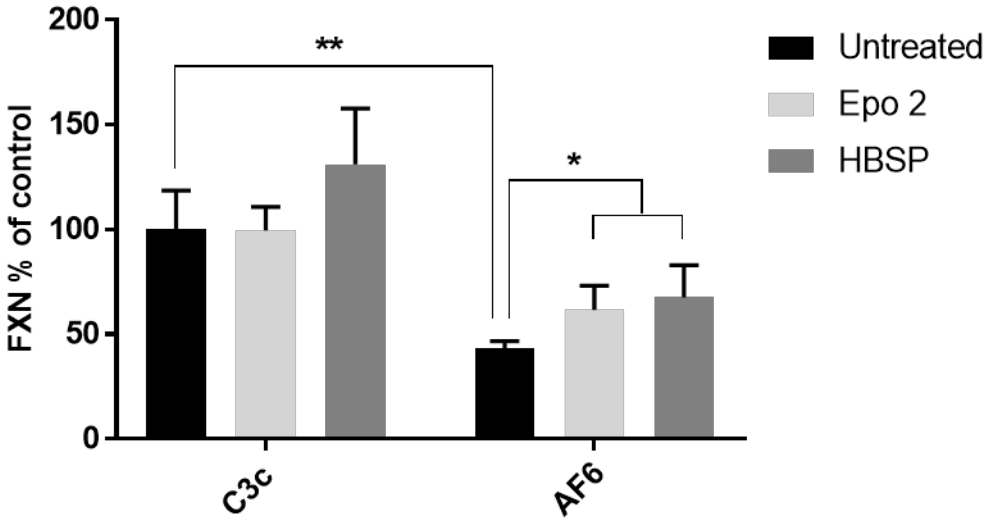

Figure 27 - Frataxin modulation in OMScs after Epo 2/HBSP treatments. Cells were treated daily for 5 days with 1 µg/ml of Epo 2 or HBSP. Frataxin levels were analyzed with an ELISA kit. Data were represented as mean ± SD and were analyzed with multiples t-tests with a n=3.

No significant effect can be seen in healthy OMS cells, while patient cells seem to responde to the treatment with both Epo 2 and HBSP peptides at the concentration used. We also analyzed peptide effects on our FRDA fibroblasts, where we did not detect changes in frataxin levels when using the concentration we used in OMScs (1 µg/ml, data not shown) and for this reason we increased the concentration of our chronic treatment to 5 µg/ml and 10 µg/ml. After five days, cells were scraped and total protein extracts were obtained and analyzed through Western blot (Fig. 28).

While for healthy fibroblast we detected an increment in frataxin levels with both peptides used for about 25~30%, results obtained in patient fibroblasts need to be further explored, even though cells seemed to respond to the treatments.

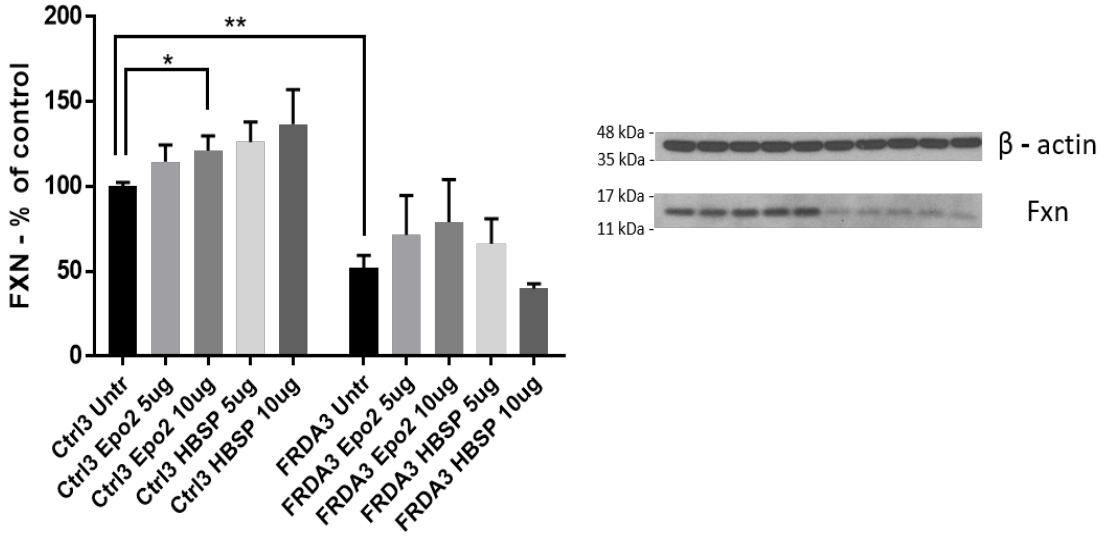

Figure 28 - Frataxin levels analysis in FRDA fibroblasts after chronic treatment with EPO2/HBSP. Cells were treated daily for 5 days with 5 µg/ml or 10 µg/ml of Epo 2 or HBSP. Frataxin levels were analyzed through Western Blot. Data were represented as mean ± SE and were analyzed with multiples t-tests with a n=4.

3. Modulation of frataxin expression *in vivo* in mouse cerebellum in response to physical activity

As we mentioned previously in the introduction, physical exercise is nowadays considered a potential new therapeutic approach for many neurodegenerative diseases. Since no direct study between physical activity and Friedreich's Ataxia has never been performed, we decided to investigate the role of the exercise upon the modulation of frataxin expression in collaboration with the laboratory of Dr. Jorge L. Ruas (Karolinska Institute, Stockholm, Sweden).

With this objective in mind, we used two different groups of C57BL6/J mice: one subjected to a spontaneous physical activity protocol, in which mice were able, on their own, to start running on a wheel positioned in their cages (n=8), and the other one without any kind of wheel, so forced to be sedentary (n=7). Wheels in cages were connected to a laptop constantly measuring the amount of spontaneous physical activity performed by the mice (expressed in meters/24h).

This spontaneous physical activity protocol lasted for 8 weeks and allowed us to identify a difference in the running behavior of the animals, with some of them running more than others along the different weeks. We, then, classified the running mice in *runners* and *high runners,* being high runners the mice that ran for more than 4000 meters/24h (Fig. 29). This separation simply worked as an internal reference for the interpretation of the results.

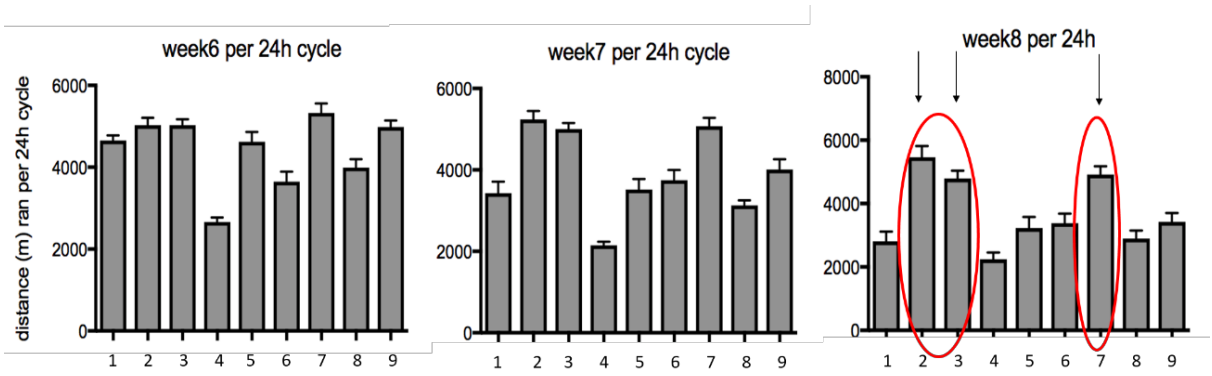

Figure 29 - Diagram showing the results of the last three weeks of the exercise protocol. Shown are the distances run by individual mice (1 to 9). The results are expressed as meters/24h. Mice are indicated with number from 1 to 9. In red, the so called *high runners* are highlighted, an arbitrary nomenclature to identify the mice that have been running more than 4000 meters/day at least in the last three weeks of the protocol. Data were represented as mean ± SD.

Once the protocol was over, we sacrificed the mice and isolated the cerebella of the animals to proceed with the analysis of frataxin levels.

3.1. Analysis of Frataxin levels in mouse cerebellum after physical exercise

After tissue extraction, we decided to analyze both protein and mRNA level to check for possible transcriptional and post-transcriptional effects of physical exercise on frataxin levels. Cerebella from both mouse groups, sedentary and runner, were processed and examined (Fig. 30).

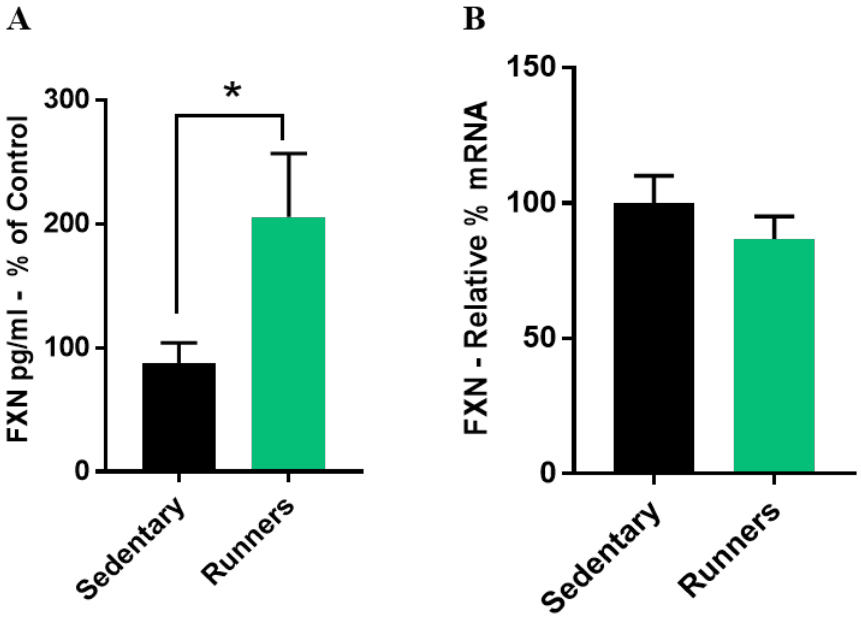

Figure 30 - Analysis of Frataxin protein and mRNA levels in mouse cerebellum after physical exercise. **A)** ELISA assay results representing Frataxin protein levels in Sedentary versus Runner mice groups. **B)** RT-qPCR results showing Frataxin mRNA levels in sedentary versus runner mice groups. Data were represented as mean ± SEM and were analyzed with an unpaired two-tailed t-test with an n=3.

While a significant difference can be seen in frataxin protein levels, the same cannot be said about mRNA. In order to check for any "activity amount"-related effects, we further analyzed the samples by splitting runner and high runner (Fig. 31). The results seem to indicate a direct correlation between physical activity amount and frataxin protein levels, being frataxin more upregulated in the mice that ran the most. These results indicate that spontaneous physical activity increase frataxin levels in the cerebellum of wild-type mice.

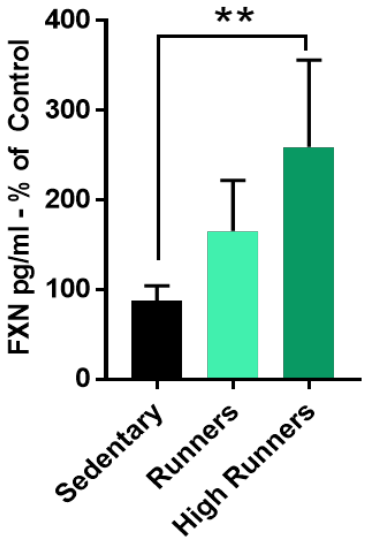

Figure 31 - Frataxin protein levels in mouse cerebellum after physical exercise. ELISA results splitting Runner and High runner group. Data were represented as mean ± SEM and were analyzed with an unpaired two-tailed t-test with an n=3

3.2. Identification of possible frataxin-regulating factors after physical exercise

Once we demonstrated that frataxin was upregulated in mouse cerebellum after spontaneous physical activity, we tried to analyze some putative mediators of this effect. Many factors have been studied in the literature, but most of the studies focused on assess the mechanisms in hippocampus, cerebrum or total brain tissue, not focusing specifically on cerebellum (Vaynman, Ying et al. 2004; Marlatt, Potter et al. 2012). For this reason, we analyzed the levels of factors we know to participate in frataxin expression regulation, based on previous work from our laboratory, like BDNF, SHH and NT-3 (Fig. 32).

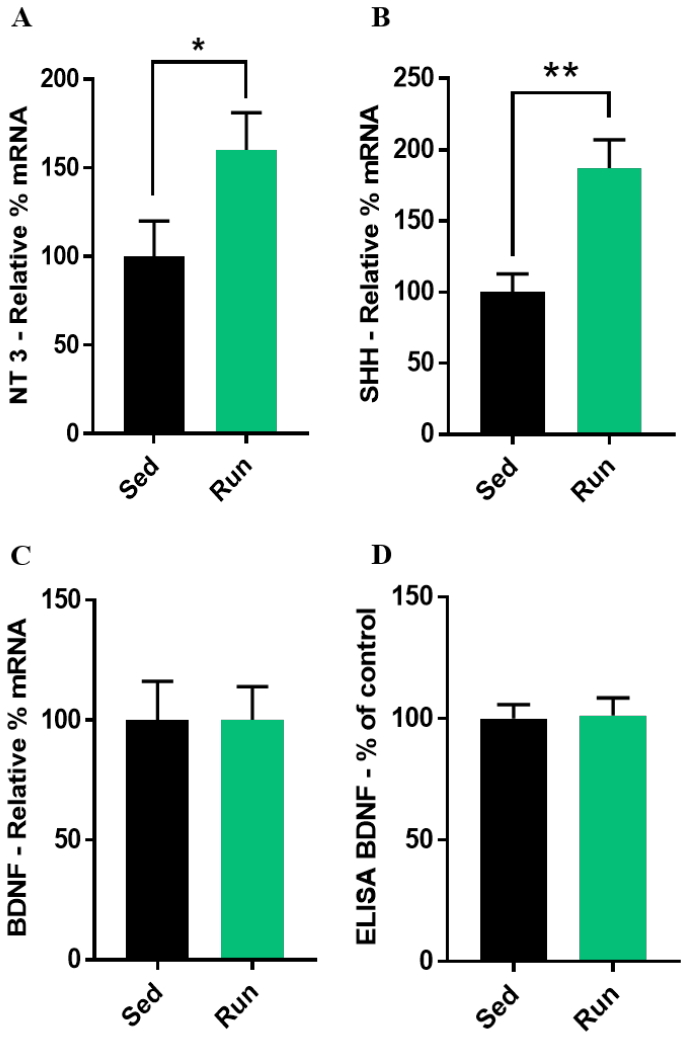

Figure 32 - Analysis of several mediators for frataxin upregulation after physical exercise. **A)** Real-time PCR amplification of NT-3 transcript of sedentary versus runner group. **B)** Real-time PCR amplification of SHH transcript of sedentary versus runner group. **C)** Real-time PCR amplification of BDNF transcript of sedentary versus runner group. **D)** ELISA results of BDNF levels between sedentary and runner group. No significant changes detected for BDNF at protein nor mRNA levels. The mRNA expression was quantified using the comparative Ct method and data were represented as mean ± SEM and were analyzed with an unpaired two-tailed t-test with an n=3.

As the picture clearly shows, both NT-3 and SHH appeared to be upregulated in the cerebellum of mice subjected to physical activity. When the analysis was performed for BDNF, we were unable to detect changes in protein levels or in mRNA, meaning that BDNF is not upregulated with this kind of physical activity, at least in the cerebellum and after the eight weeks of the protocol.

Since the effects on physical exercise on the cerebellum are not well characterized, we performed a cytokine array to identify possible changes in a wide spectrum of signaling molecules and trophic factors (Fig. 33).

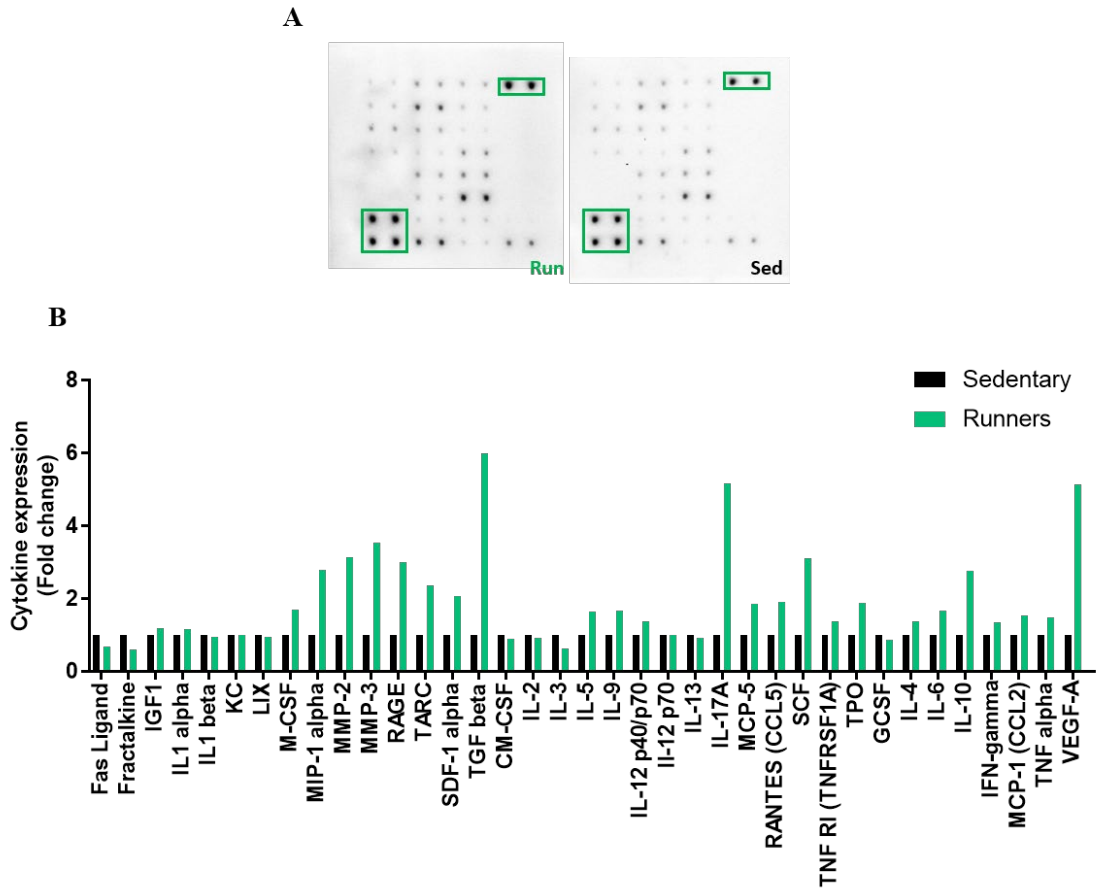

Figure 33 - Cytokine array in sedentary versus runner mice. **A)** Representative antibody cytokine array (37 cytokines) from cerebellar extracts from Runner (left) versus Sedentary (right) groups. Rectangles indicate positive controls (green). **B)** Graph showing the quantification of the array representing the cytokine expression in Runner (green) presented in fold change in respect to Sedentary (black) group.

The result of the array showed that a high number of cytokines appeared to be upregulated, like the Macrophage Inflammatory Protein-1α (MIP-1α), the Transforming Growth Factor β (TGF-β), Stem Cell Factor (SCF), the Receptor for Advanced Glycation Endproducts (RAGE), the Vascular Endotelial Factor A (VEGF-A) and the Matrix MetalloProtease 2 and 3 (MMP2/3), which are known to participate in angiogenesis processes. On the other side, some cytokines seemed to be downregulated, like Fas Ligand (FasL) or Fractalkine. Being physical activity a process involving practically the whole organism, it appeared obvious to have such a strong response after exercise. We decided to point our attention on those cytokines which might be involved in regulation of frataxin expression, such as the Macrophage Inflammatory Protein-1α (MIP-1α) and Interferon-γ (IFNγ) (Kuijpers, van Gassen et al. 2010; Wells, Seyer et al. 2015) (Fig. 34).

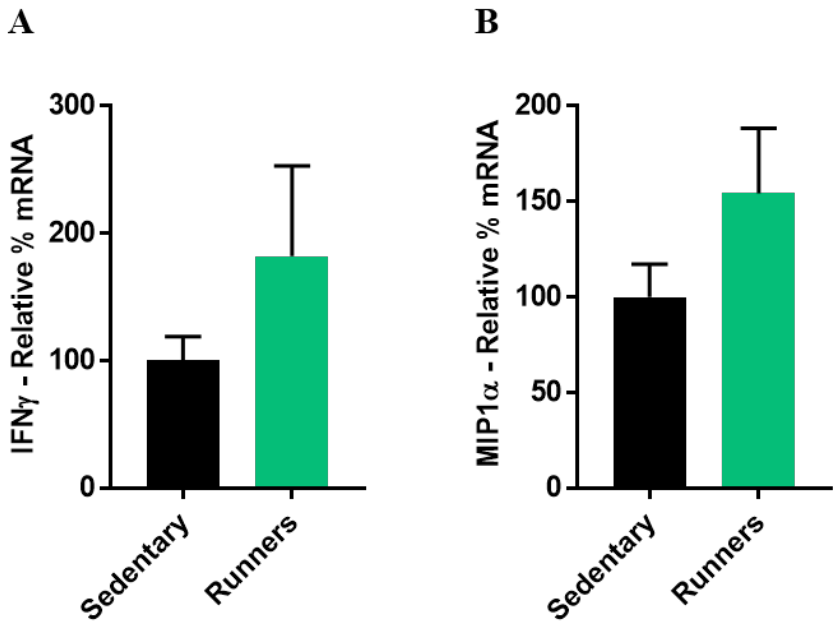

Figure 34 - RT-qPCR validation of some of the cytokines upregulated in mouse cerebellum after physical exercise. **A)** Real-time PCR amplification of IFNγ transcripts in sedentary versus runner group. **B)** Real-time PCR amplification of the transcript of MIP-1α in sedentary versus runner group. The mRNA expression was quantified using the comparative Ct method and data were represented as mean ± SEM and were analyzed with an unpaired two-tailed t-test with an n=2.

Even though differences saw in the results were not significative, a tendency of the runner group to express higher levels of IFNγ and MIP-1α mRNA can be sensed. More studies are needed in order to reach a final and stronger conclusion.

Discussion

1. Characterization of mitochondrial and extra mitochondrial frataxin isoforms

Friedreich's Ataxia is a mainly neurodegenerative disease caused, by the deficiency of the frataxin protein. Recently, several groups have reported the existence of several frataxin isoforms, with functions still not fully characterized and explored (Campuzano, Montermini et al. 1996; Xia, Cao et al. 2012), which has been a strong focus of our research. Xia et al. first described the different subcellular localization of the so-called Isoform II and III. Other authors have also described extra-mitochondrial frataxin isoforms, for example in erythrocytes it has been described an isoform (called Isoform E) quite similar to our Isoform II (Guo, Wang et al. 2018), or the existence of a pool of cytosolic frataxin involved in protecting cells from oxidative damage has also been indicated (Condo, Ventura et al. 2006). All these results opened the way for more questions about the physiological relevance of all frataxin isoforms in FRDA patients and healthy subjects, which has been one of the objectives of this work.

We focused our studies on the alternative isoforms described by Xia, mainly due to the author claims about Isoform II being enriched in cerebellum, being this one of the most affected tissues during disease development.

In all of our cell models, we have confirmed the cytosolic localization of Isoform II both by subcellular fractionation followed by Western Blot, or directly at the microscope after staining cells with specific antibodies. In contrast, we have not observed the presence of Isoform III in the cell nucleus of any of our cell models. In order to check for nuclear translocation events that could have caused our inability to observe it in the nucleus, we set up an experiment using Leptomycin B, a molecule originating from *Streptomyces* bacteria, know to interact and block the nuclear exporting pathway in humans. Not even with this setup we were able to observe its nuclear localization which is in strong contrast with Xia's assumptions (Xia, Cao et al. 2012). We also checked whether Isoform II would localize to the nucleus in its maturation process and then be exported to cytosol: we then repeated the Leptomycin B experiment after transducing cells with the lentiviral vector carrying Isoform II sequence. This time we determined that Isoform II is fully cytosolic being synthetized and eliciting its functions in this compartment. Based on these results and also following Xia's statement about the different tissue distribution of both isoforms, we focused our attention on the cytosolic Isoform II, most abundant in cerebellum which represents one of the most affected tissue by Friedreich's Ataxia.

Once Isoform II localization was fully established as cytosolic, the fact that only the over-expression of mitochondrial Isoform I was able to improve mitochondrial development by incrementing the numbers of both individual mitochondria and networks, did not surprise us.

Nonetheless, we were able to see an improvement with both isoforms in mitochondrial respiration function after the overexpression of both frataxin Isoform I and II through Seahorse assays: using our OMS cellular model we detected changes in basal respiration rate in both healthy and patient cells. This increment in basal respiration rate could indicate that OMS cells are able, when over expressing Isoform I or II, to use the metabolites we provided during the experiment (glucose and pyruvate) in a better way than untreated or GFP-transduced cells. In FRDA fibroblasts, which are clearly impaired in mitochondrial respiration when confronted with healthy fibroblasts, we saw a marked increment in maximal respiratory capacity from patient cells when transduced with Isoform I or II compared to untreated or GFP-transduced patient ones. This clearly indicated that both isoforms can rescue mitochondrial function in different manners: Isoform I by acting inside mitochondria, while cytosolic Isoform II from the outside. We do not know the molecular mechanisms behind the mitochondrial activity rescue or the basal respiration increment induced by Isoform II, but one hypothesis could be that the extra-mitochondrial isoform of frataxin could be involved in facilitating the influx of metabolites from the cytosol to the mitochondria through mechanisms which remain to be determined.

This, actually, opens the way to many questions: since there were no changes in the rest of respiratory parameters, it would be worth researching on how these metabolites are being used and for what. ATP/ADP ratios or redox state (by evaluating the nicotinamide adenine dinucleotide oxidized/reduced (NAD^+/NADH) ratio) could be evalued, especially since we also know that frataxin is involved in preventing the formation of ROS (Gakh, Park et al. 2006), thus preventing DNA damage and the activation of Poly ADP-Ribose Polymerase (PARP). PARP activation itself consumes NAD^+ and also impairs glycolysis through the inhibition of hexokinase (Andrabi, Umanah et al. 2014), thus reducing the levels of pyruvate available for oxidative phosphorylation in mitochondria.

Furthermore, many authors have shown that frataxin deficiency induces DNA damage (Chamberlain, Cramp et al. 1981; Haugen, Di Prospero et al. 2010; Coppola, Burnett et al. 2011; Khonsari, Schneider et al. 2016), by actively repressing DNA-repair pathways and, as a secondary cause, by provoking the production of ROS. The most interesting fact is that many enzymes involved in DNA repair seem to possess Fe-S clusters which are key factors for their proper functioning (Fuss, Tsai et al. 2015; Nunez, Majumdar et al. 2018), meaning that frataxin cytosolic isoform could play a crucial role in regulating and stabilizing these Fe-S clusters during DNA repair events (Rouault 2012) (Fig. 35).

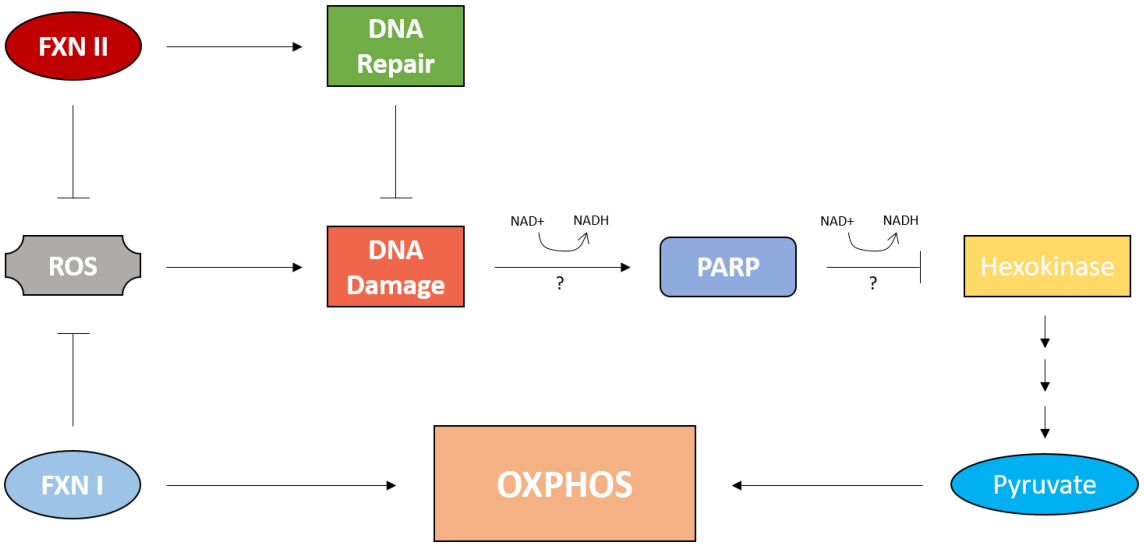

Figure 35 - Diagram showing possible involvement of frataxin isoforms in ROS action mechanism. ROS cause DNA damage and activation of PARP, prevented by the activation of DNA repair mechanisms, possibly through Frataxin Isoform II action. PARP activation impairs hexokinase, thus inhibiting glycolysis, reducing pyruvate levels available for the tricarboxylic acid cycle and oxidative phosphorylation.

Trying to elucidate these processes, we searched for hypothetical interaction partners that could participate in the events described so far. Based on the results obtained by Condó et al. (Condo, Malisan et al. 2010) that showed that their extra mitochondrial frataxin isoform was able to interact directly with the cytosolic aconitase Aco1, we checked if this would be true also for our Isoform II. In both healthy and patient OMS cellular models, we confirmed that over expression of Isoform II caused an increment in the levels of cytosolic aconitase. Aco1 levels were also increased after over expressing the canonical Isoform I of frataxin, underlying the existence of a feedback circuit between the mitochondrial and extra-mitochondrial frataxins. To further prove this hypothesis, we checked the levels of a specific mitochondrial protein like VDAC that we know to be directly modulated by mitochondrial frataxin isoform I (Jasoliya, McMackin et al. 2017). Interestingly, we saw that both isoforms are able to significantly increment VDAC levels, at least in healthy subject, while a tendency has been seen in patient OMScs. Since we know that the over expression of Isoform II is not altering the levels of Isoform I, as shown in figure 6, these increments in VDAC levels are specifically due to the presence of cytosolic frataxin, thus highlighting again the existence of some form of feedbacks between mitochondrial and extra-mitochondrial forms of frataxin, that could participate in tandem in the regulation of the homeostasis of cells, as it has been also pointed out by other groups (Condo, Ventura et al. 2006).

While it is true that many metabolic pathways crucial for cellular homeostasis take place within mitochondrial compartment, that hence is strictly regulated in regard to iron metabolism, the potential roles of cytosolic isoforms of proteins involved in the regulation of the formation/repair of Fe-S clusters is gradually gaining more interest, since cells require two different sets of machinery for cluster biogenesis: ISC mitochondrial and CIA cytosolic machinery. Frataxin is not the only protein involved in Fe-S clusters formation and regulation to express extra-mitochondrial isoforms.

This is the case of the cysteine desulfurase NSF1 (Li, Tong et al. 2006), or of Nfu, a protein necessary for correct iron sulfur clusters assembly with the role of removing sulfur from free cysteines and transfer it to scaffold ISCU proteins. Alternative splicing events of NFU1 gene cause the generation of a different, cytosolic, isoform that is able to bind Fe-S clusters and protect them from oxidative damage (Tong, Jameson et al. 2003). Moreover, cytosolic Nfu has been shown capable to transfer Fe-S clusters to IRP1, converting it into the cytosolic Aco1 isoform of aconitase. Even more proteins involved in formation and regulation of Fe-S clusters possess similar characteristics: this is the case of the scaffold IscU proteins. Transcript analysis indicated that alternative splicing events of the gene produce two different isoforms of IscU proteins with different subcellular localization: IscU1 in cytosol and IscU2, localized in the mitochondria (Tong and Rouault 2000).

Interestingly, the alternative splicing produces a change only in the N-terminal of the different IscU proteins, which indicates a difference in their 5' mRNA end, which mirrors what happens between Frataxin Isoform I and II. Canonical Frataxin is already known to participate with its mitochondrial partners in iron metabolism and Fe-S cluster homeostasis, while cytosolic frataxin II could act accordingly outside of mitochondria with the cytosolic isoforms of the other components (Fig. 36), communicating in a circuit involving membrane transporters (for example members of the ATP-Binding Cassette (ABC) family): it would be interesting to prove this working hypothesis in the future with co-immunoprecipitation assays to check for Isoform II association with possible cytosolic Fe-S cluster assembly and repair partners.

It is worth of notice that many proteins involved in Fe-S cluster biogenesis possess cytosolic and mitochondrial isoforms (Land and Rouault 1998) or are suspected to relocate (Soltys and Gupta 2000), which indicate that cells are able to direct their assembly in both compartments and, possibly, to vary their ratio according with changes in the metabolic condition of the cell itself: it

would be, thus, interesting to check for the expression pattern of the previous factors we mentioned after varying parameters of cellular homeostasis.

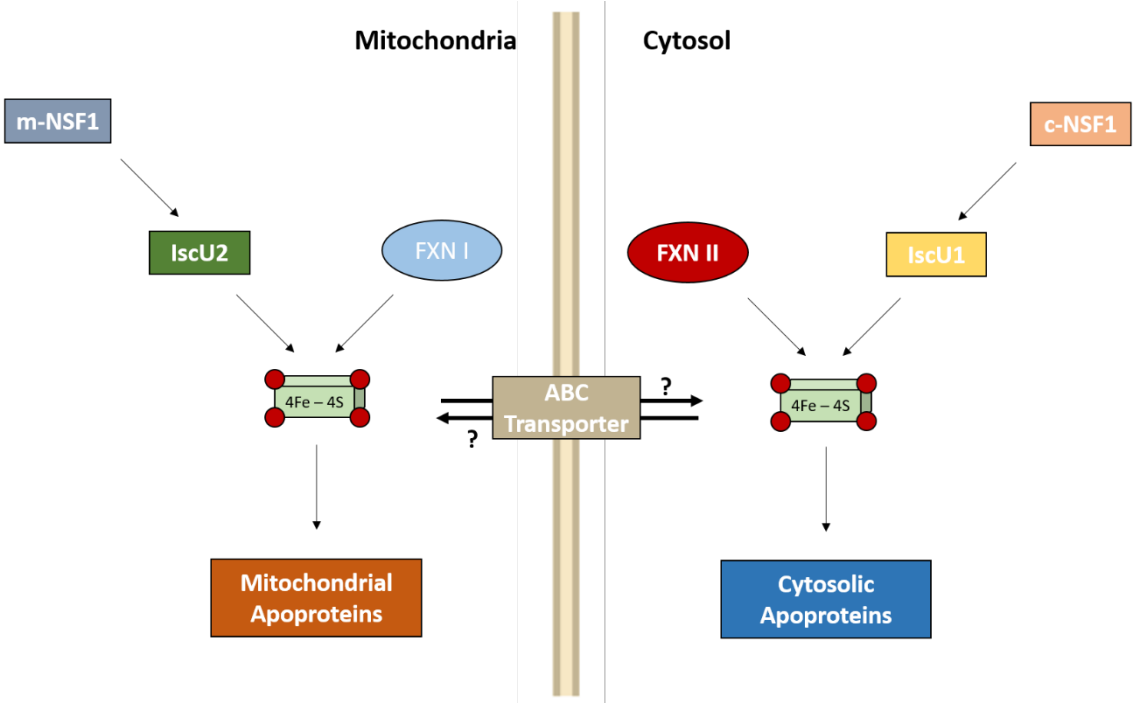

Figure 36 - Diagram showing possible mechanisms behind Fe-S clusters regulation in different subcellular compartments. Different isoforms of cysteine desulfurase NSF1 would transfer cysteine to their corresponding IscU, which would act with iron donated by the corresponding frataxin in order to regulate iron sulfur clusters formation in cytosol/mitochondria. In this view, both compartments could participate in iron sulfur cluster biogenesis thanks to transporters (ABC transporters) allowing transport of iron through the mitochondrial membrane.

Several findings have shown the existence of a cross-talk between cytosol and mitochondria regarding iron metabolism: using a conditional frataxin knockout mouse model, it has been shown that frataxin knockdown in cardiomyocytes led to an impairment in ISC biogenesis and heme synthesis, while increasing both Transferrin and Transferrin Receptor 1 (TRF1) expression and, thus, iron uptake in an emergency response. This iron was rapidly directed to the mitochondria leading to a cytosolic iron-depletion and a mitochondrial iron-overloading (Huang, Becker et al. 2009) in the effort to compensate for ISC and heme deficiency induced by frataxin silencing. The activation of Transferrin was accompanied by an inhibition of Ferritin, responsible of iron storage in cytosol, and an activation of the Mitoferrin protein, involved in the iron transport towards mitochondria, and these processes are probably regulated by iron-sensing IRP1 (Monnier, Llorens et al. 2018). Similar conclusions were achieved also in FRDA lymphoblasts (Li, Besse et al. 2008). In this view, mitochondrion and cytosol are able to send signals between them to keep the balance in iron metabolism, with frataxin isoforms being capable to mediate this cross-talk in their respective compartments. It would be interesting to integrate the results obtained by Huang

et al. and by Li et al., by specifically silencing Frataxin cytosolic Isoform II, while leaving mitochondrial isoform I in its physiological levels, to analyze what would happen to iron metabolism in that case. Another interesting analysis that could give us more inside in this argument, and that we are currently starting to perform in our group, consists in isolating proteins from healthy and patient OMS cells and fibroblasts transduced with lentiviral vectors carrying frataxin Isoform I, II, GFP or left untreated. We would then perform a proteomic analysis of mitochondrial proteome after the transduction to check for broader effects of possible modulation induced in cells after the treatments.

Apart from participating in Fe-S cluster biogenesis, frataxin may also act as a molecular chaperone to repair damaged [3Fe-4S] clusters in [4Fe-4S] one, by direct interaction with holoproteins that could contain a damaged cluster, like aconitase. As already described in the literature, one of the first causes of frataxin deficiency is shown in the decrease of mitochondrial aconitase activity (Rotig, de Lonlay et al. 1997) indicating an impairment in Fe-S cluster synthesis.

On the contrary, we demonstrated that the over expression of mature frataxin can upregulate the activity of the enzyme in OMS patient cells, as shown in figure 18. Thus, we wondered if cytosolic isoform II could also possess the ability to modulate aconitase activity. Our Western Blot results pointed at a direct upregulation of Aconitase 2 levels directly dependent on the expression of Isoform I/II, while no apparent changes in Aconitase 1 levels were seen, probably due to imprecision of the polyclonal antibody we used that was not able to detect a clear band for the protein. On the other side, when evaluating aconitase enzyme activity, our results very clearly demonstrate that both mitochondrial Isoform I and cytosolic Isoform II are able to provoke a drastic increment in aconitase activity, which is a direct indicator that both isoforms are capable of improving the Fe-S cluster biogenesis and/or repair them from, and possibly *in*, their respective cellular compartments.

Unfortunately, our protocol did not allow to distinguish between the different cytosolic or mitochondrial isoforms of aconitase and considered enzyme activity as a whole, but it would be of great interest to further confirm if Isoform I and II could specifically modulate the expression of a different isoform of the enzyme. Furthermore, apart from proving that frataxin isoforms incremented aconitase activity, we wanted to check if frataxin expression would be able to protect the Fe-S cluster of aconitase in oxidative stress conditions. For that reason, we decided to incubate neuroblastoma cells with H_2O_2 and the check for aconitase activity.

Considering that our assay allowed to check for total aconitase activity, but also the fact that each isoform express itself in a different subcellular compartment, it is of great interest the fact that both mitochondrial isoform I and cytosolic isoform II resulted able to protect the Fe-S cluster of the different aconitase isoforms they interacted with. Aco1 and Aco2 could participate, alongside their corresponding frataxin isoform partner, in maintaining a regulatory loop between the mitochondrial and cytosolic reserves of $NADP^+$/NADPH thanks to the conversion between Citrate - Isocitrate- α Ketoglutarate mediated by the different (mitochondrial and cytosolic) Isocitrate Dehydrogenase enzymes (Yoshimi, Futamura et al. 2016) (Fig. 37).

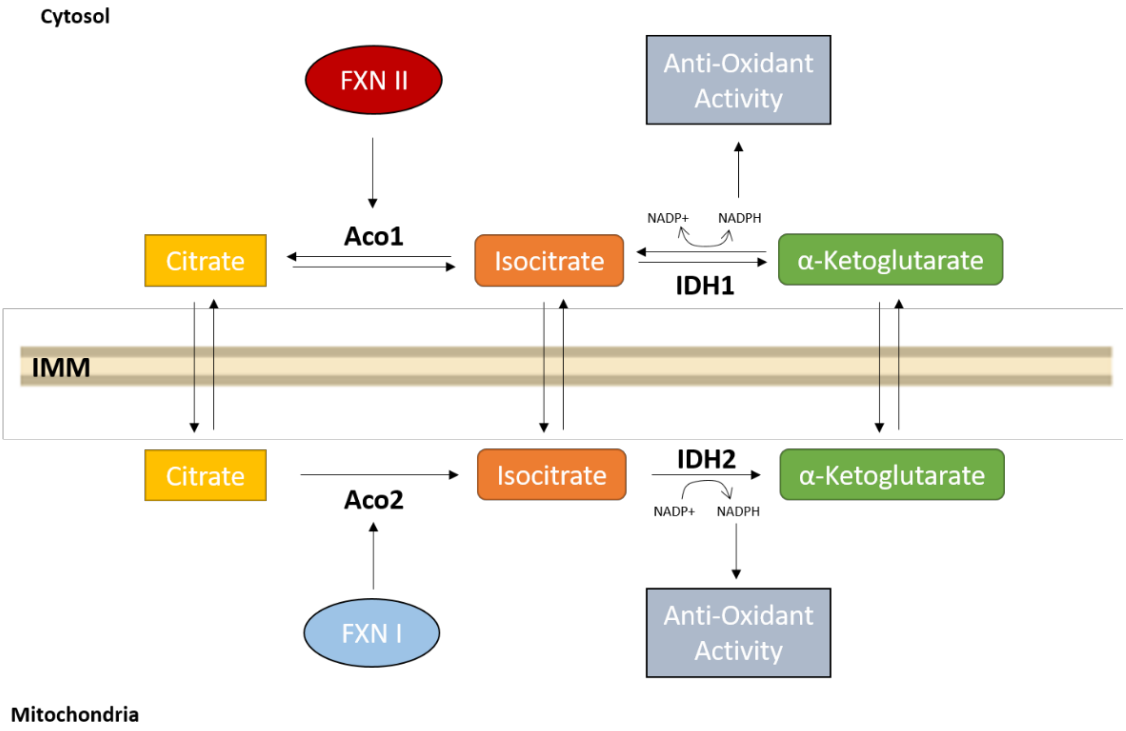

Figure 37 - Diagram showing the possible regulatory feedback loop between mitochondrial and cytosolic Aconitase isoforms.

The possible participation of Isocitrate Dehydrogenase 1 and 2 (IDH1 and IDH2) in the loss of the redox homeostasis upon frataxin deficiency is worth investigating in more detail. Interestingly, a relationship between IDH2, mitochondrial dysfunction and neurodegeneration has been indicated in some experimental models of Parkinson's Disease (Kim, Kim et al. 2016; Yang, Kim et al. 2017).

2. Frataxin regulation by non-erythropoietic EPO mimetic peptides

As mentioned in the introduction, previous work demonstrated that EPO was able to increment frataxin levels in FRDA primary lymphoblasts, lymphocytes and fibroblasts (Sturm, Stupphann et al. 2005), while rising the hematocrit (Boesch, Sturm et al. 2008), making chronic treatments with canonical EPO unviable and that is why modified versions of EPO peptide are currently being used in research. Erythropoietin is a glycoproteic hormone mainly secreted by the kidney, with the prevalent role of inducing red blood cells production, inducing mitosis in erythroid precursors and secure survival of erythroid progenitors (Gross and Goldwasser 1970; Koury and Bondurant 1990). These effects are mediated after the binding to a homodimeric Epo receptor (EPO-R), which is located on the membrane of target cells, which after the binding gets glycosylated and phosphorylated (Sawyer and Hankins 1993). EPO-R belongs to the family of cytokine receptor whose signal transduction is mediated by Janus kinase (JAK). After EPO binding, EPO-R undergoes conformational changes that allow JAK kinases to associate with it, phosphorylating itself and EPO-R. This activates a signaling cascade resulting in the increase in the modulation, apart from erythropoietic genes, of survival, cell growth and anti-apoptotic factors mediated by the signal transducer and activator of transcription factors (STAT). EPO is not only involved in erythropoiesis and several other target cells and tissues have been identified over the years, including for example mouse cerebellum and cortex (Digicaylioglu, Bichet et al. 1995), where it has been shown that EPO expression can have neuroprotective effects after the induction of several stress conditions (Letourneur, Petit et al. 2013; Si, Wang et al. 2019) . This opened the way for the proposition of different pathways for EPO action: a classical erythropoietic one and the alternative promoting cell survival and growth ameliorating metabolically stressed tissues and cells. This secondary anti-inflammatory pathway is probably activated through the binding of EPO to an alternative EPO-R receptor composed by an heterodimer between classical EPO-R monomer and the receptor of several cytokines including interleukin 5 and 3 (Brines 2010). This alternative receptor is responsible for the cytoprotective properties of Epo (Brines, Patel et al. 2008; Ueba, Brines et al. 2010). Some Epo-analogues like the carbamylated form CEPO or mimetic competitors like the small Helix-B Surface Peptide (HBSP or ARA290), can bind the alternative heterodimeric receptor without eliciting the effects of classical EPO. It has been found that HBSP, in mice, can protect cardiac functions and reduce apoptosis in cardiomyocytes after inducing ischemia (Liu, You et al. 2016) and also attenuate cardiomyopathies after inducing diabetes (Lin, Zhang et al. 2017). The drawback of HBSP seems to be its low half-life that is around 2 minutes in plasma of rats and rabbits (Brines, Patel et al. 2008) and, for this reason, it appears fundamental to search for more stable alternatives, like the retro-enantiomer peptides we focused on. After assaying various peptides with different chemical modifications in their N-

terminal domain, we focused our efforts with the EPO2 that gave us the strongest response which could be due, for example, to stronger interactions with EPO receptor due to the acetyl group the peptide expressed.

In this work, we have demonstrated the effect of EPO2 on frataxin modulation, which has been confirmed both *in vivo* and *in vitro* in different models. *In vitro*, both peptides seemed to be able to produce an increment in frataxin levels, even though not as strong as the increments spotted *in vivo*. This could be due to the fact that both our cellular models, mesenchymal stem cells and fibroblasts, could express less EPO-R levels than the ones present in the whole target organ (cerebrum, cerebellum, etc.), thus eliciting a weaker response, or maybe for some instability of the peptides reacting with cellular medium components. Being able to see the effects of the peptides in *in vivo* brain extracts after being injected intraperitoneally, it seems safe to assume that EPO2 is capable of penetrating the blood-brain barrier (BBB) which is in line with what is known about classical human-recombinant EPO (Siren, Fratelli et al. 2001; Villa, Bigini et al. 2003). Similar results on frataxin levels were seen in cerebellum extracts, where actually our EPO2 had a much stronger effect on frataxin when compared to HBSP peptide, which could be due to its stronger stability granting, thus, prolonged effects. Interestingly, other authors have used chemical agonists of alternative EPO-R (called STS-E412 and STS-E424) comparing them to rhEPO and have reported increased *in vivo* frataxin levels in their KIKO mouse model, but only in brain and heart (Miller, Rai et al. 2017).

Previous work from our laboratory and other groups (Wang, Zhang et al. 2007) suggested that between the potential mediators of EPO (and its derivatives) effects are involved partners like SHH, which is why we used its inhibitor cyclopamine when screening between the four different synthetic EPO versions, the Signal Transducer and Activator of Transcription 5 (STAT5), mitogen-activated protein kinase (MAPK) or protein kinase C (PKC) (Hernandez, Burgos et al. 2017; Suarez-Mendez, Tovilla-Zarate et al. 2018). Indeed, in order to search for possible mediators of the effects described, we performed, in cortical neurons, a qRT-PCR experiment where, as a very preliminary result, we saw a slight increase of some neurotrophins such as BDNF and NT-3 after the treatment with EPO2.

Interestingly, other authors saw that, in cortical neurons, these neurotrophins, through the binding to their receptor of the Tyrosine Receptor Kinase family (Trk) are able to activate STAT5 in a JAK-independent manner (Klein, Hempstead et al. 2005). Together this result with ours seem to indicate that EPO could activate STAT5 upregulating the expression of neurotrophins like BDNF or NT-3 that, in turn, could keep activating STAT5 in a paracrine or autocrine regulatory positive feedback. Furthermore, previous work from our lab has demonstrated that BDNF is directly related in the modulation of frataxin levels, so that could be another mechanism behind

EPO actions. Moreover, in our initial peptide screening, the frataxin upregulation observed after EPOs treatment was reduced when cells were treated with K252a, a specific inhibitor of protein kinase receptors of Trk family, target of neurotrophins (Tapley, Lamballe et al. 1992).

Together these findings indicate that there is some correlation between these factors, EPO, BDNF, Trk receptors and SHH, whose regulatory mechanisms are still to be properly investigated and unraveled (Fig. X).

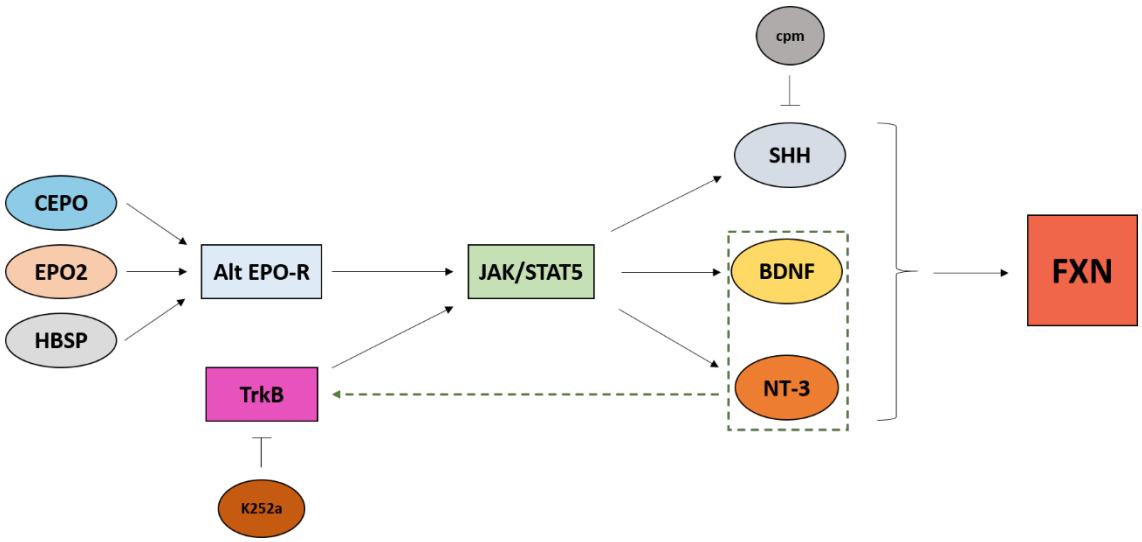

Figure 38 - Diagram showing possible regulatory mechanisms behind frataxin modulation by EPO peptides. EPO binding to the heterodimer alternative EPO receptor activates JAK-STAT5 signaling pathway upregulating Sonic Hedgehog (SHH), Neurotrophin 3 (NT-3) and Brain Derived Neurotrophic Factor (BDNF). These partners are involved in frataxin modulation, since the use of SHH pathway inhibitor cyclopamine (cpm) or an inhibitor of the Tyrosine Kinase receptors (K252a) significantly reduces frataxin upregulation by EPO. Trk receptor activation by neurotrophins activates STAT5, thus hypothesizing the existence of a positive regulatory feedback circuit.

3. Physical exercise as a non-pharmacological approach for FRDA

Finally, in the effort to elucidate novel molecular mechanisms behind frataxin regulation, we studied the effects of physical activity on the expression of frataxin in the cerebellum.

Physical activity is a field constantly gathering extreme importance as a potential treatment for many neurological diseases, including Huntington disease (Busse, Quinn et al. 2013) and neuromuscular diseases (Cup, Pieterse et al. 2007). As previously stated in the introduction, physical exercise has been shown both in human and in mouse (Fordyce and Wehner 1993; Kramer, Hahn et al. 1999) to improve neural functions and to even be able to induce hippocampal neurogenesis (van Praag, Shubert et al. 2005), probably thanks to the positive effects of exercise on the production of several neurotrophic factors, cytokines and hormones. One of these possible mediators could be, for example, the Insulin-like Growth Factor-1 (IGF-1) which is known to be activated in brain after exercise (Cotman, Berchtold et al. 2007) and to exert positive effects on FRDA patients during therapies (Sanz-Gallego, Torres-Aleman et al. 2014). It is known that in hippocampus physical activity upregulates expression of factors like BDNF (Vaynman, Ying et al. 2004; Marlatt, Potter et al. 2012), through a pathway involving the activation of PGC1α and Fibronectin Type III Domain Containing 5 (FNDC5) (Wrann, White et al. 2013). The positive effects of moderate treadmill exercise were detected in mouse models of Alzheimer's disease (AD), where PGC1α and FNDC5 upregulated BDNF levels preventing cognitive decline in these mice (Azimi, Gharakhanlou et al. 2018). Our lab has demonstrated the correlation between BDNF and frataxin (Katsu-Jimenez, Loria et al. 2016): that is why we wanted to investigate the effects of physical activity in the cerebellum on frataxin, being one of the most affected areas during FRDA development, as a potential non-pharmacological approach in FRDA treatment. In our experimental plan, we performed an eight weeks spontaneous physical activity protocol, during which the animals were free to run for the time and amount they desired, while we monitored the amount of physical activity expressed as meters/24h. Within this group, we were able to identify a subgroup of animals that ran more than other runners, which were useful to explore for regulatory effects directly dependent to the amount of exercise. We were able to see increments of frataxin protein levels in the runner group when comparing it to the sedentary one, with a stronger increment of frataxin levels in the high runner subgroup, pointing to an amount-related effect of spontaneous physical activity. Surprisingly, no frataxin mRNA changes were detected between the different groups, pointing the way for a post-transcriptional regulatory mechanism induced by spontaneous physical activity.

Searching for mediators, we investigated whether there were changes in the factors we had already hypothesized to be involved in frataxin expression modulation. We saw increments in the

levels of NT-3 and SHH. SHH is also thought, in rat and mouse hippocampus, to be involved, with mechanisms not yet fully known, in adult neurogenesis, being activated after physical exercise (Banerjee, Rajendran et al. 2005; Fabel and Kempermann 2008).

Surprisingly, we were not able to detect changes in BDNF levels, protein or mRNA, while it is well known to be upregulated after physical exercise in hippocampus (Vaynman, Ying et al. 2004). This could be interpreted not as a lack of upregulation of BDNF but, as suggested by other authors, to the fact that this neurotrophin could be upregulated in the first time-window upon physical exercise, being transient and characteristic of the first "phase" (Klintsova, Dickson et al. 2004). In their study, Klintsova et al. saw that, after a protocol of just two weeks of voluntary physical exercise (versus our eight), there were no changes in BDNF levels (mRNA or protein) in mouse cerebellum after the whole fourteen days period, while they were able to observe increments in BDNF levels during the first week of their experiment. So, BDNF could be an early mediator of physical exercise induced in the first phases, acting transiently to upregulate more downstream factors, like the previously mentioned NT-3 and SHH. To gain further insight on the possible mediators involved in frataxin increment post-exercise, we decided to upscale the screening with a Cytokine Array testing it with our cerebellar lysates, always comparing the sedentary and runner groups. We were able to identify several upregulated cytokines after physical exercise: between the highly upregulated ones, we found the Vascular Endothelial Growth Factor A (VEGF-A), which was expected, being a factor involved in promoting angiogenesis and vasculogenesis, events clearly promoted by any kind of physical activity (Morland, Andersson et al. 2017) and the Transforming Growth Factor β (TGF-β), which has been described to promote the "fatigue" sensation and to be upregulated by physical exercise (Inoue, Yamazaki et al. 1999).

Besides, we identified several upregulated cytokines related to frataxin regulation and expression, which were the most interesting for our aims: MIP-1α, SCF, IFNγ and IL-6. Interleukin 6, considered to be a pro-inflammatory cytokine produced after several stimuli, was initially thought to be related only to the maturation of B-cells into antibody producing cell types, while later evidences demonstrated that it was expressed also in some neural cell lines (Yasukawa, Hirano et al. 1987), opening the way for its roles in axonal sprouting and regeneration in hippocampus (Hakkoum, Stoppini et al. 2007) and in adult neurogenesis (Bauer, Kerr et al. 2007), which is a phenomenon affected by a plethora of factors, including precisely physical exercise. In regards to MIP-1α and IFNγ, these two cytokines are known to be involved in inflammatory processes in the immune system, where secretion of MIP-1α from macrophages after recognition of pathogens, promotes IFNγ synthesis in Natural Killer (NK) cells (Schroder, Hertzog et al. 2004) and there have been evidences of IFNγ release also by many cellular types of CNS, like

microglia, sensory neurons and astrocytes (Neumann, Schmidt et al. 1997; Lau and Yu 2001; Makela, Osterlund et al. 2011).

Furthermore, MIP-1α receptors have been identified in several areas of CNS like hippocampus, cortex, cerebellum and brain stem (Van Der Meer, Goldberg et al. 2001; Xu, Long et al. 2009) and there have been evidences that, in rat hippocampus, chronic treatments with MIP-1α improved neuronal activity by upregulating the N-methyl-D-aspartate receptor (NMDAR) and, consequently, Ca^{2+} signals, improving neuronal plasticity (Kuijpers, van Gassen et al. 2010). IFNγ, which is also involved in iron metabolism (Byrd and Horwitz 1993), has also shown promising effects *in vitro* in FRDA patient fibroblasts where it was able to increase frataxin mRNA levels (Wells, Seyer et al. 2015), and *in vivo* in YG8r mice, where, in dorsal root ganglia, IFNγ treatment resulted in improved coordination and locomotor activity (Tomassini, Arcuri et al. 2012). Finally, there have been evidences of IFNγ upregulating SHH mRNA and protein expression in cerebellum, showing a deep regulatory web between all the factors involved (Wang, Lin et al. 2004). Taken together into account, all these data seem to point to a deep regulatory mechanism started by physical activity that ultimately leads to frataxin upregulation, giving a stronger emphasis on exercise as a potential non-invasive treatment for FRDA (Fig. 39). It would be very interesting to investigate also the potential effect of a forced exercise, in a context of physical exhaustion, versus our voluntary running experiments to check which pathways are activated in that other model.

In addition, as mentioned previously, one of the principal mediators of physical exercise effects is PGC-1α and, recently, it has been described that alternative promoters can be activated under different stimuli, resulting in the transcription of different PGC-1α isoforms, in particular the so called PGC-1α1 and PGC-1α4. The α4 isoform, after overexpression in skeletal muscle, seems to be involved in muscle hypertrophy, granting muscle mass and strength (Ruas, White et al. 2012), while isoform α1 seems to participate in oxidative metabolism and mitochondrial biogenesis, being responsible of improving endurance in muscle fibers (Arany 2008; Agudelo, Femenia et al. 2014).

Under these interesting highlights, we are going to investigate the effects on frataxin regulation in transgenic mouse models constitutively expressing the different PGC-1α isoform in skeletal muscle, under the promotor of the muscle creatine kinase, which will further clarify the molecular mechanisms behind frataxin upregulation after physical exercise. Since we were able to obtain the samples just very recently, there has been no time to perform the appropriate analyses, but this will undoubtedly one of the most intriguing future focuses of our research.

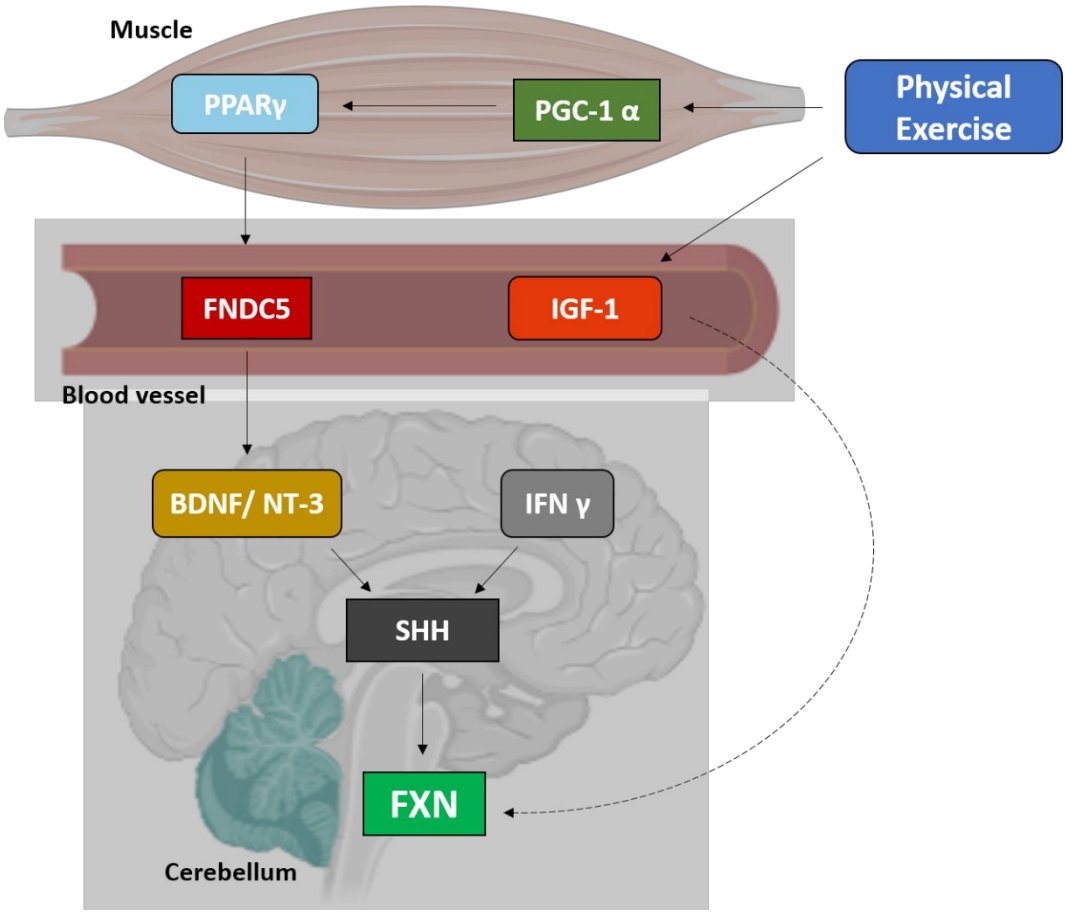

Figure 39 - Model of frataxin regulation in cerebellum after spontaneous physical activity. Physical exercise, through a pathway involving PGC-1α, PPARγ and FNDC5, promotes the expressions of several neurotrophins and cytokines which are able to induce several positive effects on cells and, ultimately, to positively modulate frataxin levels.

4. Frataxin expression regulation mechanisms in FRDA

There is no cure for Friedreich's Ataxia, at the moment. Many therapeutic strategies are being currently investigated and explored, with some avenues being more promising than others. We have tried to elucidate some of the potential mechanisms behind frataxin expression by several factors which are getting more interest from a therapeutic point of view, like physical exercise or epomimetic peptides, showing that there is a direct effect of physical activity on frataxin levels involving many potential mediators that are also important in the epomimetic peptides response in our models, putting under the spotlight factors like neurotrophins, tyrosike kinase receptors and the Sonic Hedgehog signaling pathway (Fig. 40). Furthermore, we have also tried to enlighten the roles and functions on a controversial topic, like frataxin isoforms, which has been debated in FRDA literature without reaching clear conclusions on the potential roles of the different isoforms described. While we have not confirmed the existence of the nuclear isoform III, we have shown some of the potential cross-talk mechanisms between the mitochondrial Isoform I and the cytosolic Isoform II, which could prove useful in the unraveling of the molecular mechanisms during FRDA development.

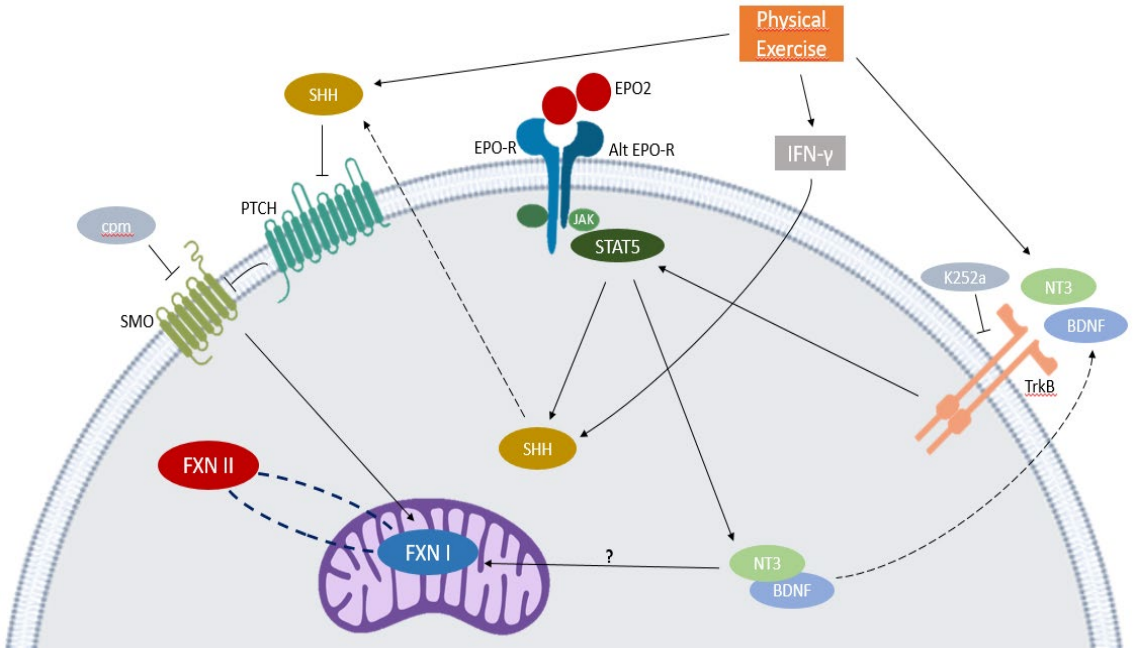

Figure 40 - Model of Frataxin regulation of the different approaches analyzed in this thesis. The model depicted in the figure illustrates the possible mechanisms behind frataxin regulation after physical activity or Epo mimetic peptides treatment. Physical exercise leads to the upregulation of the mediators of frataxin expression IFNg, NT-3 and BDNF and, consequently, to frataxin increased levels. Meanwhile, EPO2 binding to the heterodimer composed by EPO receptor and the alternative EPO-R, causes upregulation of neurotrophins like NT-3 and BDNF and activates the SHH pathway. In the presence of SHH, the cell-surface transmembrane protein Patched (PTCH) is inhibited, allowing the receptor Smoothenhead (SMO) to start its signaling cascade, ultimately leading to Frataxin increment. The cross-talk between mitochondria and cytosol frataxin isoforms is briefly shown in the picture using the dotted circle.

Conclusions

1. An extra mitochondrial pool of frataxin has been observed in several cellular models. The cytosolic localization of Frataxin Isoform II has been confirmed, while no nuclear Frataxin Isoform III has been detected.

2. Frataxin Isoform I overexpression increase the mitochondrial network, while Isoform II overexpression does not have any observable effect in this aspect.

3. The overexpression of both mitochondrial and cytosolic Frataxin isoforms improves mitochondrial respiration in FRDA patient cells and also increases the expression of some mitochondrial biomarkers (VDAC and aconitase).

4. The overexpression of both mitochondrial and cytosolic Frataxin isoforms increases Aconitase activity, and furthermore protects the enzyme from oxidative stress inactivation.

5. The retro-enantiomer erythropoietin-derived EPO2 peptide increases Frataxin expression in different cellular models and *in vivo*, in the cerebellum.

6. Spontaneous physical activity in wild type mice leads to an increase in Frataxin levels in the cerebellum. This may be due at least in part to a post-transcriptional mechanism.

7. Physical exercise in mice also increases the levels of some factors including SHH, NT-3, MIP-1α and IFN-γ, which might be putative mediators of the effects of physical activity on frataxin expression.

Bibliography

Abeti, R., A. Baccaro, et al. (2018). "Novel Nrf2-Inducer Prevents Mitochondrial Defects and Oxidative Stress in Friedreich's Ataxia Models." Front Cell Neurosci **12**: 188.

Acquaviva, F., I. Castaldo, et al. (2008). "Recombinant human erythropoietin increases frataxin protein expression without increasing mRNA expression." Cerebellum **7**(3): 360-365.

Adamec, J., F. Rusnak, et al. (2000). "Iron-dependent self-assembly of recombinant yeast frataxin: implications for Friedreich ataxia." Am J Hum Genet **67**(3): 549-562.

Agudelo, L. Z., T. Femenia, et al. (2014). "Skeletal muscle PGC-1alpha1 modulates kynurenine metabolism and mediates resilience to stress-induced depression." Cell **159**(1): 33-45.

Al-Mahdawi, S., R. M. Pinto, et al. (2006). "GAA repeat expansion mutation mouse models of Friedreich ataxia exhibit oxidative stress leading to progressive neuronal and cardiac pathology." Genomics **88**(5): 580-590.

Anderson, P. R., K. Kirby, et al. (2005). "RNAi-mediated suppression of the mitochondrial iron chaperone, frataxin, in Drosophila." Hum Mol Genet **14**(22): 3397-3405.

Andrabi, S. A., G. K. Umanah, et al. (2014). "Poly(ADP-ribose) polymerase-dependent energy depletion occurs through inhibition of glycolysis." Proc Natl Acad Sci U S A **111**(28): 10209-10214.

Ang, E. T., P. T. Wong, et al. (2003). "Neuroprotection associated with running: is it a result of increased endogenous neurotrophic factors?" Neuroscience **118**(2): 335-345.

Anjomani Virmouni, S., V. Ezzatizadeh, et al. (2015). "A novel GAA-repeat-expansion-based mouse model of Friedreich's ataxia." Dis Model Mech **8**(3): 225-235.

Arany, Z. (2008). "PGC-1 coactivators and skeletal muscle adaptations in health and disease." Curr Opin Genet Dev **18**(5): 426-434.

Azimi, M., R. Gharakhanlou, et al. (2018). "Moderate treadmill exercise ameliorates amyloid-beta-induced learning and memory impairment, possibly via increasing AMPK activity and up-regulation of the PGC-1alpha/FNDC5/BDNF pathway." Peptides **102**: 78-88.

Banerjee, S. B., R. Rajendran, et al. (2005). "Recruitment of the Sonic hedgehog signalling cascade in electroconvulsive seizure-mediated regulation of adult rat hippocampal neurogenesis." Eur J Neurosci **22**(7): 1570-1580.

Baralle, M., T. Pastor, et al. (2008). "Influence of Friedreich ataxia GAA noncoding repeat expansions on pre-mRNA processing." Am J Hum Genet **83**(1): 77-88.

Bauer, S., B. J. Kerr, et al. (2007). "The neuropoietic cytokine family in development, plasticity, disease and injury." Nat Rev Neurosci **8**(3): 221-232.

Bencze, K. Z., T. Yoon, et al. (2007). "Human frataxin: iron and ferrochelatase binding surface." Chem Commun (Camb)(18): 1798-1800.

Boesch, S., W. Nachbauer, et al. (2014). "Safety and tolerability of carbamylated erythropoietin in Friedreich's ataxia." Mov Disord **29**(7): 935-939.

Boesch, S., B. Sturm, et al. (2008). "Neurological effects of recombinant human erythropoietin in Friedreich's ataxia: a clinical pilot trial." Mov Disord **23**(13): 1940-1944.

Bolinches-Amoros, A., B. Molla, et al. (2014). "Mitochondrial dysfunction induced by frataxin deficiency is associated with cellular senescence and abnormal calcium metabolism." Front Cell Neurosci **8**: 124.

Braymer, J. J. and R. Lill (2017). "Iron-sulfur cluster biogenesis and trafficking in mitochondria." J Biol Chem **292**(31): 12754-12763.

Brines, M. (2010). "The therapeutic potential of erythropoiesis-stimulating agents for tissue protection: a tale of two receptors." Blood Purif **29**(2): 86-92.

Brines, M. and A. Cerami (2005). "Emerging biological roles for erythropoietin in the nervous system." Nat Rev Neurosci **6**(6): 484-494.

Brines, M., N. S. Patel, et al. (2008). "Nonerythropoietic, tissue-protective peptides derived from the tertiary structure of erythropoietin." Proc Natl Acad Sci U S A **105**(31): 10925-10930.

Brittenham, G. M., D. G. Nathan, et al. (2003). "Deferiprone and hepatic fibrosis." Blood **101**(12): 5089-5090; author reply 5090-5081.

Bulteau, A. L., H. A. O'Neill, et al. (2004). "Frataxin acts as an iron chaperone protein to modulate mitochondrial aconitase activity." Science **305**(5681): 242-245.

Busse, M., L. Quinn, et al. (2013). "A randomized feasibility study of a 12-week community-based exercise program for people with Huntington's disease." J Neurol Phys Ther **37**(4): 149-158.

Butler, J. S. and M. Napierala (2015). "Friedreich's ataxia--a case of aberrant transcription termination?" Transcription **6**(2): 33-36.

Byrd, T. F. and M. A. Horwitz (1993). "Regulation of transferrin receptor expression and ferritin content in human mononuclear phagocytes. Coordinate upregulation by iron transferrin and downregulation by interferon gamma." J Clin Invest **91**(3): 969-976.

Calap-Quintana, P., J. A. Navarro, et al. (2018). "Drosophila melanogaster Models of Friedreich's Ataxia." Biomed Res Int **2018**: 5065190.

Calatrava-Ferreras, L., R. Gonzalo-Gobernado, et al. (2016). "Liver Growth Factor (LGF) Upregulates Frataxin Protein Expression and Reduces Oxidative Stress in Friedreich's Ataxia Transgenic Mice." Int J Mol Sci **17**(12).

Campos, C., N. B. Rocha, et al. (2016). "Exercise-induced neuroprotective effects on neurodegenerative diseases: the key role of trophic factors." Expert Rev Neurother **16**(6): 723-734.

Campuzano, V., L. Montermini, et al. (1997). "Frataxin is reduced in Friedreich ataxia patients and is associated with mitochondrial membranes." Hum Mol Genet **6**(11): 1771-1780.

Campuzano, V., L. Montermini, et al. (1996). "Friedreich's ataxia: autosomal recessive disease caused by an intronic GAA triplet repeat expansion." Science **271**(5254): 1423-1427.

Cnop, M., H. Mulder, et al. (2013). "Diabetes in Friedreich ataxia." J Neurochem **126 Suppl 1**: 94-102.

Colcombe, S. and A. F. Kramer (2003). "Fitness effects on the cognitive function of older adults: a meta-analytic study." Psychol Sci **14**(2): 125-130.

Colin, F., A. Martelli, et al. (2013). "Mammalian frataxin controls sulfur production and iron entry during de novo Fe4S4 cluster assembly." J Am Chem Soc **135**(2): 733-740.

Condo, I., F. Malisan, et al. (2010). "Molecular control of the cytosolic aconitase/IRP1 switch by extramitochondrial frataxin." Hum Mol Genet **19**(7): 1221-1229.

Condo, I., N. Ventura, et al. (2006). "A pool of extramitochondrial frataxin that promotes cell survival." J Biol Chem **281**(24): 16750-16756.

Coppola, G., R. Burnett, et al. (2011). "A gene expression phenotype in lymphocytes from Friedreich ataxia patients." Ann Neurol **70**(5): 790-804.

Coppola, G., D. Marmolino, et al. (2009). "Functional genomic analysis of frataxin deficiency reveals tissue-specific alterations and identifies the PPARgamma pathway as a therapeutic target in Friedreich's ataxia." Hum Mol Genet **18**(13): 2452-2461.

Cossee, M., H. Puccio, et al. (2000). "Inactivation of the Friedreich ataxia mouse gene leads to early embryonic lethality without iron accumulation." Hum Mol Genet **9**(8): 1219-1226.

Cossee, M., M. Schmitt, et al. (1997). "Evolution of the Friedreich's ataxia trinucleotide repeat expansion: founder effect and premutations." Proc Natl Acad Sci U S A **94**(14): 7452-7457.

Cotman, C. W., N. C. Berchtold, et al. (2007). "Exercise builds brain health: key roles of growth factor cascades and inflammation." Trends Neurosci **30**(9): 464-472.

Cup, E. H., A. J. Pieterse, et al. (2007). "Exercise therapy and other types of physical therapy for patients with neuromuscular diseases: a systematic review." Arch Phys Med Rehabil **88**(11): 1452-1464.

Chamberlain, S., W. A. Cramp, et al. (1981). "Defects in newly synthesised DNA in skin fibroblasts from patients with Friedreich's ataxia." Lancet **1**(8230): 1165.

Chamberlain, S., J. Shaw, et al. (1988). "Mapping of mutation causing Friedreich's ataxia to human chromosome 9." Nature **334**(6179): 248-250.

Chattaragada, M. S., C. Riganti, et al. (2018). "FAM49B, a novel regulator of mitochondrial function and integrity that suppresses tumor metastasis." Oncogene **37**(6): 697-709.

Chiang, S., Z. Kovacevic, et al. (2016). "Frataxin and the molecular mechanism of mitochondrial iron-loading in Friedreich's ataxia." Clin Sci (Lond) **130**(11): 853-870.

Chiocchetti, A. G., D. Haslinger, et al. (2016). "Transcriptomic signatures of neuronal differentiation and their association with risk genes for autism spectrum and related neuropsychiatric disorders." Transl Psychiatry **6**(8): e864.

de Assis, G. G. and K. M. de Almondes (2017). "Exercise-dependent BDNF as a Modulatory Factor for the Executive Processing of Individuals in Course of Cognitive Decline. A Systematic Review." Front Psychol **8**: 584.

De Castro, M., J. Garcia-Planells, et al. (2000). "Genotype and phenotype analysis of Friedreich's ataxia compound heterozygous patients." Hum Genet **106**(1): 86-92.

Digicaylioglu, M., S. Bichet, et al. (1995). "Localization of specific erythropoietin binding sites in defined areas of the mouse brain." Proc Natl Acad Sci U S A **92**(9): 3717-3720.

Ding, Q., S. Vaynman, et al. (2006). "Insulin-like growth factor I interfaces with brain-derived neurotrophic factor-mediated synaptic plasticity to modulate aspects of exercise-induced cognitive function." Neuroscience **140**(3): 823-833.

Evans-Galea, M. V., N. Carrodus, et al. (2012). "FXN methylation predicts expression and clinical outcome in Friedreich ataxia." Ann Neurol **71**(4): 487-497.

Fabel, K. and G. Kempermann (2008). "Physical activity and the regulation of neurogenesis in the adult and aging brain." Neuromolecular Med **10**(2): 59-66.

Finocchiaro, G., G. Baio, et al. (1988). "Glucose metabolism alterations in Friedreich's ataxia." Neurology **38**(8): 1292-1296.

Fleming, J., A. Spinoulas, et al. (2005). "Partial correction of sensitivity to oxidant stress in Friedreich ataxia patient fibroblasts by frataxin-encoding adeno-associated virus and lentivirus vectors." Hum Gene Ther **16**(8): 947-956.

Fontecave, M. (2006). "Iron-sulfur clusters: ever-expanding roles." Nat Chem Biol **2**(4): 171-174.

Fordyce, D. E. and J. M. Wehner (1993). "Physical activity enhances spatial learning performance with an associated alteration in hippocampal protein kinase C activity in C57BL/6 and DBA/2 mice." Brain Res **619**(1-2): 111-119.

Foury, F. and O. Cazzalini (1997). "Deletion of the yeast homologue of the human gene associated with Friedreich's ataxia elicits iron accumulation in mitochondria." FEBS Lett **411**(2-3): 373-377.

Fuss, J. O., C. L. Tsai, et al. (2015). "Emerging critical roles of Fe-S clusters in DNA replication and repair." Biochim Biophys Acta **1853**(6): 1253-1271.

Gakh, O., J. Adamec, et al. (2002). "Physical evidence that yeast frataxin is an iron storage protein." Biochemistry **41**(21): 6798-6804.

Gakh, O., T. Bedekovics, et al. (2010). "Normal and Friedreich ataxia cells express different isoforms of frataxin with complementary roles in iron-sulfur cluster assembly." J Biol Chem **285**(49): 38486-38501.

Gakh, O., S. Park, et al. (2006). "Mitochondrial iron detoxification is a primary function of frataxin that limits oxidative damage and preserves cell longevity." Hum Mol Genet **15**(3): 467-479.

Galea, C. A., A. Huq, et al. (2016). "Compound heterozygous FXN mutations and clinical outcome in friedreich ataxia." Ann Neurol **79**(3): 485-495.

Gimenez-Cassina, A., F. Lim, et al. (2006). "Differentiation of a human neuroblastoma into neuron-like cells increases their susceptibility to transduction by herpesviral vectors." J Neurosci Res **84**(4): 755-767.

Gomez-Sebastian, S., A. Gimenez-Cassina, et al. (2007). "Infectious Delivery and Expression of a 135 kb Human FRDA Genomic DNA Locus Complements Friedreich's Ataxia Deficiency in Human Cells." Mol Ther **15**(2): 248-254.

Goncalves, S., V. Paupe, et al. (2008). "Deferiprone targets aconitase: implication for Friedreich's ataxia treatment." BMC Neurol **8**: 20.

Gonzalez-Cabo, P., R. P. Vazquez-Manrique, et al. (2005). "Frataxin interacts functionally with mitochondrial electron transport chain proteins." Hum Mol Genet **14**(15): 2091-2098.

Gross, M. and E. Goldwasser (1970). "On the mechanism of erythropoietin-induced differentiation. VII. The relationship between stimulated deoxyribonucleic acid synthesis and ribonucleic acid synthesis." J Biol Chem **245**(7): 1632-1636.

Guo, L., Q. Wang, et al. (2018). "Characterization of a new N-terminally acetylated extra-mitochondrial isoform of frataxin in human erythrocytes." Sci Rep **8**(1): 17043.

Hakkoum, D., L. Stoppini, et al. (2007). "Interleukin-6 promotes sprouting and functional recovery in lesioned organotypic hippocampal slice cultures." J Neurochem **100**(3): 747-757.

Haugen, A. C., N. A. Di Prospero, et al. (2010). "Altered gene expression and DNA damage in peripheral blood cells from Friedreich's ataxia patients: cellular model of pathology." PLoS Genet **6**(1): e1000812.

Herman, D., K. Jenssen, et al. (2006). "Histone deacetylase inhibitors reverse gene silencing in Friedreich's ataxia." Nat Chem Biol **2**(10): 551-558.

Hernandez, C. C., C. F. Burgos, et al. (2017). "Neuroprotective effects of erythropoietin on neurodegenerative and ischemic brain diseases: the role of erythropoietin receptor." Neural Regen Res **12**(9): 1381-1389.

Hick, A., M. Wattenhofer-Donze, et al. (2013). "Neurons and cardiomyocytes derived from induced pluripotent stem cells as a model for mitochondrial defects in Friedreich's ataxia." Dis Model Mech **6**(3): 608-621.

Huang, M. L., E. M. Becker, et al. (2009). "Elucidation of the mechanism of mitochondrial iron loading in Friedreich's ataxia by analysis of a mouse mutant." Proc Natl Acad Sci U S A **106**(38): 16381-16386.

Inoue, K., H. Yamazaki, et al. (1999). "Transforming growth factor-beta activated during exercise in brain depresses spontaneous motor activity of animals. Relevance To central fatigue." Brain Res **846**(2): 145-153.

Isaya, G., H. A. O'Neill, et al. (2004). "Functional studies of frataxin." Acta Paediatr Suppl **93**(445): 68-71; discussion 72-63.

Jasoliya, M. J., M. Z. McMackin, et al. (2017). "Frataxin deficiency impairs mitochondrial biogenesis in cells, mice and humans." Hum Mol Genet **26**(14): 2627-2633.

Jauslin, M. L., S. Vertuani, et al. (2007). "Protective effects of Fe-Aox29, a novel antioxidant derived from a molecular combination of Idebenone and vitamin E, in immortalized fibroblasts and fibroblasts from patients with Friedreich Ataxia." Mol Cell Biochem **302**(1-2): 79-85.

Kakhlon, O., H. Manning, et al. (2008). "Cell functions impaired by frataxin deficiency are restored by drug-mediated iron relocation." Blood **112**(13): 5219-5227.

Katsu-Jimenez, Y., F. Loria, et al. (2016). "Gene Transfer of Brain-derived Neurotrophic Factor (BDNF) Prevents Neurodegeneration Triggered by FXN Deficiency." Mol Ther **24**(5): 877-889.

Kauppila, J. H. K., N. A. Bonekamp, et al. (2018). "Base-excision repair deficiency alone or combined with increased oxidative stress does not increase mtDNA point mutations in mice." Nucleic Acids Res **46**(13): 6642-6669.

Kearney, M., R. W. Orrell, et al. (2016). "Pharmacological treatments for Friedreich ataxia." Cochrane Database Syst Rev(8): CD007791.

Kemp, K. C., N. Cerminara, et al. (2017). "Cytokine therapy-mediated neuroprotection in a Friedreich's ataxia mouse model." Ann Neurol **81**(2): 212-226.

Kempermann, G., E. P. Brandon, et al. (1998). "Environmental stimulation of 129/SvJ mice causes increased cell proliferation and neurogenesis in the adult dentate gyrus." Curr Biol **8**(16): 939-942.

Khdour, O. M., I. Bandyopadhyay, et al. (2018). "Lipophilic methylene blue analogues enhance mitochondrial function and increase frataxin levels in a cellular model of Friedreich's ataxia." Bioorg Med Chem **26**(12): 3359-3369.

Khonsari, H., M. Schneider, et al. (2016). "Lentivirus-meditated frataxin gene delivery reverses genome instability in Friedreich ataxia patient and mouse model fibroblasts." Gene Ther **23**(12): 846-856.

Kim, H., S. H. Kim, et al. (2016). "IDH2 deficiency promotes mitochondrial dysfunction and dopaminergic neurotoxicity: implications for Parkinson's disease." Free Radic Res **50**(8): 853-860.

Klein, M., B. L. Hempstead, et al. (2005). "Activation of STAT5-dependent transcription by the neurotrophin receptor Trk." J Neurobiol **63**(2): 159-171.

Klintsova, A. Y., E. Dickson, et al. (2004). "Altered expression of BDNF and its high-affinity receptor TrkB in response to complex motor learning and moderate exercise." Brain Res **1028**(1): 92-104.

Koeppen, A. H. and J. E. Mazurkiewicz (2013). "Friedreich ataxia: neuropathology revised." J Neuropathol Exp Neurol **72**(2): 78-90.

Koury, M. J. and M. C. Bondurant (1990). "Erythropoietin retards DNA breakdown and prevents programmed death in erythroid progenitor cells." Science **248**(4953): 378-381.

Kramer, A. F. and S. Colcombe (2018). "Fitness Effects on the Cognitive Function of Older Adults: A Meta-Analytic Study-Revisited." Perspect Psychol Sci **13**(2): 213-217.

Kramer, A. F., S. Hahn, et al. (1999). "Ageing, fitness and neurocognitive function." Nature **400**(6743): 418-419.

Kudo, N., N. Matsumori, et al. (1999). "Leptomycin B inactivates CRM1/exportin 1 by covalent modification at a cysteine residue in the central conserved region." Proc Natl Acad Sci U S A **96**(16): 9112-9117.

Kuijpers, M., K. L. van Gassen, et al. (2010). "Chronic exposure to the chemokine CCL3 enhances neuronal network activity in rat hippocampal cultures." J Neuroimmunol **229**(1-2): 73-80.

Kumari, D. and K. Usdin (2012). "Is Friedreich ataxia an epigenetic disorder?" Clin Epigenetics **4**(1): 2.

Land, T. and T. A. Rouault (1998). "Targeting of a human iron-sulfur cluster assembly enzyme, nifs, to different subcellular compartments is regulated through alternative AUG utilization." Mol Cell **2**(6): 807-815.

Lau, L. T. and A. C. Yu (2001). "Astrocytes produce and release interleukin-1, interleukin-6, tumor necrosis factor alpha and interferon-gamma following traumatic and metabolic injury." J Neurotrauma **18**(3): 351-359.

Letourneur, A., E. Petit, et al. (2013). "Brain ischemic injury in rodents: the protective effect of EPO." Methods Mol Biol **982**: 79-101.

Li, D. S., K. Ohshima, et al. (1999). "Knock-out of the cyaY gene in Escherichia coli does not affect cellular iron content and sensitivity to oxidants." FEBS Lett **456**(1): 13-16.

Li, K., E. K. Besse, et al. (2008). "Iron-dependent regulation of frataxin expression: implications for treatment of Friedreich ataxia." Hum Mol Genet **17**(15): 2265-2273.

Li, K., W. H. Tong, et al. (2006). "Roles of the mammalian cytosolic cysteine desulfurase, ISCS, and scaffold protein, ISCU, in iron-sulfur cluster assembly." J Biol Chem **281**(18): 12344-12351.

Lim, F., G. M. Palomo, et al. (2007). "Functional recovery in a Friedreich's ataxia mouse model by frataxin gene transfer using an HSV-1 amplicon vector." Mol Ther **15**(6): 1072-1078.

Lin, C., M. Zhang, et al. (2017). "Helix B surface peptide attenuates diabetic cardiomyopathy via AMPK-dependent autophagy." Biochem Biophys Res Commun **482**(4): 665-671.

Lin, H., J. Magrane, et al. (2017). "Early cerebellar deficits in mitochondrial biogenesis and respiratory chain complexes in the KIKO mouse model of Friedreich ataxia." Dis Model Mech **10**(11): 1343-1352.

Liu, P., W. You, et al. (2016). "Helix B Surface Peptide Protects against Acute Myocardial Ischemia-Reperfusion Injury via the RISK and SAFE Pathways in a Mouse Model." Cardiology **134**(2): 109-117.

Lodi, R., J. M. Cooper, et al. (1999). "Deficit of in vivo mitochondrial ATP production in patients with Friedreich ataxia." Proc Natl Acad Sci U S A **96**(20): 11492-11495.

Loria, F. and J. Diaz-Nido (2015). "Frataxin knockdown in human astrocytes triggers cell death and the release of factors that cause neuronal toxicity." Neurobiol Dis **76**: 1-12.

Lu, C., R. Schoenfeld, et al. (2009). "Frataxin deficiency induces Schwann cell inflammation and death." Biochim Biophys Acta **1792**(11): 1052-1061.

Makela, S. M., P. Osterlund, et al. (2011). "TLR ligands induce synergistic interferon-beta and interferon-lambda1 gene expression in human monocyte-derived dendritic cells." Mol Immunol **48**(4): 505-515.

Mariotti, C., R. Fancellu, et al. (2012). "Erythropoietin in Friedreich ataxia: no effect on frataxin in a randomized controlled trial." Mov Disord **27**(3): 446-449.

Marlatt, M. W., M. C. Potter, et al. (2012). "Running throughout middle-age improves memory function, hippocampal neurogenesis, and BDNF levels in female C57BL/6J mice." Dev Neurobiol **72**(6): 943-952.

Marmolino, D. (2011). "Friedreich's ataxia: past, present and future." Brain Res Rev **67**(1-2): 311-330.

Marmolino, D., F. Acquaviva, et al. (2009). "PPAR-gamma agonist Azelaoyl PAF increases frataxin protein and mRNA expression: new implications for the Friedreich's ataxia therapy." Cerebellum **8**(2): 98-103.

Mascalchi, M., N. Toschi, et al. (2016). "Regional Cerebral Disease Progression in Friedreich's Ataxia: A Longitudinal Diffusion Tensor Imaging Study." J Neuroimaging **26**(2): 197-200.

Miller, J. L., M. Rai, et al. (2017). "Erythropoietin and small molecule agonists of the tissue-protective erythropoietin receptor increase FXN expression in neuronal cells in vitro and in Fxn-deficient KIKO mice in vivo." Neuropharmacology **123**: 34-45.

Mincheva-Tasheva, S., E. Obis, et al. (2014). "Apoptotic cell death and altered calcium homeostasis caused by frataxin depletion in dorsal root ganglia neurons can be prevented by BH4 domain of Bcl-xL protein." Hum Mol Genet **23**(7): 1829-1841.

Miranda, C. J., M. M. Santos, et al. (2002). "Frataxin knockin mouse." FEBS Lett **512**(1-3): 291-297.

Monnier, V., J. V. Llorens, et al. (2018). "Impact of Drosophila Models in the Study and Treatment of Friedreich's Ataxia." Int J Mol Sci **19**(7).

Morland, C., K. A. Andersson, et al. (2017). "Exercise induces cerebral VEGF and angiogenesis via the lactate receptor HCAR1." Nat Commun **8**: 15557.

Nabhan, J. F., K. M. Wood, et al. (2016). "Intrathecal delivery of frataxin mRNA encapsulated in lipid nanoparticles to dorsal root ganglia as a potential therapeutic for Friedreich's ataxia." Sci Rep **6**: 20019.

Navarro, J. A., E. Ohmann, et al. (2010). "Altered lipid metabolism in a Drosophila model of Friedreich's ataxia." Hum Mol Genet **19**(14): 2828-2840.

Neumann, H., H. Schmidt, et al. (1997). "Interferon gamma gene expression in sensory neurons: evidence for autocrine gene regulation." J Exp Med **186**(12): 2023-2031.

Nguyen, L. A., H. He, et al. (2006). "Chiral drugs: an overview." Int J Biomed Sci **2**(2): 85-100.

Nunez, N. N., C. Majumdar, et al. (2018). "Fe-S Clusters and MutY Base Excision Repair Glycosylases: Purification, Kinetics, and DNA Affinity Measurements." Methods Enzymol **599**: 21-68.

Palomo, G. M., T. Cerrato, et al. (2011). "Silencing of frataxin gene expression triggers p53-dependent apoptosis in human neuron-like cells." Hum Mol Genet **20**(14): 2807-2822.

Paredes, F., K. Sheldon, et al. (2018). "Poldip2 is an oxygen-sensitive protein that controls PDH and alphaKGDH lipoylation and activation to support metabolic adaptation in hypoxia and cancer." Proc Natl Acad Sci U S A **115**(8): 1789-1794.

Parkinson, M. H., S. Boesch, et al. (2013). "Clinical features of Friedreich's ataxia: classical and atypical phenotypes." J Neurochem **126 Suppl 1**: 103-117.

Perdomini, M., B. Belbellaa, et al. (2014). "Prevention and reversal of severe mitochondrial cardiomyopathy by gene therapy in a mouse model of Friedreich's ataxia." Nat Med **20**(5): 542-547.

Perez-Luz, S., A. Gimenez-Cassina, et al. (2015). "Delivery of the 135 kb human frataxin genomic DNA locus gives rise to different frataxin isoforms." Genomics **106**(2): 76-82.

Pianese, L., A. Tammaro, et al. (2002). "Identification of a novel transcript of X25, the human gene involved in Friedreich ataxia." Neurosci Lett **320**(3): 137-140.

Piguet, F., C. de Montigny, et al. (2018). "Rapid and Complete Reversal of Sensory Ataxia by Gene Therapy in a Novel Model of Friedreich Ataxia." Mol Ther **26**(8): 1940-1952.

Regner, S. R., S. J. Lagedrost, et al. (2012). "Analysis of echocardiograms in a large heterogeneous cohort of patients with friedreich ataxia." Am J Cardiol **109**(3): 401-405.

Ribeiro, S. M., A. Gimenez-Cassina, et al. (2015). "Measurement of mitochondrial oxygen consumption rates in mouse primary neurons and astrocytes." Methods Mol Biol **1241**: 59-69.

Rotig, A., P. de Lonlay, et al. (1997). "Aconitase and mitochondrial iron-sulphur protein deficiency in Friedreich ataxia." Nat Genet **17**(2): 215-217.

Rouault, T. A. (2012). "Biogenesis of iron-sulfur clusters in mammalian cells: new insights and relevance to human disease." Dis Model Mech **5**(2): 155-164.

Rouault, T. A. and N. Maio (2017). "Biogenesis and functions of mammalian iron-sulfur proteins in the regulation of iron homeostasis and pivotal metabolic pathways." J Biol Chem **292**(31): 12744-12753.

Ruas, J. L., J. P. White, et al. (2012). "A PGC-1alpha isoform induced by resistance training regulates skeletal muscle hypertrophy." Cell **151**(6): 1319-1331.

Sacca, F., R. Piro, et al. (2011). "Epoetin alfa increases frataxin production in Friedreich's ataxia without affecting hematocrit." Mov Disord **26**(4): 739-742.

Sakamoto, N., K. Ohshima, et al. (2001). "Sticky DNA, a self-associated complex formed at long GAA*TTC repeats in intron 1 of the frataxin gene, inhibits transcription." J Biol Chem **276**(29): 27171-27177.

Salehi, M. H., B. Kamalidehghan, et al. (2014). "Gene expression profiling of mitochondrial oxidative phosphorylation (OXPHOS) complex I in Friedreich ataxia (FRDA) patients." PLoS One **9**(4): e94069.

Sanz-Gallego, I., I. Torres-Aleman, et al. (2014). "IGF-1 in Friedreich's Ataxia - proof-of-concept trial." Cerebellum Ataxias **1**: 10.

Sawyer, S. T. and W. D. Hankins (1993). "The functional form of the erythropoietin receptor is a 78-kDa protein: correlation with cell surface expression, endocytosis, and phosphorylation." Proc Natl Acad Sci U S A **90**(14): 6849-6853.

Schroder, K., P. J. Hertzog, et al. (2004). "Interferon-gamma: an overview of signals, mechanisms and functions." J Leukoc Biol **75**(2): 163-189.

Seznec, H., D. Simon, et al. (2005). "Friedreich ataxia: the oxidative stress paradox." Hum Mol Genet **14**(4): 463-474.

Shan, Y., R. A. Schoenfeld, et al. (2013). "Frataxin deficiency leads to defects in expression of antioxidants and Nrf2 expression in dorsal root ganglia of the Friedreich's ataxia YG8R mouse model." Antioxid Redox Signal **19**(13): 1481-1493.

Shulman, E., V. Belakhov, et al. (2014). "Designer aminoglycosides that selectively inhibit cytoplasmic rather than mitochondrial ribosomes show decreased ototoxicity: a strategy for the treatment of genetic diseases." J Biol Chem **289**(4): 2318-2330.

Si, W., J. Wang, et al. (2019). "Erythropoietin protects neurons from apoptosis via activating PI3K/AKT and inhibiting Erk1/2 signaling pathway." 3 Biotech **9**(4): 131.

Siren, A. L., T. Fasshauer, et al. (2009). "Therapeutic potential of erythropoietin and its structural or functional variants in the nervous system." Neurotherapeutics **6**(1): 108-127.

Siren, A. L., M. Fratelli, et al. (2001). "Erythropoietin prevents neuronal apoptosis after cerebral ischemia and metabolic stress." Proc Natl Acad Sci U S A **98**(7): 4044-4049.

Soltys, B. J. and R. S. Gupta (2000). "Mitochondrial proteins at unexpected cellular locations: export of proteins from mitochondria from an evolutionary perspective." Int Rev Cytol **194**: 133-196.

Sturm, B., U. Bistrich, et al. (2005). "Friedreich's ataxia, no changes in mitochondrial labile iron in human lymphoblasts and fibroblasts: a decrease in antioxidative capacity?" J Biol Chem **280**(8): 6701-6708.

Sturm, B., M. Helminger, et al. (2010). "Carbamylated erythropoietin increases frataxin independent from the erythropoietin receptor." Eur J Clin Invest **40**(6): 561-565.

Sturm, B., D. Stupphann, et al. (2005). "Recombinant human erythropoietin: effects on frataxin expression in vitro." Eur J Clin Invest **35**(11): 711-717.

Suarez-Mendez, S., C. A. Tovilla-Zarate, et al. (2018). "Erythropoietin: A potential drug in the management of diabetic neuropathy." Biomed Pharmacother **105**: 956-961.

Tapley, P., F. Lamballe, et al. (1992). "K252a is a selective inhibitor of the tyrosine protein kinase activity of the trk family of oncogenes and neurotrophin receptors." Oncogene **7**(2): 371-381.

Tomassini, B., G. Arcuri, et al. (2012). "Interferon gamma upregulates frataxin and corrects the functional deficits in a Friedreich ataxia model." Hum Mol Genet **21**(13): 2855-2861.

Tong, W. H., G. N. Jameson, et al. (2003). "Subcellular compartmentalization of human Nfu, an iron-sulfur cluster scaffold protein, and its ability to assemble a [4Fe-4S] cluster." Proc Natl Acad Sci U S A **100**(17): 9762-9767.

Tong, W. H. and T. Rouault (2000). "Distinct iron-sulfur cluster assembly complexes exist in the cytosol and mitochondria of human cells." EMBO J **19**(21): 5692-5700.

Ueba, H., M. Brines, et al. (2010). "Cardioprotection by a nonerythropoietic, tissue-protective peptide mimicking the 3D structure of erythropoietin." Proc Natl Acad Sci U S A **107**(32): 14357-14362.

Valente, A. J., L. A. Maddalena, et al. (2017). "A simple ImageJ macro tool for analyzing mitochondrial network morphology in mammalian cell culture." Acta Histochem **119**(3): 315-326.

Van Der Meer, P., S. H. Goldberg, et al. (2001). "Expression pattern of CXCR3, CXCR4, and CCR3 chemokine receptors in the developing human brain." J Neuropathol Exp Neurol **60**(1): 25-32.

van Praag, H., T. Shubert, et al. (2005). "Exercise enhances learning and hippocampal neurogenesis in aged mice." J Neurosci **25**(38): 8680-8685.

Vannocci, T., R. Notario Manzano, et al. (2018). "Adding a temporal dimension to the study of Friedreich's ataxia: the effect of frataxin overexpression in a human cell model." Dis Model Mech **11**(6).

Vaynman, S., Z. Ying, et al. (2004). "Exercise induces BDNF and synapsin I to specific hippocampal subfields." J Neurosci Res **76**(3): 356-362.

Vazquez-Manrique, R. P., P. Gonzalez-Cabo, et al. (2006). "Reduction of Caenorhabditis elegans frataxin increases sensitivity to oxidative stress, reduces lifespan, and causes lethality in a mitochondrial complex II mutant." FASEB J **20**(1): 172-174.

Villa, P., P. Bigini, et al. (2003). "Erythropoietin selectively attenuates cytokine production and inflammation in cerebral ischemia by targeting neuronal apoptosis." J Exp Med **198**(6): 971-975.

Wang, J., W. Lin, et al. (2004). "Inducible production of interferon-gamma in the developing brain causes cerebellar dysplasia with activation of the Sonic hedgehog pathway." Mol Cell Neurosci **27**(4): 489-496.

Wang, L., Z. G. Zhang, et al. (2007). "The Sonic hedgehog pathway mediates carbamylated erythropoietin-enhanced proliferation and differentiation of adult neural progenitor cells." J Biol Chem **282**(44): 32462-32470.

Wells, M., L. Seyer, et al. (2015). "IFN-gamma for Friedreich ataxia: present evidence." Neurodegener Dis Manag **5**(6): 497-504.

Wrann, C. D., J. P. White, et al. (2013). "Exercise induces hippocampal BDNF through a PGC-1alpha/FNDC5 pathway." Cell Metab **18**(5): 649-659.

Wu, Z., P. Puigserver, et al. (1999). "Mechanisms controlling mitochondrial biogenesis and respiration through the thermogenic coactivator PGC-1." Cell **98**(1): 115-124.

Xia, H., Y. Cao, et al. (2012). "Novel frataxin isoforms may contribute to the pathological mechanism of Friedreich ataxia." PLoS One **7**(10): e47847.

Xu, J. H., L. Long, et al. (2009). "CCR3, CCR2A and macrophage inflammatory protein (MIP)-1a, monocyte chemotactic protein-1 (MCP-1) in the mouse hippocampus during and after pilocarpine-induced status epilepticus (PISE)." Neuropathol Appl Neurobiol **35**(5): 496-514.

Yandim, C., T. Natisvili, et al. (2013). "Gene regulation and epigenetics in Friedreich's ataxia." J Neurochem **126 Suppl 1**: 21-42.

Yang, J., M. J. Kim, et al. (2017). "Isocitrate protects DJ-1 null dopaminergic cells from oxidative stress through NADP+-dependent isocitrate dehydrogenase (IDH)." PLoS Genet **13**(8): e1006975.

Yasukawa, K., T. Hirano, et al. (1987). "Structure and expression of human B cell stimulatory factor-2 (BSF-2/IL-6) gene." EMBO J **6**(10): 2939-2945.

Yoshimi, N., T. Futamura, et al. (2016). "Cerebrospinal fluid metabolomics identifies a key role of isocitrate dehydrogenase in bipolar disorder: evidence in support of mitochondrial dysfunction hypothesis." Mol Psychiatry **21**(11): 1504-1510.

Zeitlberger, A. M., G. Thomas-Black, et al. (2018). "Plasma Markers of Neurodegeneration Are Raised in Friedreich's Ataxia." Front Cell Neurosci **12**: 366.

Zhang, S., M. Napierala, et al. (2019). "Therapeutic Prospects for Friedreich's Ataxia." Trends Pharmacol Sci **40**(4): 229-233.